

AD/A-004 219

ANALYSIS OF THE MUTUAL INDUCTANCE
PARTICLE VELOCIMETER (MIPV)

Joseph D. Renick

Air Force Weapons Laboratory

Prepared for:

Defense Nuclear Agency

November 1974

DISTRIBUTED BY:

NTIS

National Technical Information Service
U. S. DEPARTMENT OF COMMERCE

This final report was prepared for the Air Force Weapons Laboratory. Mr. Joseph D. Renick (DEX) was the Laboratory Project Officer in Charge.

When US Government Drawings, specifications, or other data are used for any purpose other than a definitely related Government procurement operation, the Government thereby incurs no responsibility nor any obligation whatsoever, and the fact that the Government may have formulated, furnished, or in any way supplied the said drawings, specifications, or other data is not to be regarded by implication or otherwise as in any manner licensing the holder or any other person or corporation or conveying any rights or permission to manufacture, use, or sell any patented invention that may in any way be related thereto.

This technical report has been reviewed and is approved for publication.

Joseph D. Renick

JOSEPH D. RENICK
Project Officer

FOR THE COMMANDER

Wilfred F. Bucklew

WILFRED F. BUCKLEW
Lt Colonel, USAF
Chief, Experimental Branch

William B. Liddicoet

WILLIAM B. LIDDICOET
Colonel, USAF
Chief, Evil Engineering
Research Division

ACCESSION NO.	
NTIS	UNIT NO.
DOC	NO.
UNCLASSIFIED	43
JUSTIFICATION	
BY	
DISTRIBUTION AVAILABILITY CODES	
Dist.	APPROPRIATE SPECIAL
A	

DO NOT RETURN THIS COPY. RETAIN OR DESTROY.

UNCLASSIFIED

SECURITY CLASSIFICATION OF THIS PAGE (When Data Entered)

AD/A004 219

REPORT DOCUMENTATION PAGE		READ INSTRUCTIONS BEFORE COMPLETING FORM
1. REPORT NUMBER AFWL-TR-74-205	2. GOVT ACCESSION NO.	3. RECIPIENT'S CATALOG NUMBER
4. TITLE (and Subtitle) ANALYSIS OF THE MUTUAL INDUCTANCE PARTICLE VELOCIMETER (MIPV)		5. TYPE OF REPORT & PERIOD COVERED Final report; June 1973-June 1974
7. AUTHOR(s) Joseph D. Renick		6. PERFORMING ORG. REPORT NUMBER
9. PERFORMING ORGANIZATION NAME AND ADDRESS Air Force Weapons Laboratory (DEX) Kirtland Air Force Base, New Mexico 87117		8. CONTRACT OR GRANT NUMBER(s)
11. CONTROLLING OFFICE NAME AND ADDRESS Defense Nuclear Agency (SPSS) Washington, DC 20305		10. PROGRAM ELEMENT, PROJECT, TASK AREA & WORK UNIT NUMBERS 62710H; WDNS0303; J11AASX352
14. MONITORING AGENCY NAME & ADDRESS (if different from Controlling Office)		12. REPORT DATE November 1974
		13. NUMBER OF PAGES 140 133
		15. SECURITY CLASS. (of this report) UNCLASSIFIED
		15a. DECLASSIFICATION/DOWNGRADING SCHEDULE
16. DISTRIBUTION STATEMENT (of this Report) Approved for public release; distribution unlimited.		
17. DISTRIBUTION STATEMENT (of the abstract entered in Block 20, if different from Report) Reproduced by NATIONAL TECHNICAL INFORMATION SERVICE US Department of Commerce Springfield, VA. 22151		
18. SUPPLEMENTARY NOTES PRICES SUBJECT TO CHANGE		
19. KEY WORDS (Continue on reverse side if necessary and identify by block number) Mutual inductance; Soil motion measurements; Hydrodynamic flow		
20. ABSTRACT (Continue on reverse side if necessary and identify by block number) Three analytical areas supporting development of the mutual inductance particle velocimeter (MIPV) are investigated. First, the basic theory is extended to permit calculation of gage factors and determination of design criteria for complex geometry gages. A finite element model is developed to investigate the effects of divergent/off-axis flow upon the gage response. Finally, an electromechanical mathematical model of the gage is developed to		

133

UNCLASSIFIED

SECURITY CLASSIFICATION OF THIS PAGE(When Data Entered)

investigate the effects of shock-induced self-inductance and resistance changes upon gage response. The mathematical model identifies the influence of different conductor materials upon gage design, therefore a brief study is conducted to further define conductor resistance-stress and shock equilibration time characteristics. Numerical data are presented for each analytical area. As a result of the numerical investigations, the following conclusions are made: (1) The gage length-to-width ratio should be greater than 5 after shock transit through the gage to ensure a constant gage factor. Generally a gage designed with a length-to-width ratio of 10 or greater will satisfy this requirement; (2) Increased gage factors without sacrifice in electrical rise time are available with a design which, instead of alternating single loops of primary and secondary turns, uses alternating multiple primary and single secondary turns; (3) The MIPV is essentially insensitive to divergent flow effects for normal gage designs where the width is less than 3 inches and the source is at a range of 1 meter or greater; (4) The gage is relatively insensitive to off-axis flow in the plane of the gage loops, the error induced being approximately equal to $\frac{1}{2}(1 - \cos \gamma)$ where γ is the off-axis angle. However, flow off-axis in a plane normal to the loop plane results in much larger errors approximately equal to $3(1 - \cos \theta)$ where θ is the off-axis angle; (5) Errors caused by shock-induced self-inductance and resistance changes in the gage are effectively controlled with a large ballast inductance in the gage primary; (6) Three metals, aluminum, magnesium, and beryllium, all exhibit favorable shock impedance, electrical resistivity, and pressure-induced $\Delta R/l$ characteristics; each presents a relatively low neutron cross section, with beryllium being the most favorable.

ia

UNCLASSIFIED

PREFACE

Appreciation is expressed to Lt Colonel Giles Willis who provided the solution methods in the electromechanical modeling of section VI and to Mr. Gerald Perry, GE-TEMPO, who assisted in the assembly of this report.

CONTENTS

<u>Section</u>	<u>Page</u>
I INTRODUCTION	7
General	7
Description	8
Background	9
II EXTENSION OF THEORY TO COMPLEX GAGE DESIGNS	12
Basic Theory	12
Extension of Theory for Complex Gage Geometries	17
Numerical Results	21
Summary	26
III OFF-AXIS, DIVERGENT FLOW RESPONSE	28
Development of Computer Model	28
Summary of Numerical Results	31
Summary	41
IV ELECTROMECHANICAL MODELING	42
Previous Work	42
Electromechanical Model	43
Numerical Results	50
Summary	62
V CONCLUSIONS AND RECOMMENDATIONS	65
APPENDIXES	
A. Tabulated Numerical Data for MIPV Designs	67
B. Computer Code Listing--DIVE	93
C. Selection of Optimum Gage Conductor	106
D. Computer Code Listing--ELMEK	115
REFERENCES	131

ILLUSTRATIONS

<u>Figure</u>		<u>Page</u>
1	MIPV Used in Gas Gun Testing	10
2	Mutual Inductance Particle Velocimeter Nomenclature	13
3	MIPV Undergoing Deformation Due to Shock	16
4	Cross Section of MIPV Loops, Type I Gage	18
5	Cross Sections of MIPV Loops, Type II Design	21
6	Gage Factor as a Function of Width and Number of Primary and Secondary Turns, Type I Gage	23
7	Gage Factor as a Function of Spacing between Loops and Number of Primary and Secondary Turns, Type I Gage	24
8	Variation of Gage Factor and η with Gage Length-to-Width Ratio for a Typical Type I Gage Design	26
9	Comparison of Types I and II Gages	27
10	Nomenclature for Development of Divergent/ Off-Axis Flow Model of MIPV	29
11	Effects of Divergent Flow upon Gage Response	33
12	Effects of Off-Axis Flow upon Gage Response	34
13	Effects of Off-Axis Flow upon Gage Response	35
14	Effects of Off-Axis Flow upon Gage Response	36
15	Effects of Off-Axis Flow upon Gage Response	37
16	Effects of Off-Axis Flow upon Gage Response	38
17	Comparisons of DIVE Calculations with Cosine Function	39
18	Gage Undergoing Deformation for Off-Axis Shock, $\theta=0$, $\gamma \neq 0$	39
19	Gage Undergoing Deformation for Off-Axis Shock, $\gamma=0$, $\theta \neq 0$	40
20	Simplified Schematic of Power Supply and Velocity Gage with Open Secondary	44

ILLUSTRATIONS (cont'd)

<u>Figure</u>		<u>Page</u>
21	Electrical Network of Velocity Measuring System	44
22	Graph of Network Shown in Figure 21, Tree Indicated by Solid Lines, Branches by Dashed Lines	45
23	MIPV Undergoing Shock Deformation and Nomenclature for Determining $L(t)$ and $\dot{L}(t)$	49
24	Nomenclature for Determining Gage $R(t)$	49
25	Glass Gage	52
26	Shock Response of AEDC Gage as Calculated by ELMEK, $K = .4$	55
27	Shock Response of AEDC Gage as Calculated by ELMEK, $K = 2$	56
28	Calculated Gage Response Using ELMEK, Inductance Changes Only, AEDC Gage	57
29	Calculated Gage Response Using ELMEK, Resistance Changes Only, AEDC Gage	58
30	Calculated Gage Response Using ELMEK, Normal Resistance and Inductance Changes, AEDC Gage	60
31	Shock Response of Field Design Gage as Calculated by ELMEK, $K = 0.2$, $L_{11} = 500 \mu h$	63
C-1	Change in Resistance as a Function of Stress for Several Metals	109
C-2	Geometry for One-Dimensional Shock Response Analysis	111
C-3	Shock Equilibration of Copper in Tuff	111
C-4	Resistance Change Per-Unit-Length as a Function of Equilibration Time, t_e , for Several Conductor Materials, 200 Kbar	114

SECTION I

INTRODUCTION

1. GENERAL

The Air Force Nuclear Weapons Effects Research Council has established a requirement for the experimental investigation of the radiative and kinetic energy partitioning during the initial coupling into the ground of a near surface nuclear burst. An understanding of the initial energy coupling is essential to the accurate computer predictions of crater formation and ground motion used in the survivability/vulnerability assessment of Air Force weapon systems. Ideally, this information would be obtained through experiments utilizing megaton yields in near surface nuclear bursts. However, the Limited Nuclear Test Ban Treaty of 1963 prevents atmospheric testing of nuclear weapons; thus, all nuclear testing in this country subsequent to the treaty has been conducted underground. As a result, the near surface burst geometry, which represents the actual threat geometry, is replaced by a room geometry. An additional ground shock system is generated by the room effects which overtake the shock system generated by the initial coupling and obscure information about the initial coupling. To obtain any information about the initial coupling, soil stress and motion measurements in the unobscured region very close in to the nuclear source would be required. Supposedly, this would require measurements in the stress region of 2 to 3 Mbar; however, any measurements above 100 Kbar would provide useful information.

It appears to be feasible to conduct an experiment with a room configuration such that the near surface burst geometry is preserved for early times. With soil motion and stress instrumentation suitably placed, the effects of the shock generated by the initial coupling could then be observed. However, the ability of the scientific community to successfully conduct an experiment of this type has been seriously questioned since the capability to make the required temperature, radiative, and ground stress and

motion measurements has never been demonstrated. Until considerable confidence is developed in the instrumentation to be fielded, a full-scale coupling experiment is not justifiable. This level of confidence might be achieved through evaluation of the instrumentation systems in add-on experiments to scheduled underground nuclear tests.

Instrumentation for use in an underground nuclear event would also be suitable for use in the region close-in to a large-scale high-explosive event since the material flow in each case is described by a hydrodynamic model. Any calculations of cratering and ground motion for the purpose of assessing structures survivability/vulnerability must begin with the coupling of the source into the soil; therefore, measurements in this region would be essential to verifying the calculated dynamic soil loading.

The Air Force Weapons Laboratory has been conducting a program of analysis, testing, and evaluation in an effort to develop instrumentation which can make the required soil stress and motion measurements. Included in this program have been investigations of the Impedance-Mismatch-High-Stress-Transducer (IMHST) (ref. 1), Thermoelectric-Thermopile-Transducer (T^3) (ref. 2), Mutual Inductance Particle Velocimeter (MIPV) (ref. 3), and waveguide displacement system (ref. 4). Other systems, such as the crescent velocity gage (ref. 5), DX pendulum velocity gage (ref. 6), electrolytic stress gage (ref. 7), and the laser interferometer system (ref. 8) were also considered but did not appear to have potential for making the required measurements.

The MIPV was judged to have the best potential for providing the soil motion measurements, and a development program consisting of analyses and testing was initiated at AFWL in late 1971. The purpose of this report is to describe the significant analysis of the MIPV completed by AFWL. Recent testing of the MIPV is reported elsewhere.

2. DESCRIPTION

The MIPV consists of two sets of rectangular-shaped loops of wire. The gage is embeded in a media (geology, grout, epoxy, etc.) of interest and oriented so that the shock front propagates along

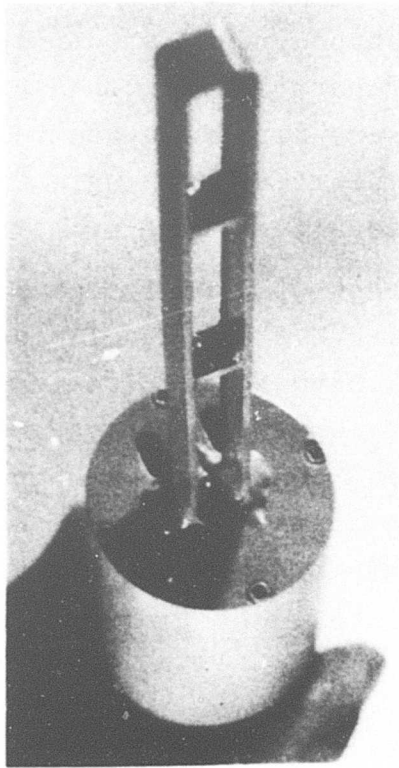
its major axis. A constant current is supplied to the primary loop, and a voltage which is proportional to the rate of collapse of the loops is induced in the secondary. Any number of primary and secondary turns with any desired grouping may be utilized. Typical gage designs have utilized alternating primary and secondary loops.

Figure 1 is a photograph of a design utilized in gas gun testing at AFWL. The loops are 0.020-inch diameter aluminum wire embedded in a strap of aluminum-oxide-loaded polymethylmethacrylate (PMMA) which electrically insulates the gage and holds the gage dimensions. A capacitive discharge power supply provides a constant current pulse to the gage primary. The secondary is connected to a 50-ohm coaxial cable which in turn is terminated in 50 ohms at the recording instrumentation.

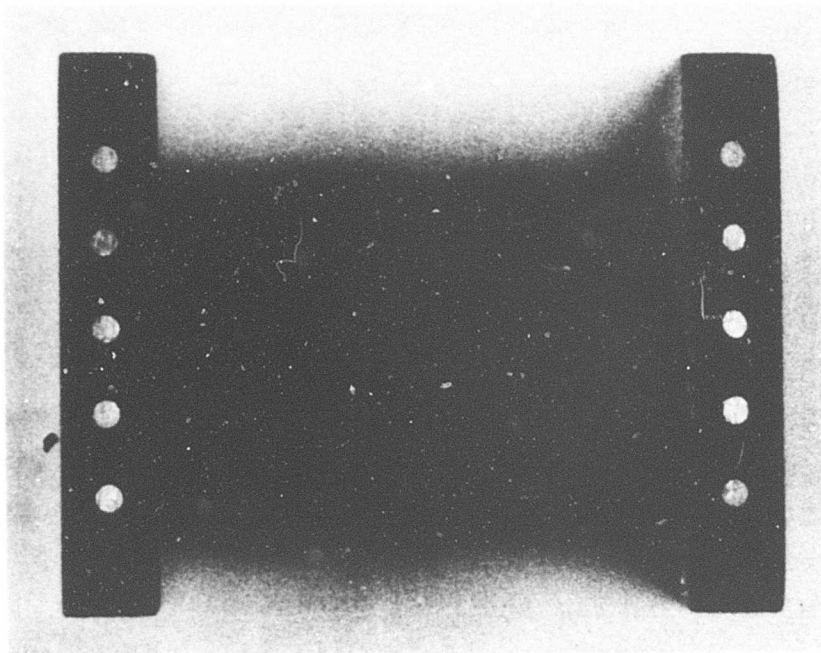
3. BACKGROUND

In 1963, DASA, presently called the Defense Nuclear Agency (DNA), awarded a contract to the Engineering Physics Company (EPCO) for development of a soil particle velocity gage for use in underground nuclear tests (refs. 3, 9, 10, 11). The gage was to have the capability of making measurements in the 50- to 1000-Kbar stress region. After considering several schemes, EPCO selected the mutual inductance principle as the most promising. Development continued through 1965 and resulted in what appeared to be a reliable velocity gage. The gage was fielded in RED HOT (ref. 12) in 1966 and DISTANT PLAIN, event VI (ref. 13) in 1967 with limited success. There has been no further use of the EPCO-designed gage since these field tests.

Stanford Research Institute (SRI) since 1971 has been conducting a program for DNA to determine constitutive relations in rocks and soils by in-material stress and particle velocity measurements and analysis techniques. During the initial phase of the program, SRI selected the MIPV as having the best potential for making the required velocity measurements (refs. 14, 15). Excellent results have been obtained in gas gun and explosive tests (ref. 16), where the gage was evaluated in the stress range of from a few Kbars to 40 Kbars. Recent fielding of the MIPV in ESSEX (1973-1974) has produced good data in the 1- to 10-Kbar stress region.



(a) Assembled gage



(b) Cross section showing 20-mil aluminum wires in aluminum-oxide-loaded acrylic

Figure 1. MIPV Used in Gas Gun Testing

During the AFWL development program, gages were fielded in MIDDLE GUST IV and V (ref. 17) and in MIXED COMPANY (ref. 18) which, respectively, were 100-ton surface-tangent, 20-ton half-buried, and 500-ton surface-tangent TNT events. During these tests, gage survivability well after shock passage was demonstrated. However, gage shorting due to electrical breakdown of the gage insulation in the 150-Kbar stress environment was observed. This dictated further investigation to obtain insulating materials which would maintain their properties at high-stress levels.

A series of gas gun experiments was conducted at AFWL in 1973 to evaluate the gage response in the 15- to 50-Kbar region. Loading, unloading, repeatability, off-axis response, and self-generating response were investigated with very good results. Testing in explosive and hypervelocity gas gun experiments was conducted during the spring of 1974. The results of these tests are to be published in a forthcoming AFWL technical report.

Three major analytical areas were investigated to provide an improved understanding of the gage response to the intense shock environment. These analytical areas, which are the subject of this report, are presented in individual sections as follows:

Extension of Theory to Complex Gage Designs

Divergent/Off-Axis Flow Response

Electromechanical Modeling

The specific requirements for investigating these problems are presented in introductory remarks in each section.

SECTION II

EXTENSION OF THEORY TO COMPLEX GAGE DESIGNS

The MIPV theory of operation developed by EPCO was applied specifically to a single primary, multiple secondary gage design (ref. 3). Expressions were derived for a rectangular gage geometry for calculating the gage mutual inductance, M , and dM/da , where "a" is gage length (figure 2). These relations cannot be applied directly in making calculations for gages consisting of multiple turns of primary and secondary loops such as utilized in the AFWL- and SRI-designed gages. A requirement, therefore, existed to extend the basic theory so that gage parameters could be calculated for a given design prior to fabrication. This permits designing a gage to meet the requirements of a particular test.

The basic theory developing the expressions for mutual inductance and dM/da will be summarized. The theory will then be extended to consider complex gage designs. The results of numerical investigation of the effects of changing gage design parameters upon sensitivity will be presented, and design parameters will be tabulated for several designs.

1. BASIC THEORY

Consider the simple model of the velocity gage shown in figure 2. If the magnetic flux, Φ , linking the secondary loop changes, a voltage, E , will be induced in the secondary that is equal to the negative time rate of change of the magnetic flux such that

$$E = - \frac{d\Phi}{dt} \quad (1)$$

The magnetic flux through the surface of the gage secondary (in the x-y plane) may be expressed in terms of the magnetic flux density, \vec{B} ,

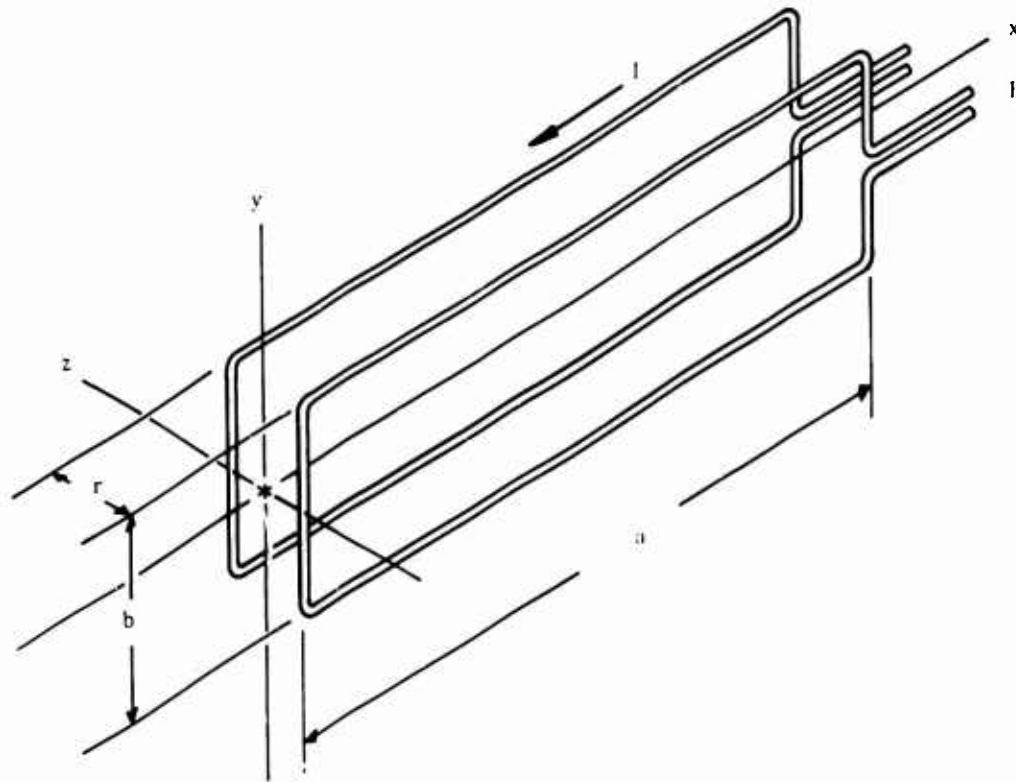


Figure 2. Mutual Inductance Particle Velocimeter Nomenclature

$$\Phi = \iint \vec{B} \cdot d\vec{S} \quad (2)$$

where $d\vec{S}$ is an element of area of the surface.

A vector, \vec{A} , the magnetic vector potential, may be defined such that

$$(\vec{\nabla} \times \vec{A}) \equiv \vec{B} \quad (3)$$

Applying Stokes' theorem,

$$\iint (\vec{\nabla} \times \vec{A}) \cdot d\vec{S} = \oint \vec{A} \cdot d\vec{\ell}_s \quad (4)$$

where $d\vec{\ell}_s$ is an increment of length along the secondary loop. Equations (1) through (4) may be combined to obtain the induced voltage in terms of the magnetic vector potential

$$E = - \frac{d}{dt} \oint \vec{A} \cdot d\vec{\ell}_s \quad (5)$$

The magnetic vector potential at any point, Q, on the secondary is

$$\vec{A}|_Q = \frac{\mu_o}{4\pi} \oint \frac{I d\vec{\ell}_p}{d} \quad (6)$$

where

μ_o is the magnetic permeability of air

I is the primary loop current

$d\vec{\ell}_p$ is an element of length along the primary loop

d is the distance from point Q to the element $d\vec{\ell}_p$

Combining equations (5) and (6),

$$E = - \frac{\mu_o}{4\pi} \frac{d}{dt} \oint \oint \frac{I d\vec{\ell}_p}{d} \cdot d\vec{\ell}_s \quad (7)$$

Since by definition the mutual inductance is the flux in the secondary per unit current in the primary,

$$\Phi = MI$$

and

$$M = \frac{\mu_o}{4\pi} \oint \oint \frac{d\vec{\ell}_p}{d} \cdot d\vec{\ell}_s \quad (8)$$

which is seen to be simply a function of geometry. Equation (7) may then be rewritten as

$$E = - \frac{d(MI)}{dt} \quad (9)$$

if we require that the current be held constant, then

$$E = - I \frac{dM}{dt} \quad (10)$$

Consider figure 3 where a plane shock wave propagates down the gage major axis, x , at a shock velocity, c . Assuming that the loops flow with the media at the particle velocity, u , it is apparent that

$$u = - \frac{da}{dt}$$

Expanding the term dM/dt

$$\frac{dM}{dt} = \frac{dM}{da} \frac{da}{dt}$$

The expression for the secondary induced voltage now becomes

$$E = I \frac{dM}{da} u \quad (11)$$

recalling that M is defined by equation (8). EPCO obtained a closed form solution to equation (8) in terms of generalized gage dimensions (ref. 3). Their result is repeated here as equation (12).

$$M = \frac{\mu_0}{\pi} \left\{ 2r - 2\sqrt{r^2+b^2} - 2\sqrt{r^2+a^2} + 2\sqrt{r^2+b^2+a^2} \right. \\ \left. + a \ln \left[\frac{\sqrt{r^2+b^2} (a+\sqrt{r^2+a^2})}{r(a+\sqrt{r^2+b^2+a^2})} \right] + b \ln \left[\frac{\sqrt{r^2+a^2} (b+\sqrt{r^2+b^2})}{r(b+\sqrt{r^2+b^2+a^2})} \right] \right\} \quad (12)$$

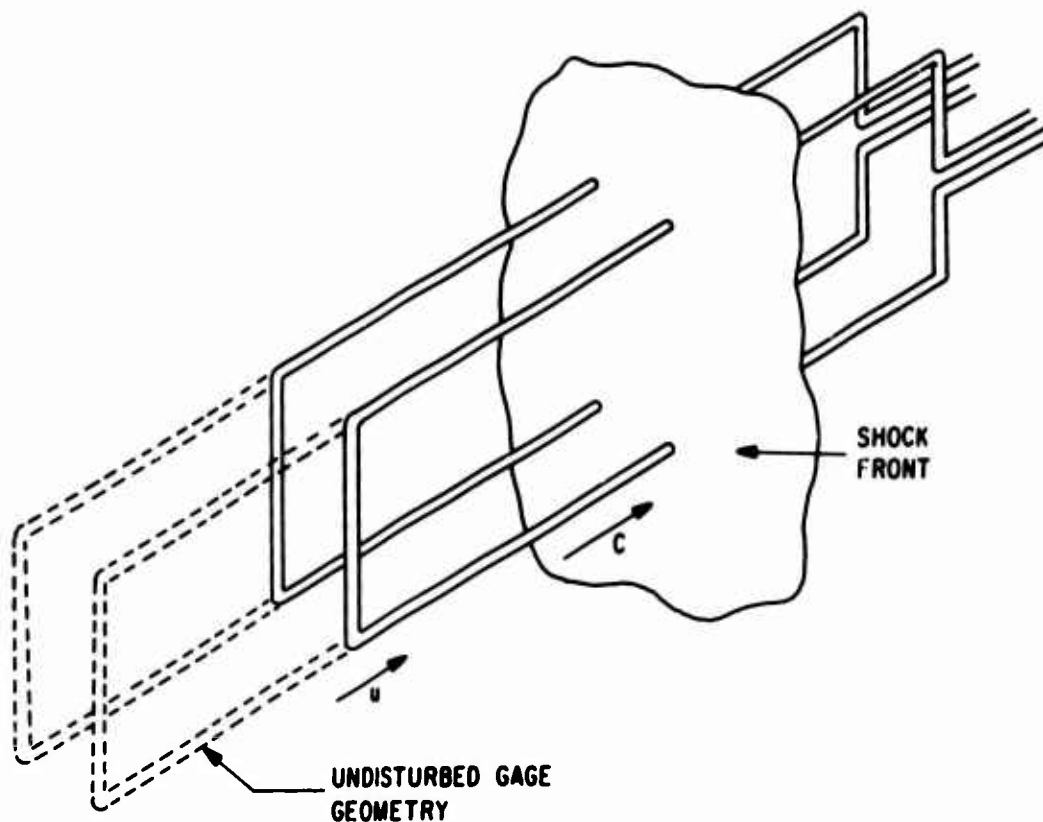


Figure 3. MIPV Undergoing Deformation Due to Shock

where the nomenclature of figure 2 applies. Differentiating with respect to "a,"

$$\frac{dM}{da} = \frac{\mu_c}{\pi} \left\{ \ln \frac{(\sqrt{r^2+b^2})(a+\sqrt{a^2+r^2})}{(r(a+\sqrt{a^2+b^2+r^2}))} + a \frac{(\sqrt{a^2+b^2+r^2} - \sqrt{a^2+r^2})}{a^2+r^2} \right\} \quad (13)$$

Equations (12) and (13) permit calculation of gage parameters for simple geometries consisting of a constant distance, r , between primary and secondary loops. This would be possible for a single primary, multiple secondary (or vice versa) design such as that of EPCO.

There is no way known to measure the term dM/da for a given gage design. To establish confidence in the gage sensitivity,

some method of experimentally determining the magnitude of dM/da is required. EPCO noted that by assuming

$$\frac{M}{a} \approx \frac{dM}{da} \quad (14)$$

an experimental estimation of dM/da could be obtained simply by measuring the gage mutual inductance and length. Numerical investigations indicated that for a gage whose length was 10 to 15 times greater than the width, the difference between M/a and dM/da was less than ≈ 5 percent. Further improvements to the determination of dM/da are obtained by applying the error term as a correction factor. The correction factor, η , is defined as

$$\eta = \frac{\frac{dM}{da} - \frac{M}{a}}{\frac{dM}{da}} = 1 - \frac{M}{a} \frac{1}{\frac{dM}{da}} \quad (15)$$

and dM/da is expressed as

$$\frac{dM}{da} = \frac{M}{a} \frac{1}{(1-\eta)} \quad (16)$$

In equation (15) M and dM/da are calculated values from equations (12) and (13), respectively. In equation (16) M and " a " are measured values. This method of using a calculated factor (η) to correct measured parameters (M/a) is applicable providing the calculated and measured values of M agree very closely. As will be shown later, this has routinely been the case.

Extension of the previous analysis is required to calculate η for more complex geometries.

2. EXTENSION OF THEORY FOR COMPLEX GAGE GEOMETRIES

Consider a gage geometry consisting of m primary and n secondary turns. For the i th primary turn and j th secondary turn, the mutual inductance is M_{ij} and the total gage mutual inductance M , may be expressed as

$$M = \sum_{i=1}^m \sum_{j=1}^n M_{ij} \quad (17)$$

As an example, consider the 4-primary, 3-secondary turn design depicted in figure 4.

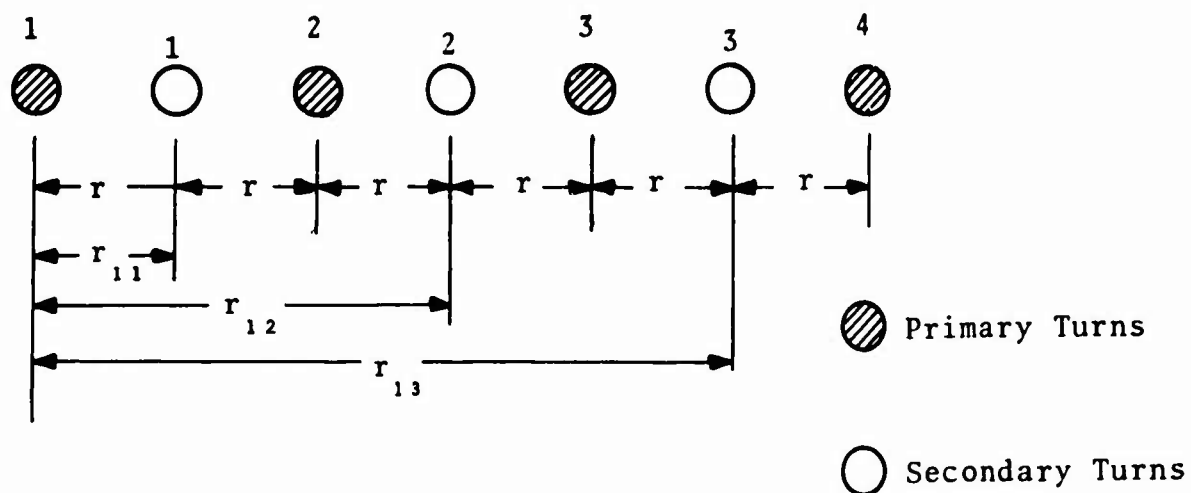


Figure 4. Cross Section of MIPV Loops, Type I Gage

The mutual inductance is calculated as

$$\begin{aligned}
 M &= \sum_{i=1}^4 \sum_{j=1}^3 M_{ij} \\
 &= M_{11} + M_{12} + M_{13} + M_{21} + M_{22} + M_{23} \\
 &\quad + M_{31} + M_{32} + M_{33} + M_{41} + M_{42} + M_{43}
 \end{aligned}$$

Note that due to the same distance, r , between loops.

$$M_{11} = M_{21} = M_{22} = M_{32} = M_{33} = M_{43},$$

$$M_{12} = M_{23} = M_{31} = M_{42}, \text{ and}$$

$$M_{13} = M_{41}$$

The mutual inductance may then be expressed as

$$M = 6M_{11} + 4M_{12} + 2M_{13}$$

In this case, by calculating the mutual inductances M_{11} , M_{12} , and M_{13} with equation (12) utilizing the distances r_{11} , r_{12} , and r_{13} , the total gage mutual inductance may be calculated. By requiring that the loops be separated by the same distances and specifying that there is one more primary turn than secondary turn, the generalized expression for gages with alternating primary and secondary turns is

$$M = \sum_{j=1}^n \left[n+m+1-2j \right] M_{1j} \quad (18)$$

Recalling equation (15) and substituting equations (16) and (17),

$$\eta = 1 - \frac{\sum_{i=1}^m \sum_{j=1}^n M_{ij}}{\sum_{i=1}^m \sum_{j=1}^n \frac{M_{ij}}{1-\eta_{ij}}} \quad (19)$$

where

$$\eta_{ij} = 1 - \frac{M_{ij}}{a \frac{dM_{ij}}{da}}$$

and dM_{ij}/da is calculated from equation (13). Utilizing equation (18) in equation (19),

$$\eta = 1 - \frac{\sum_{j=1}^n \left[\frac{n+m+1-2j}{a} \right] M_{1j}}{\sum_{j=1}^n \left[\frac{n+m+1-2j}{a} \right] \frac{dM_{1j}}{da}} \quad (20)$$

which applies to the same geometry as that associated with equation (18). A more general expression for η would utilize equation (17) in equation (15), resulting in

$$\eta = 1 - \frac{\sum_{i=1}^n \sum_{j=1}^m M_{ij}}{a \sum_{i=1}^n \sum_{j=1}^m \frac{dM_{ij}}{da}} \quad (21)$$

Considering the example from before (figure 4),

$$\eta = 1 - \frac{6M_{11} + 4M_{12} + 2M_{13}}{a \left[6 \frac{dM_{11}}{da} + 4 \frac{dM_{12}}{da} + 2 \frac{dM_{13}}{da} \right]}$$

Equations (11) and (16) may be combined to define a term, gage factor, GF, such that

$$GF \equiv \frac{E}{uI} = \frac{M}{a} \left(\frac{1}{1-\eta} \right) \quad (22)$$

where

M is measured mutual inductance, henries

a is measured length, meters

n is calculated from equation (21)

GF has the units volts/amp \cdot mps but is more conveniently expressed as mv/(amp \cdot mm/ μ sec)

Thus during a test, two measurements, secondary output voltage and primary current, must be made to obtain particle velocity.

3. NUMERICAL RESULTS

A generalized computer code (DSIN1, appendix A) calculates gage mutual inductance, gage factor, and error term (or correction factor) for gages utilizing alternating primary and secondary turns. This will be referred to as the Type I gage. A specialized code (DSIN2, appendix A) calculates the same parameters for the designs shown in figure 5. This will be referred to as the Type II gage. Numerical results for a variety of designs for each type gage are tabulated in appendix A.

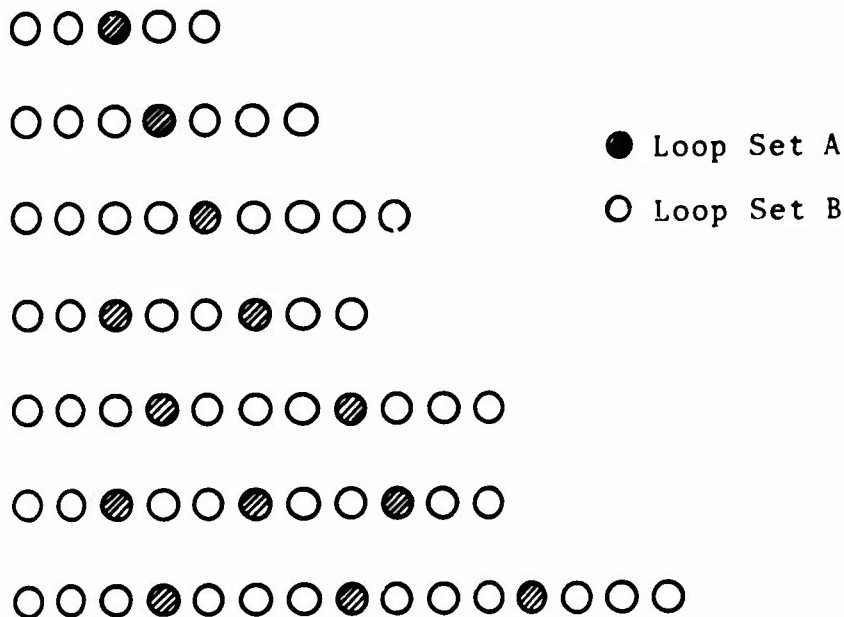


Figure 5. Cross Sections of MIPV Loops, Type II Design

a. Comparison of Calculated and Measured Mutual Inductance

Table 1 shows the results of calculations made for gages designed for fielding in MIXED COMPANY, a 500-ton TNT event. Measured values of mutual inductance are compared with the

calculated values and the error between the two indicated. Inductance measurements were made with a GR Type 1632-A Inductance Bridge. The slight variation in measured values is primarily due to slight variations in length between individual gages which results from the fabrication technique. For gages which have a length-to-width ratio, a/b , greater than approximately 5, the mutual inductance essentially varies directly with length. Therefore, by considering the individual gage length and controlling other gage dimensions, a very accurate value of the gage factor, which, as will be shown, is essentially independent of gage length, may be determined. The results of table 1 are typical, i.e., gages can be constructed routinely to within less than 1 percent design gage factor.

Table 1

COMPARISON OF MEASURED AND CALCULATED VALUES OF
MUTUAL INDUCTANCE FOR MIXED COMPANY GAGES

<u>Gage No.</u>	<u>Measured mutual inductance (μh)</u>	<u>Calculated mutual inductance (μh)</u>	<u>Error (%)</u>
1	4.411	4.356	1.2
2	4.385	4.356	0.6
3	4.398	4.356	0.9
4	4.386	4.356	0.6

b. Parametric Analysis

Figures 6 and 7 show the influence upon gage factor of varying gage width, spacing between turns, and number of primary and secondary turns for typical Type I gage designs. The results are not unexpected, i.e., increasing gage width, increasing number of turns, and decreasing loop spacing all result in increased gage factor.

Since, as shown in figure 6, a wide range of gage factors is available, the gage may be used over a wide range of particle velocity inputs and still produce measurable signals. For instance, a signal of 400 mv is produced for a 0.1-mm/ μ sec velocity input (≈ 5 Kbar) with a gage factor of 40 mv/(amp \cdot mm/ μ sec) and 100 amperes current in the primary. For applications in the stress region above 100

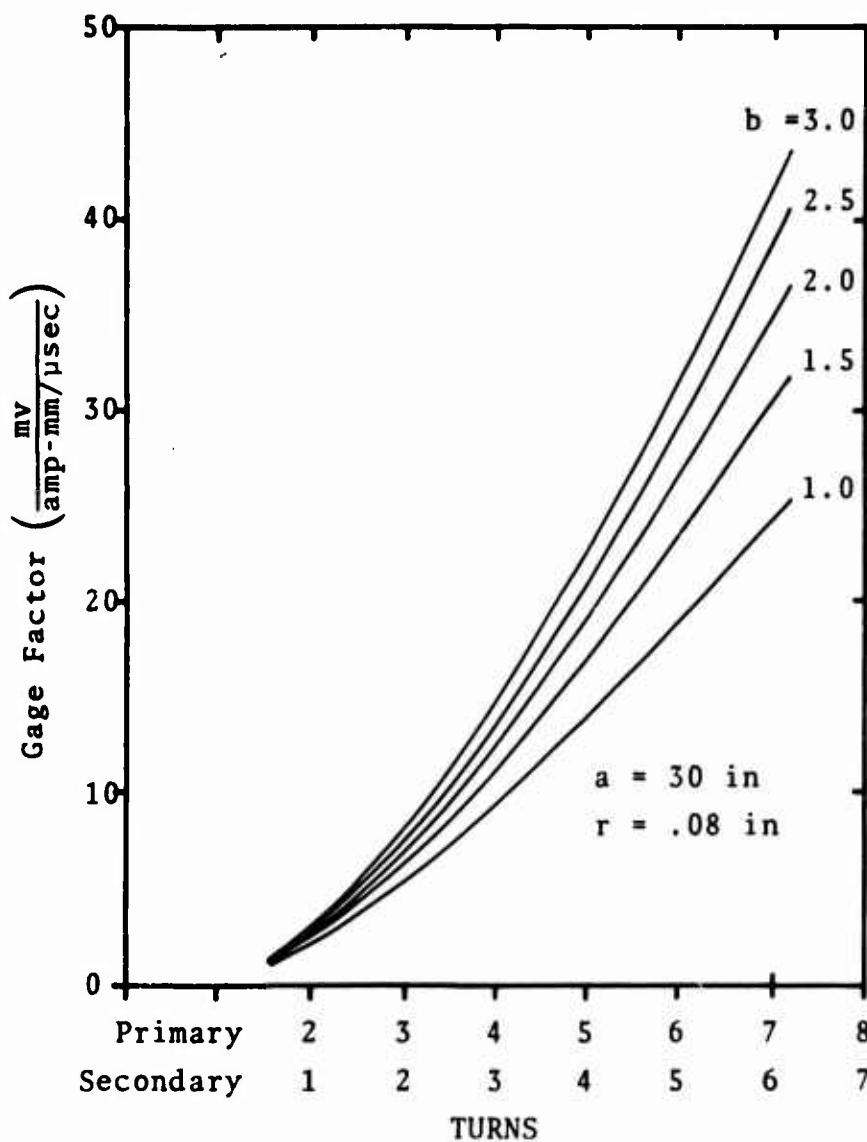


Figure 6. Gage Factor as a Function of Width and Number of Primary and Secondary Turns, Type I Gage

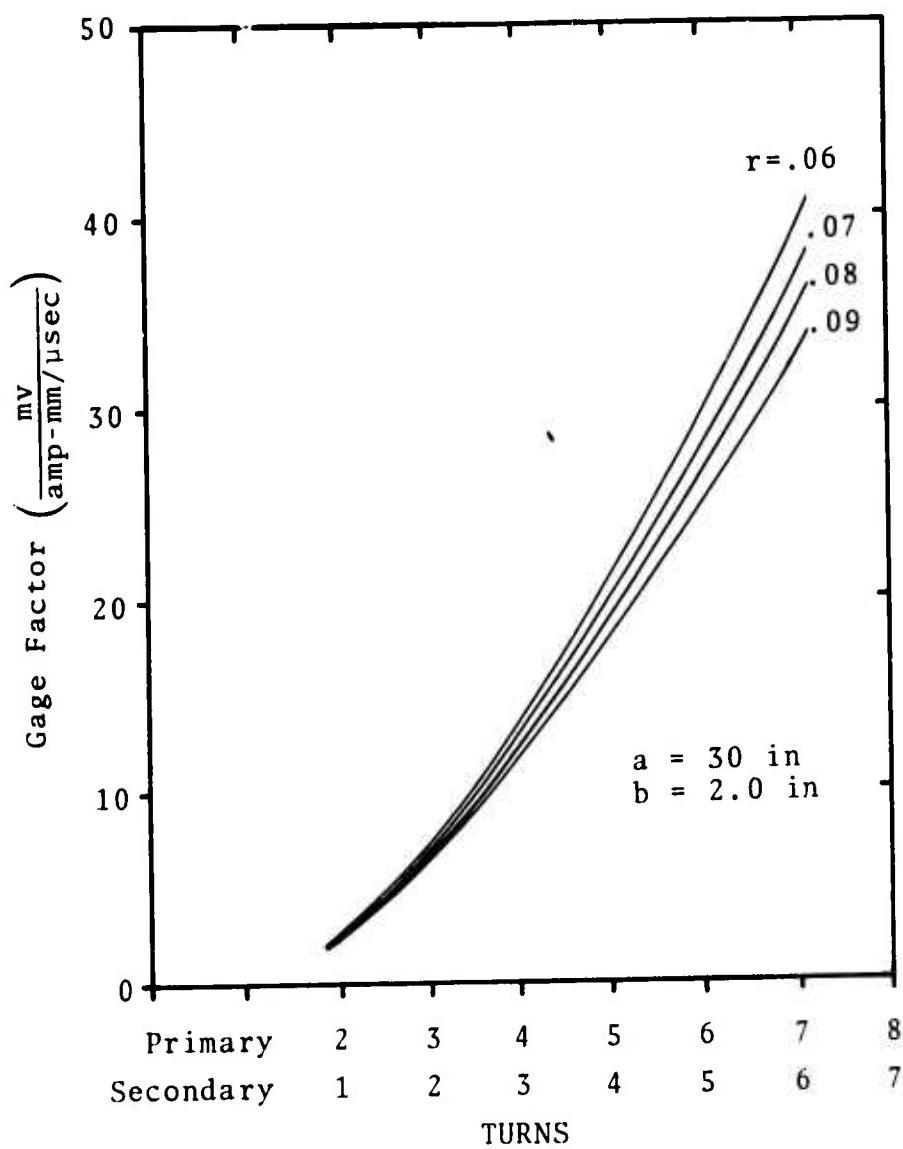


Figure 7. Gage Factor as a Function of Spacing between Loops and Number of Primary and Secondary Turns, Type I Gage

Kbar, the particle velocity would generally be greater than 1 mm/ μ sec, and signals above 2 volts are easily obtainable.

Note in figure 7 that loop spacing has a relatively small influence upon gage factor. This would suggest that one would be free to choose from a wide range of wire diameters without seriously affecting gage factor. Past designs by AFWL have utilized wire diameters varying from 0.020 to 0.0625 inch. Loop spacing is generally 2 to 2.5 times the wire diameter to ensure adequate separation to prevent mechanical contact and hence electrical shorting between loops. Typical designs employ spacings ranging from around 0.040 to 0.160 inch.

In many geologies at very high stress levels and for long duration stress pulses, a gage deformation of up to 50 percent may be experienced during the shock transit. This introduces questions as to the influence of changing gage length upon gage factor. The numerical results shown in figure 8 indicate that certain geometrical limitations do exist, beyond which the gage factor would undergo significant changes. For a length-to-width ratio greater than 4 or 5, the gage factor for this design (which is typical) is constant within 0.5 percent. Therefore, a gage of any desired length might be utilized, as long as the length-to-width ratio after shock transit did not decrease below 4 or 5.

The correction factor, η , is plotted in figure 8 to clarify its role in determining gage factor. Note that as a/b decreases, large changes in the value of η result. This is of little consequence since the proper application of η is in determining the initial value of the gage factor. The results of figure 8 clearly indicate a constant gage factor for $a/b \geq 5$ even though η is obviously changing.

c. Comparison of Type I and Type II Gages

To form a basis for a detailed comparison of the Type I and Type II gages, many factors such as desired signal rise time, recording duration, stress and particle velocity, geology, and type and length of cables must be considered. This, however, would be a very involved discussion and beyond the intent of this analysis. Therefore, a simple comparison is made which illustrates how one of the

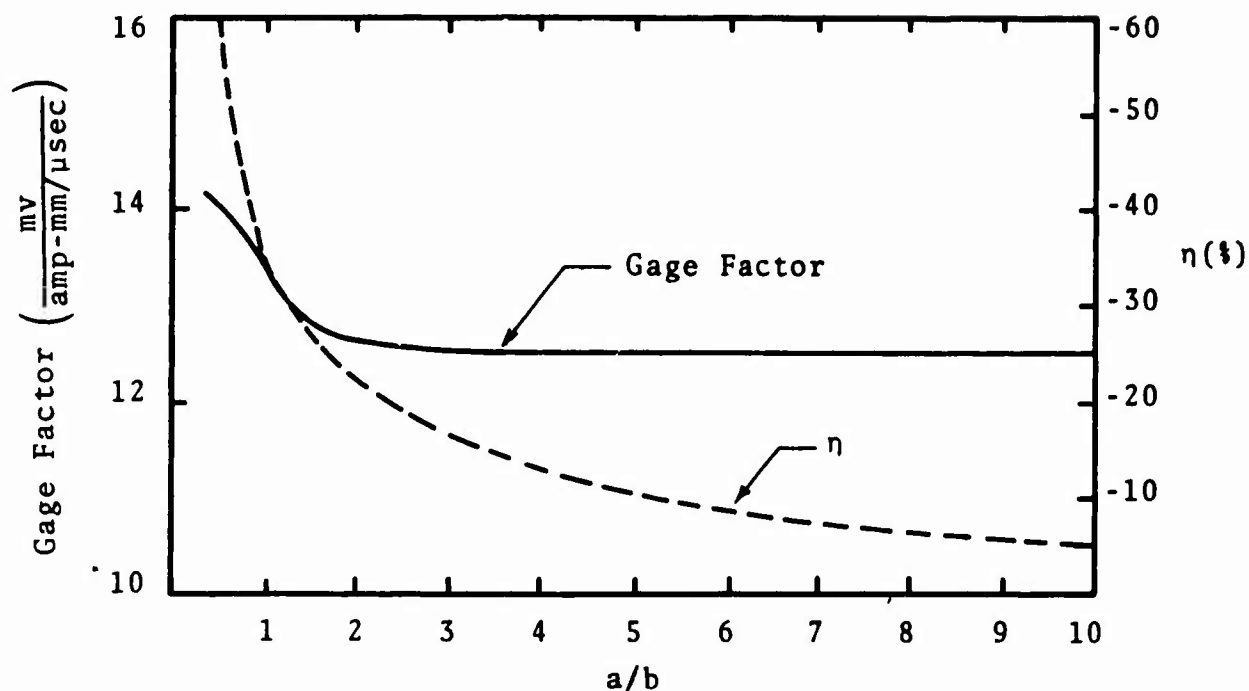


Figure 8. Variation of Gage Factor and η with Gage Length-to-Width Ratio for a Typical Type I Gage Design

designs can be used to advantage. In general, an analysis based upon the requirements of a particular test would be required to identify the most favorable design.

Consider figure 9 where it has been specified that loop set A in the Type II gage is the secondary, and the definitions set forth in figures 4 and 5 apply. Significant increases in gage factor are available with the Type II gage without increasing the number of secondary turns. This is important in that likewise there will be no increase in the secondary self-inductance and thus no increase in electrical rise time. This advantage would be particularly important in improving the rise time performance for gages designed for the low kilobar stress region where a large gage factor, and hence many primary and secondary turns, are required.

4. SUMMARY

Gages of any desired design may be fabricated routinely to within 1 percent of the design gage factor. In the Type II gage

significant increases in gage factor are available without affecting gage rise time. A complete analysis would be required to determine the optimum gage design to meet the requirements of a particular experiment.

Considering only the requirement for a constant gage factor during gage deformation, any length gage may be chosen as long as $a/b \geq 5$ after shock transit.

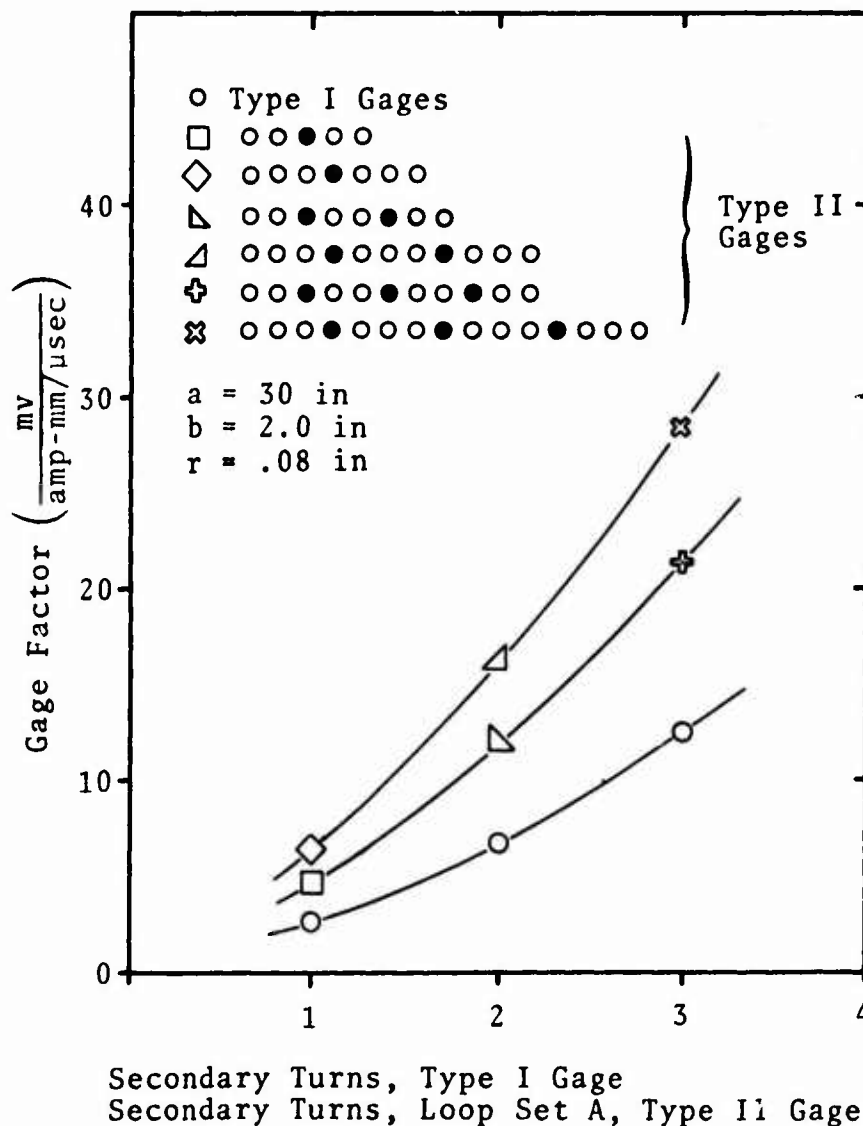


Figure 9. Comparison of Types I and II Gages

SECTION III

OFF-AXIS DIVERGENT FLOW RESPONSE

The theory previously presented in section II was based upon one-dimensional flow along the major axis (x-axis) of the gage. This environment is easily created in laboratory-type experiments utilizing flyer plates or plane wave explosive lenses, and in fact these types of experiments are very useful in comparing the gage experimental and theoretical responses. However, in large-scale TNT or nuclear events, the flow field will likely be oriented off the gage major axis and be spherical in nature. Flow components in the y or z directions will clearly distort the gage geometry and consequently change the gage mutual inductance. The end result is a response which is not totally defined by the one-dimensional, on-axis analysis. To establish the usefulness of the mutual inductance particle velocimeter as a field gage, it is necessary to investigate the sensitivity of the gage to nonideal flow effects.

1. DEVELOPMENT OF COMPUTER MODEL

A simplified gage design, consisting of one primary and one secondary turn, is chosen to reduce the computation time which becomes prohibitive for multiple turn designs. The geometry of the problem is shown in figure 10, where the coordinate system origin is located at the center of the front end of the gage, and the source is located at some selected position (x_s, y_s, z_s) ahead of the gage. A spherical shock front propagates at a velocity c , and behind the shock front the material flows outwardly at a velocity u , along radial lines emanating from the source. Typical values of u and c are chosen to simulate realistic field conditions. A step particle velocity is chosen to investigate the worst case and to simplify the calculations. The conservative relations would not allow an actual step in particle velocity for constant stress loading at the source of the spherical flow. However, where the spherical flow approximates one-dimensional flow (source at a relatively large distance from the gage), this is a good approximation.

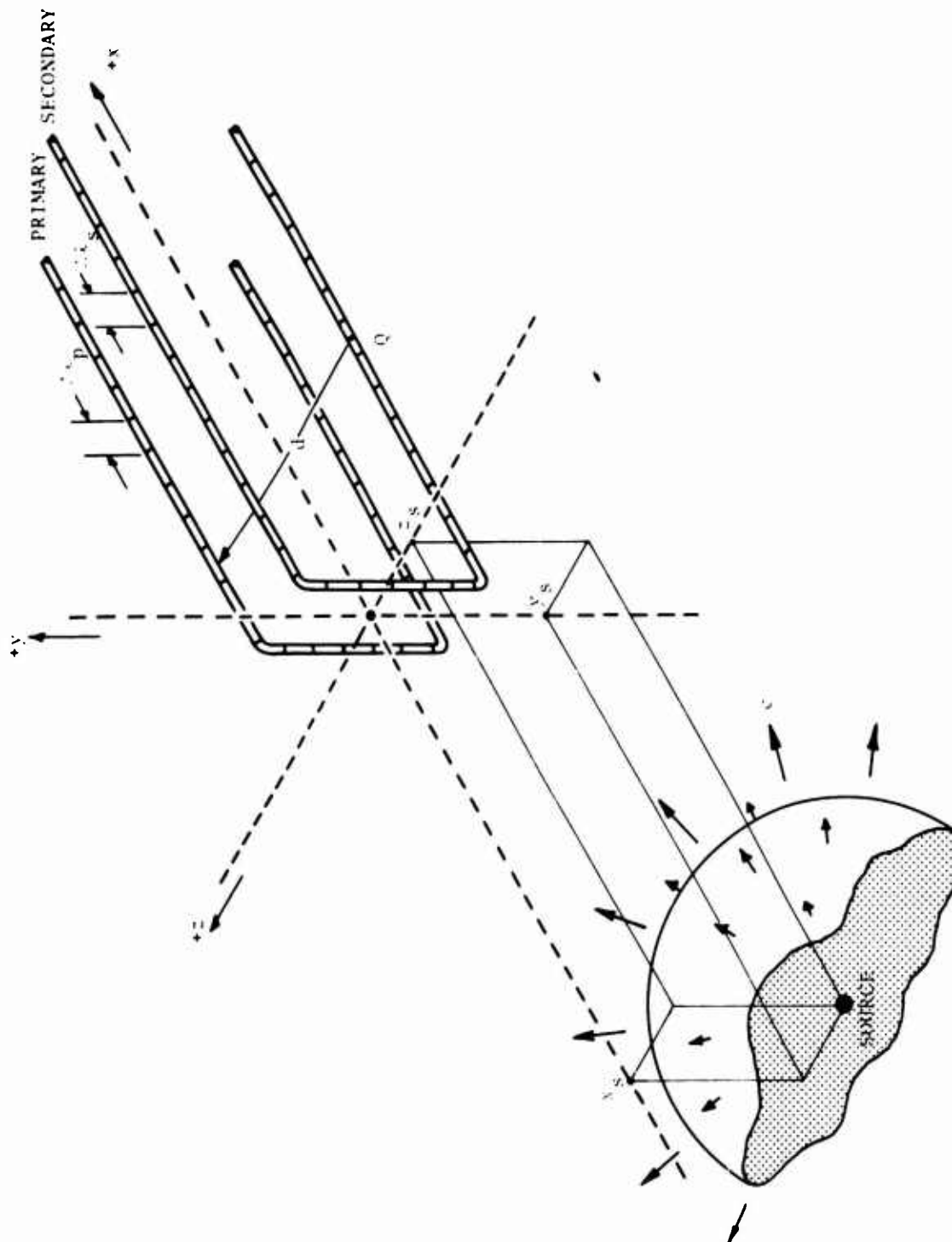


Figure 10. Nomenclature for Development of Divergent/Off-Axis Flow Model of MPV

As shown in figure 10, the gage primary and secondary are divided into small segments. Time is stepped in increments of Δt , and as the shock front propagates through the gage, the segment positions are calculated. At selected intervals, the gage mutual inductance is calculated, resulting in the mutual inductance time history, $M(t)$. By numerically differentiating $M(t)$ with respect to time

$$\dot{M}_t = \frac{M_{t+\Delta t} - M_{t-\Delta t}}{2\Delta t}$$

$\dot{M}(t)$ is determined. $\dot{M}(t)$ is then multiplied by the current (assumed constant) to give the gage output voltage $E(t)$. This output is then compared with the one-dimensional, on-axis response calculated by equation (11).

The mutual inductance is determined at each time increment by first calculating the magnetic vector potential at each segment midpoint on the secondary utilizing the finite difference form of equation (6)

$$\vec{A}|_Q = \frac{\mu_0 I}{4\pi} \sum_{\ell_p} \frac{\Delta \vec{\ell}_p}{r} \quad (23)$$

and then using the relationship

$$M = \frac{1}{I} \sum_{\ell_s} \vec{A} \cdot \Delta \vec{\ell}_s \quad (24)$$

which results from equation (23) and the finite difference form of equation (8).

A computer code, DIVE, was developed to make the calculations. This code is listed in appendix B.

2. SUMMARY OF NUMERICAL RESULTS

Initial numerical investigation of the problem involved selecting time increments and number of primary and secondary segments which would minimize the computation time while providing a reasonable accuracy in the numerical results. M for the real flow model is calculated by placing the source on-axis and at a great distance so that one-dimensional flow is approximated. It is then legitimate to compare the ideal and real flow results for the purpose of determining computational accuracy. The result was a gage consisting of 868 segments for each loop. The difference in the numerically calculated mutual inductance and that determined from equation (12) was approximately 0.008 percent. The difference in the numerically calculated \dot{M} and the ideal \dot{M} was less than 0.2 percent. It is apparent that the errors due to the finite elements are insignificant and may be neglected.

All numerical results are based upon the following gage design and flow environment:

Gage length	-	19.5 inches
Gage width	-	1.5 inches
Loop spacing	-	0.080 inch
Primary turns	-	1
Secondary turns	-	1
Shock velocity	-	4000 meters per second
Particle velocity	-	2000 meters per second

The values of the shock and particle velocities are important here only in their relative magnitudes. A worst case of $c/u = 2$ is selected here, where the case of very high pressure (over 500 Kbar) in geologic materials is approximated. At lower pressures $c/u \approx 3$.

As a first analysis of the real flow effects, it is considered sufficient to investigate only the single gage geometry described above. The expense of expanding the effort to include other geometries is not justifiable, since it is intended here only to show the general effects of the real flow upon a typical gage design.

The effects of divergent flow are shown in figure 11. Here the results are shown as a percentage error in gage response as a function of time. The source is located on the gage centerline in each case. Note that for a source position as close as 1/2 meter, the error in gage output is less than -2 percent and for 5 meters and beyond is less than -0.2 percent. Generally, it may be concluded that for anticipated field flow environments, the error generated due to spherical flow is negligible.

Figures 12 through 16 show the off-axis response of the gage in terms of the output of the gage, normalized by the ideal output. Source radius was located at 5 meters in every case to observe only the off-axis effects. The two major effects are identified clearly in figures 12 and 13.

In figure 12 the angle off in the x-z plane, θ , is held at zero, while the source position is varied by the angle γ in the x-y plane. The obvious effect is an increase in rise time and slight overshoot before returning to essentially a constant level slightly below ideal. For $\gamma \neq 0$, a finite time interval is required for the shock to transverse the front of the gage, and hence the increasing rise time with increasing γ is observed. Further analysis would lead to the intuitive notion that the output of the gage would be reduced in proportion to the angle γ , or simply, to the x component of the particle velocity u_x , where

$$u_x = u \cos \gamma$$

However, this is not the case as seen in figure 17, where the normalized velocity is compared with u_x . It is apparent that there must be some compensating effects to explain the discrepancy. Observe in figure 18 the nature of the gage deformation. Since shock arrival occurs at one side of the gage prior to the other, the gage width is reduced somewhat behind the shock front. The effect is to decrease the mutual inductance with time and hence results in an additional positive output voltage in the gage secondary. The result is that, except for the early time peak, the gage is relatively insensitive to off-axis flow in the x-y plane.

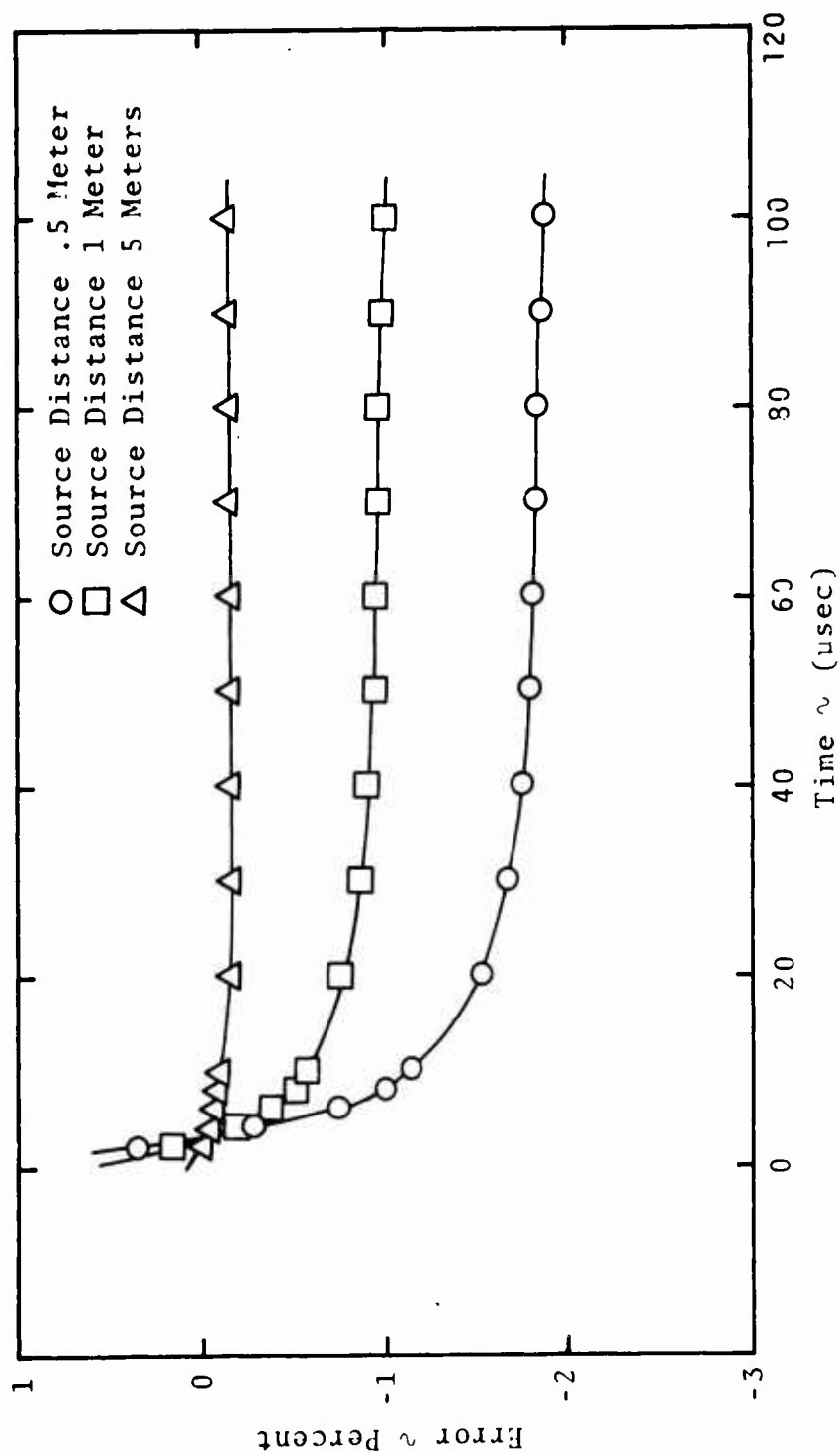


Figure 11. Effects of Divergent Flow upon Gage Response

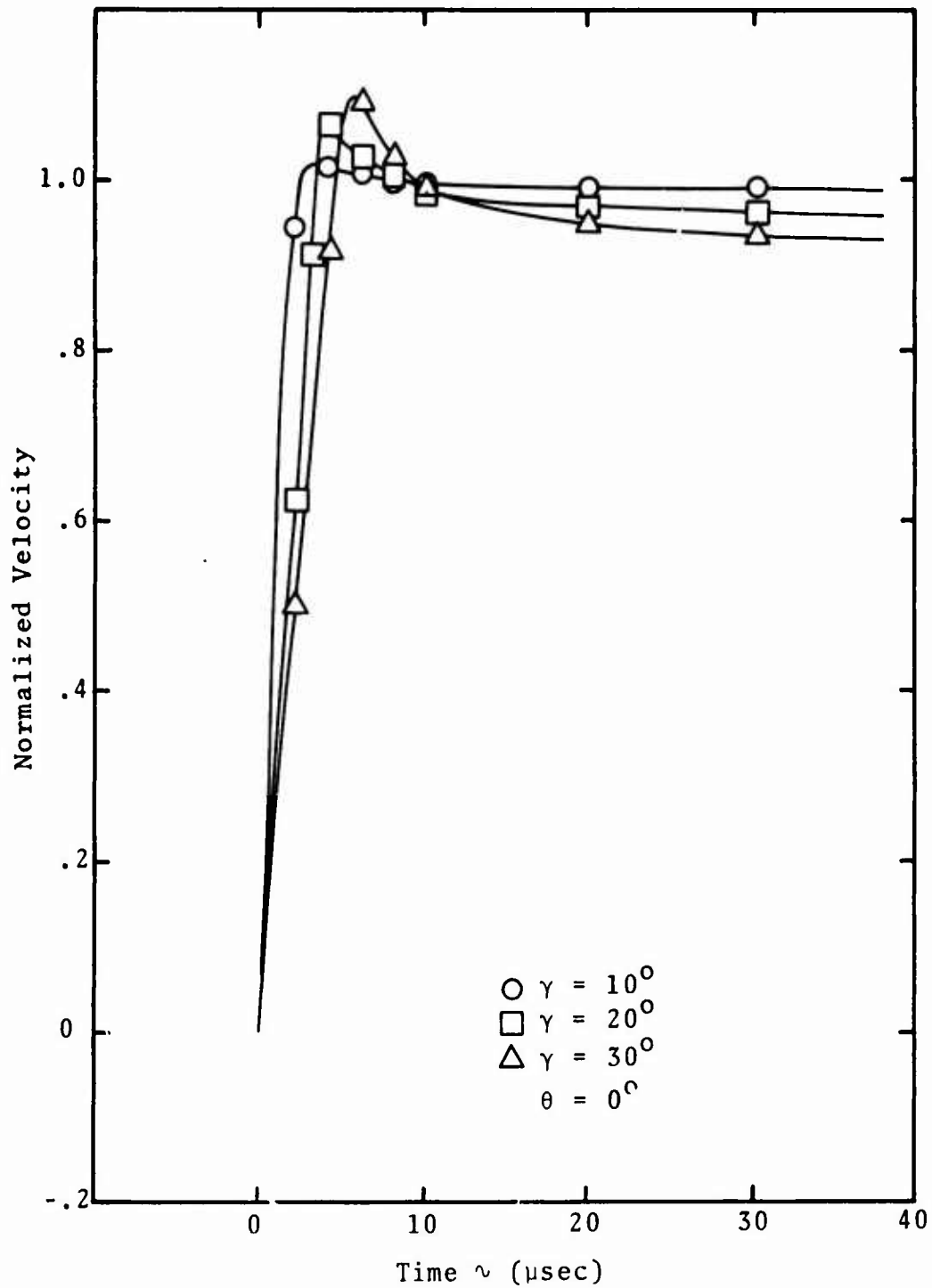


Figure 12. Effects of Off-Axis Flow upon Gage Response

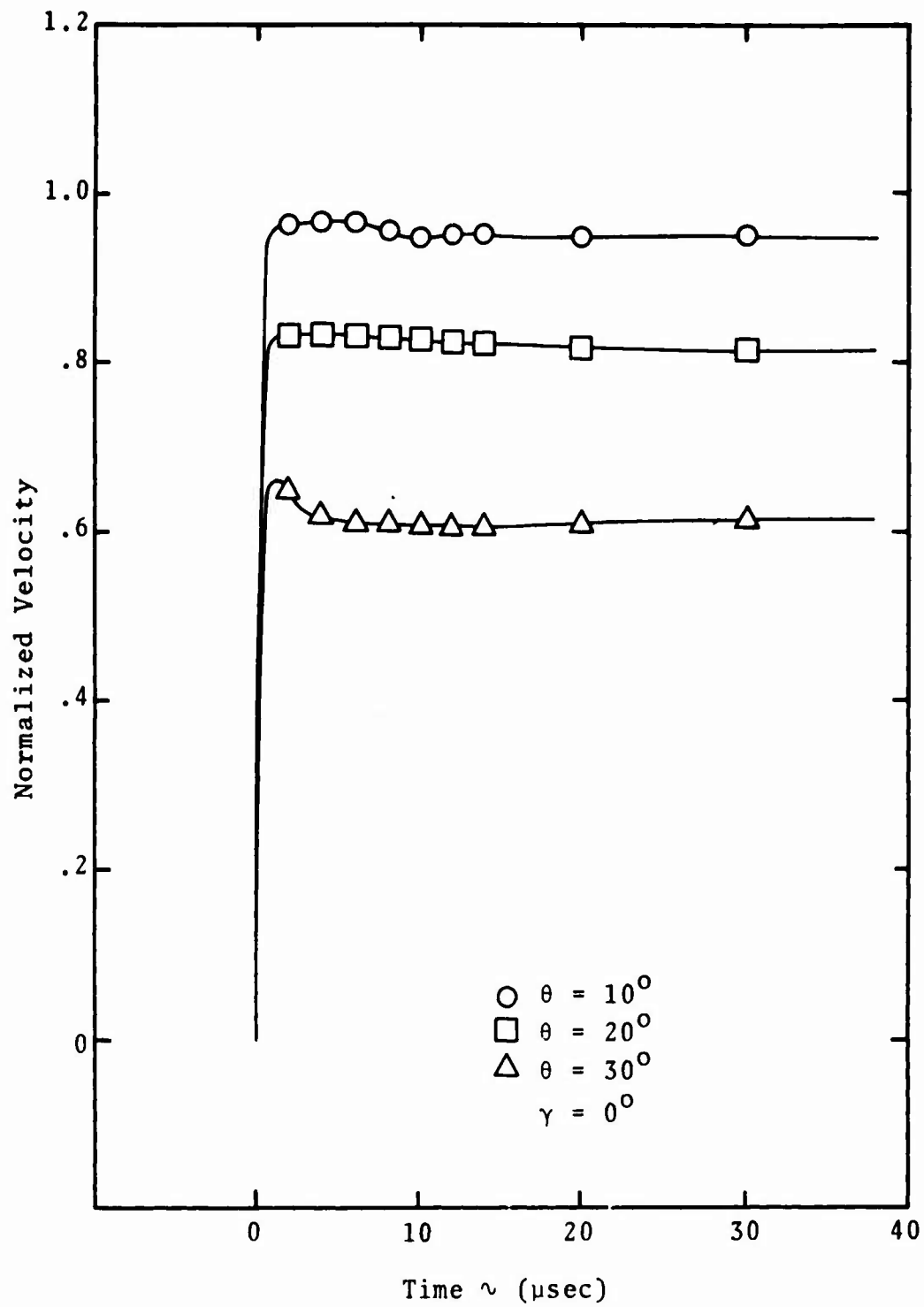


Figure 13. Effects of Off-Axis Flow upon Gage Response

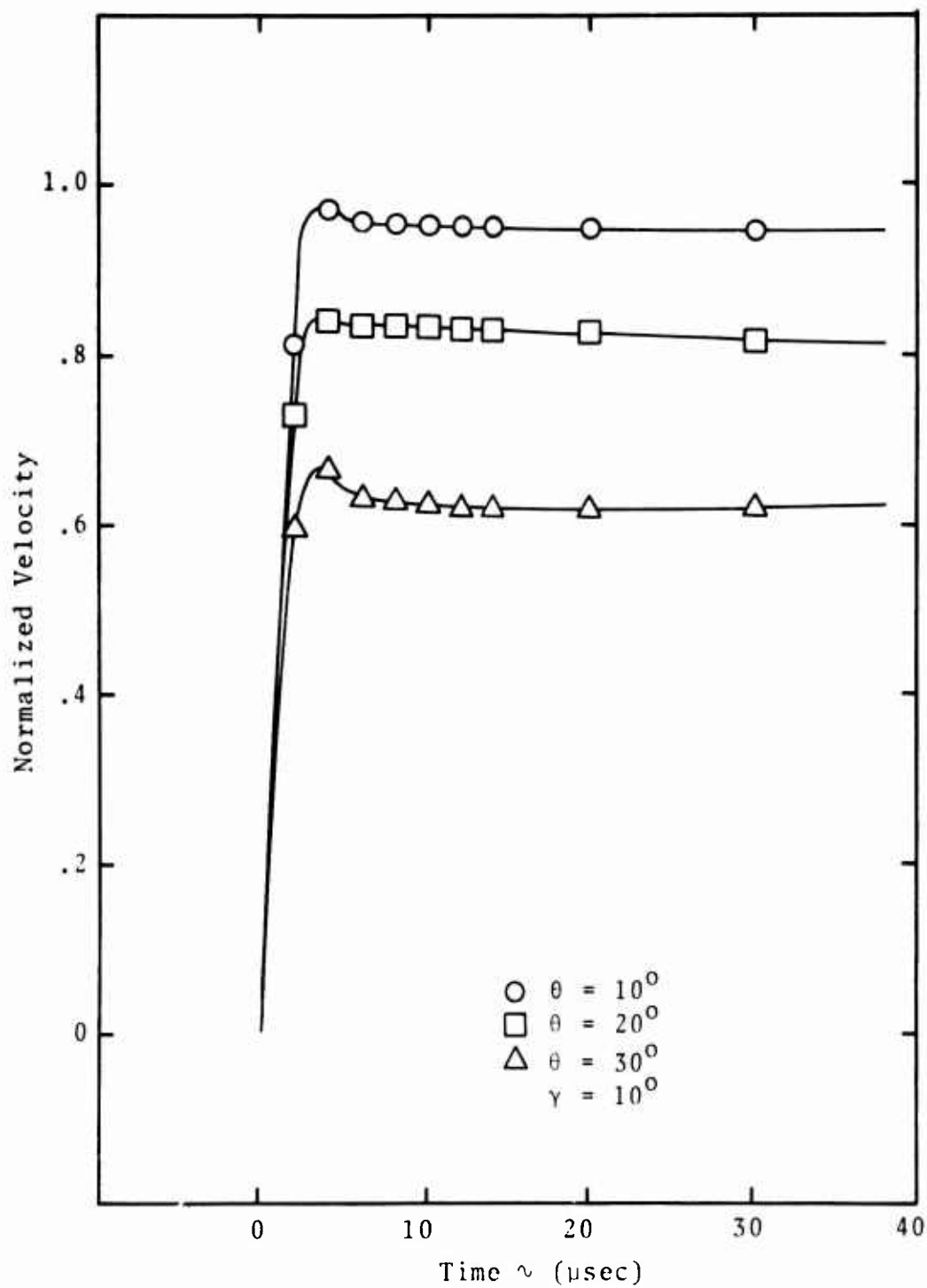


Figure 14. Effects of Off-Axis Flow upon Gage Response

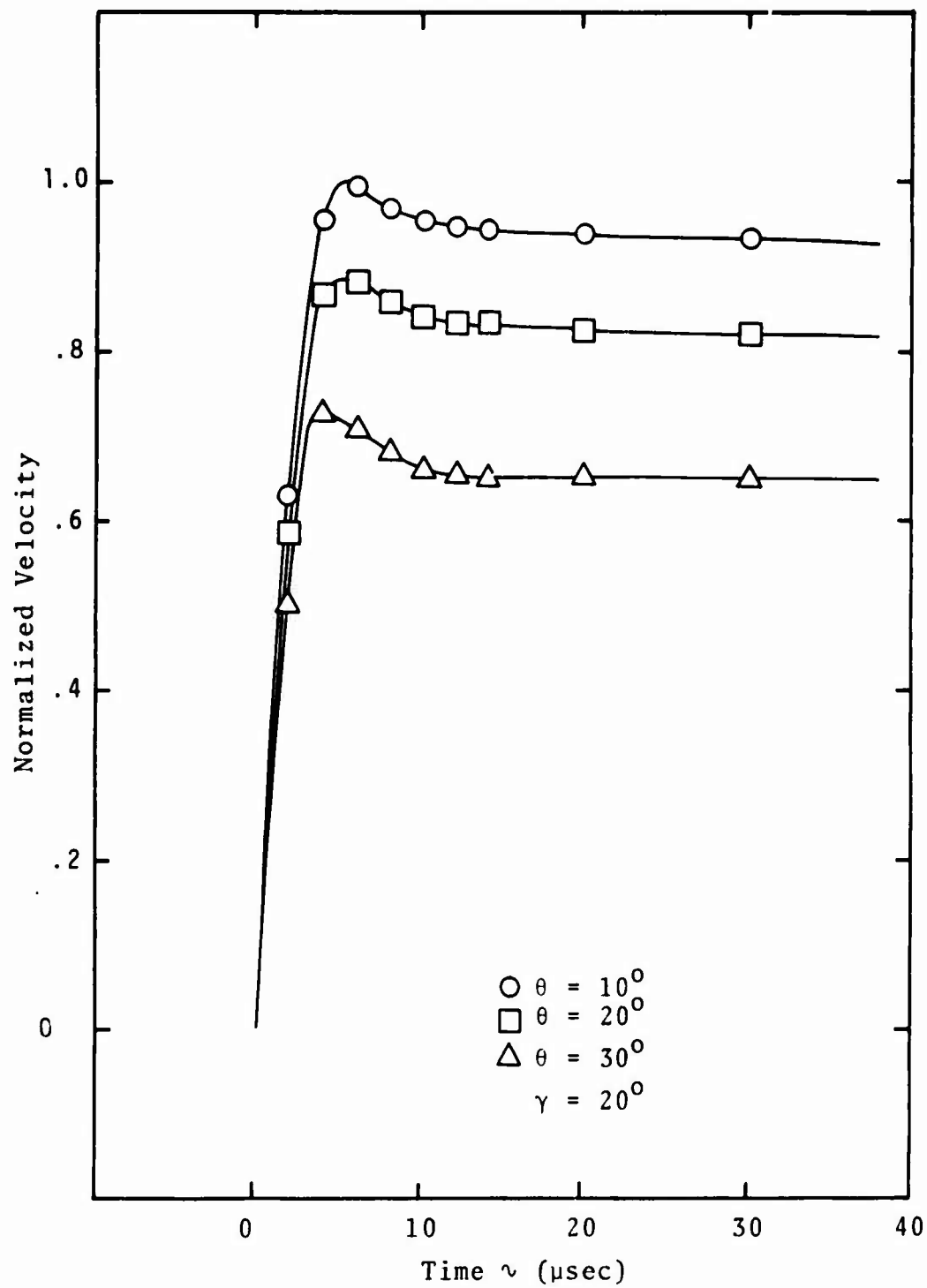


Figure 15. Effects of Off-Axis Flow upon Gage Response

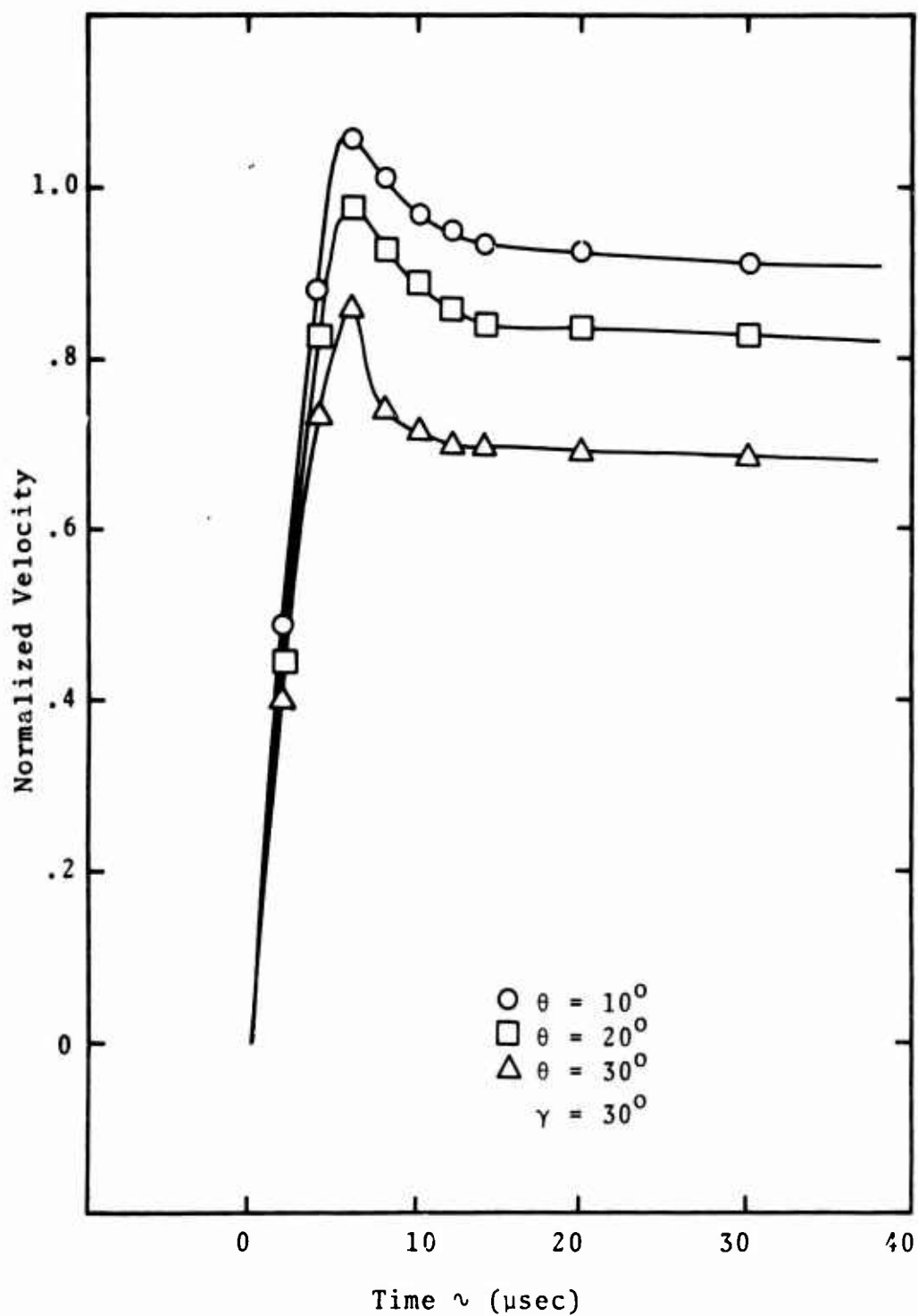


Figure 16. Effects of Off-Axis Flow upon Gage Response

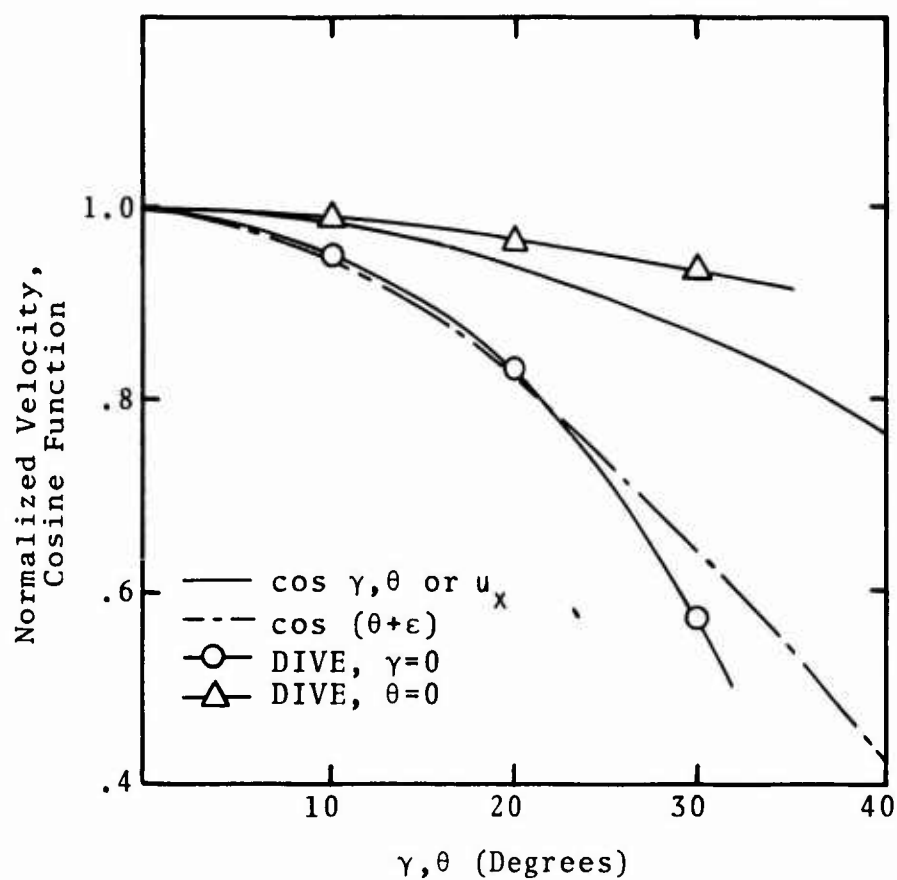
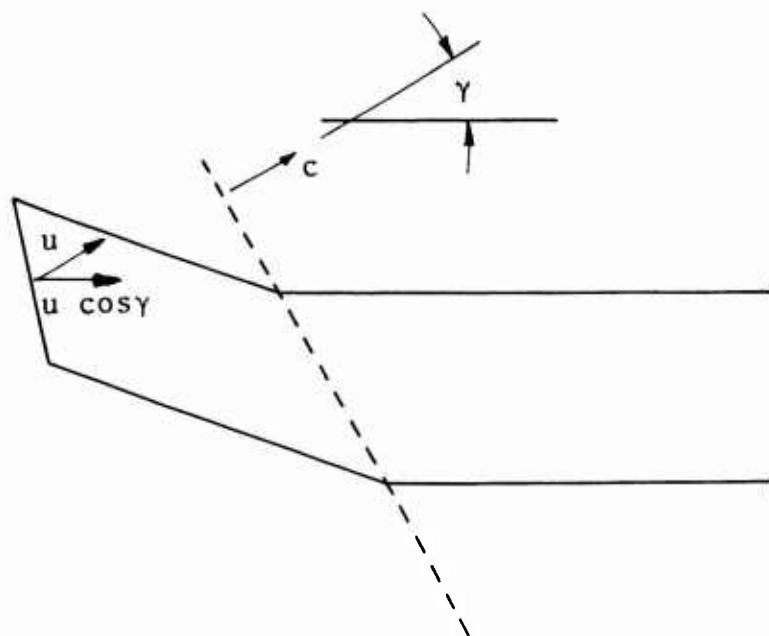


Figure 17. Comparisons of DIVE Calculations with Cosine Function

Figure 13. Gage Undergoing Deformation for Off-Axis Shock, $\theta=0$, $\gamma \neq 0$

In figure 13 the shock propagation is off-axis by the angle θ in the x - z plane, while $\gamma = 0$. The gage rise time is relatively unaffected, while the level is significantly influenced. It must be pointed out that for multiple primary and secondary turns, the z dimension will be much greater, and hence, the rise time would also be increased.

Comparing the gage response with u_x in figure 17, an error in gage response much greater than anticipated is observed. This is explained by considering figure 19. Note that as the gage deforms, its orientation relative to the shock front propagation direction changes so that the effective component of u down the deflected gage axis is not $u \cos \theta$ but rather $u \cos (\theta + \epsilon)$. In figure 17 $\cos (\theta + \epsilon)$ has been plotted, and we see that it conforms fairly well with the actual gage response, especially for $\theta \leq 20$ degrees. The angle ϵ is obviously a function of the ratio of c/u , therefore, as c/u increases, ϵ would, for a given θ , decrease. Again, for $c/u = 2$, the worst case results.

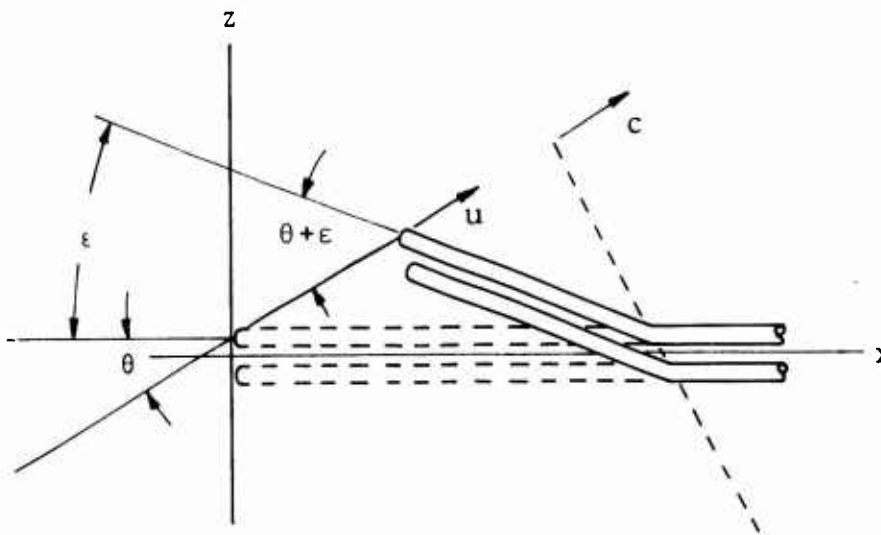


Figure 19. Gage Undergoing Deformation for Off-Axis Shock, $\gamma=0$, $\theta \neq 0$

The intention of figures 17, 18, and 19 and the related discussion is to attempt a logical explanation of the numerical results and provide an improved intuitive feeling for the gage response. The remaining data in figures 14, 15, and 16 show the gage response for various combinations of θ and γ . As might be expected, it is observed that the effects portrayed in figures 12 and 13 combine to provide the results of figures 14, 15, and 16.

3. SUMMARY

The results of the numerical investigation of the off-axis/divergent flow response are summarized as follows:

a. For anticipated field flow environments, the error generated due to spherical flow is negligible.

b. The gage is relatively insensitive to off-axis flow in the x-y plane, the error induced being approximately equal to $1/2 (1 - \cos \gamma)$. However, off-axis flow in the x-z plane results in much larger errors approximately equal to $3 (1 - \cos \theta)$. An immediate result is that if in a field test there is a plane in which the uncertainty in shock propagation direction is a maximum, then the preferred orientation of the gage is with the x-y plane aligned with the plane of uncertainty.

SECTION IV

ELECTROMECHANICAL MODELING

The development in section II leading to equation (11), the expression for the gage output voltage, was based upon the assumptions that the media and gage flow were ideal, i.e., one-dimensional and aligned with the gage major axis and that no electrical parameters other than the gage mutual inductance were changing. The nonideal flow effects were investigated in section III. In this section the effects of nonideal electrical behavior are treated.

It is obvious that as the gage shortens, the primary and secondary self-inductances will decrease. Also, the gage resistance will change due to the very high stress behind the shock front. These effects are totally ignored in the analysis of section II and must be considered separately. The approach is to evaluate the effects of changes in self-inductance and resistance on gage response and, by proper circuit design, control the effects so that equation (11) adequately describes the gage response.

1. PREVIOUS WORK

The Engineering Physics Company, during their development program, performed a detailed analysis of the error generated in the gage output by changes in self-inductance and resistance in the gage primary (ref. 10). A closed form solution was obtained for a model utilizing a voltage source as the power supply. The solution was developed by linearizing the differential equations, neglecting self-inductance and resistance changes in the secondary, and making other simplifications.

An analysis was performed (ref. 16) that used a simplified voltage source model, linearized equations, and neglected resistance changes in the gage. This is an adequate model for applications in the low Kbar stress region.

Neither of these analyses were considered completely adequate for application in the very high-pressure region because of the

approximations used. A more detailed model was required that would consider inductance and resistance changes in the primary and secondary. Additionally, it was desirable to incorporate a capacitive discharge power supply in the model.

2. ELECTROMECHANICAL MODEL

A simplified schematic of the power supply and gage, assuming an open secondary, is shown in figure 20. The elements L_0 and R_0 are controllable parameters used to minimize the undesired effects of changes in self-inductance and resistance in the gage loops. The basic problem is to determine the proper values for L_0 and R_0 for a given gage design under some specified test conditions. The circuit in figure 20 is described by a set of nonlinear differential equations with time-varying coefficients which are not amenable to closed form solution by conventional methods.

a. Approach

The approach taken in obtaining a solution is to determine a set of first order differential equations in the normal form (state variable equations) that will describe the electrical model. Given initial conditions, these equations may then be solved to obtain numerical results. Due to the ease with which more complex models may be handled by this method, it is possible to utilize a detailed model of the gage that introduces as few assumptions as practical.

The electrical network that models the system is shown in figure 21. Elements 2, 6, 12, and 13 represent the power supply; elements 1, 10, and 11 represent the primary cable capacitance, control resistance, and inductance; the gage consists of elements 5, 9, 4, and 8; and elements 7 and 3 represent the secondary line cable capacitance and termination resistance. In the network, it is assumed that the distributed parameters may be lumped. It now remains to determine the appropriate mathematical model that describes the network.

b. State Variable Equations

Stern (ref. 19) describes the procedures for applying the linear graph and electrical network theory of Seshu and Reed (ref.

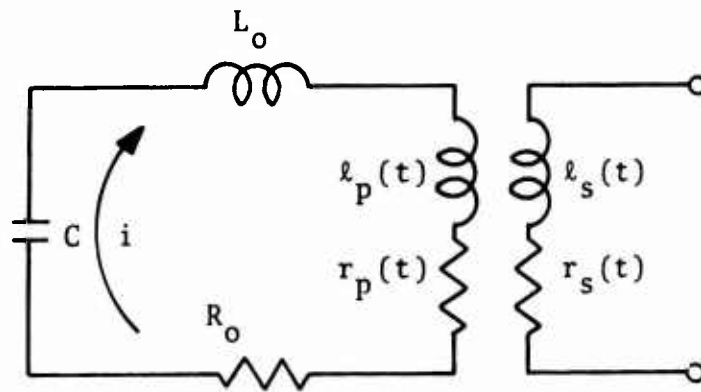


Figure 20. Simplified Schematic of Power Supply and Velocity Gage with Open Secondary

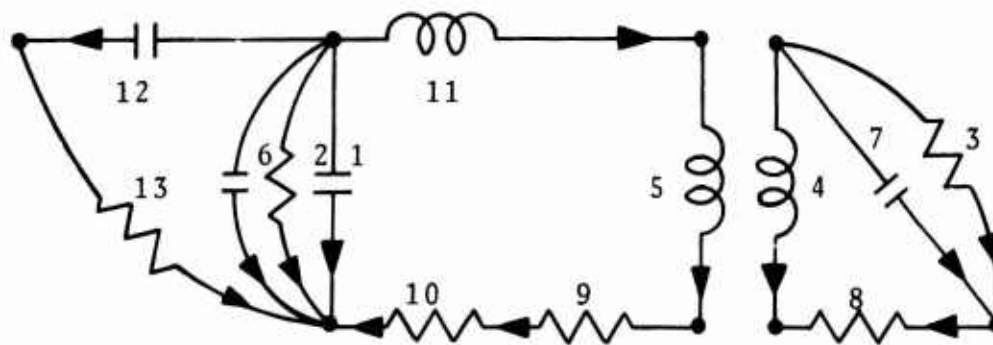


Figure 21. Electrical Network of Velocity Measuring System

20) to determine the linearly independent loop and node equations, equations (23) through (35), which mathematically describe the network. A graph of the network is shown in figure 22. The equations are based upon the choice of the sign convention shown in figure 21 and the tree of the graph shown in figure 22.

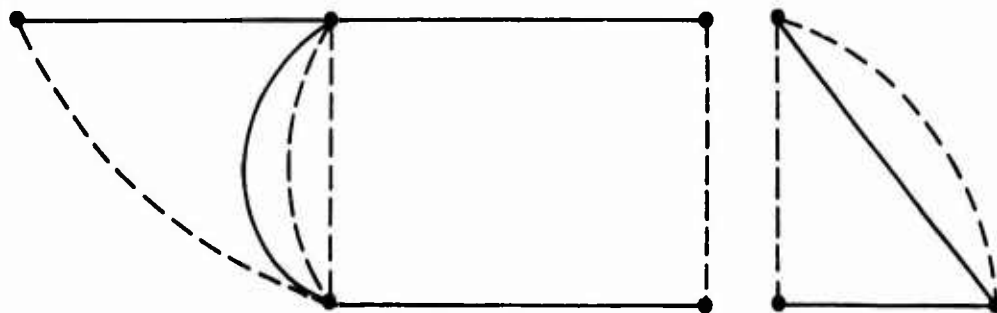


Figure 22. Graph of Network Shown in Figure 21, Tree Indicated by Solid Lines, Branches by Dashed Lines

$$e_1 = e_6 \quad (23)$$

$$e_2 = e_6 \quad (24)$$

$$e_3 = e_7 \quad (25)$$

$$e_{13} = e_6 - e_{12} \quad (26)$$

$$e_4 = e_7 + e_8 \quad (27)$$

$$e_5 = e_6 - e_9 - e_{10} - e_{11} \quad (28)$$

$$i_6 = -i_1 - i_2 - i_{13} - i_5 \quad (29)$$

$$i_7 = -i_3 - i_4 \quad (30)$$

$$i_{12} = i_{13} \quad (31)$$

$$i_8 = -i_4 \quad (32)$$

$$i_9 = i_5 \quad (33)$$

$$i_{10} = i_5 \quad (34)$$

$$i_{11} = i_5 \quad (35)$$

The tree branch charges, q_6 , q_7 , and q_{12} , and chord flux linkages, λ_4 and λ_5 , are chosen as state variables. By applying the basic relations

$$\begin{aligned} q &= Ce, & \dot{q} &= i, \\ \lambda &= Li, & \dot{\lambda} &= e, \\ e &= iR, \end{aligned}$$

to equations (27) through (31), expressions for the state variables may be obtained resulting in

$$\dot{\lambda}_4 = e_7 + e_8 \quad (36)$$

$$\dot{\lambda}_5 = e_6 - e_9 - e_{10} - e_{11} \quad (37)$$

$$\dot{q}_6 = -i_1 - i_2 - i_{13} - i_5 \quad (38)$$

$$\dot{q}_7 = -i_3 - i_4 \quad (39)$$

$$\dot{q}_{12} = i_{12} - i_{13} \quad (40)$$

The basic relations are then applied throughout, except for elements 4 and 5 where the coupling relations

$$\lambda_4 = L_4 i_4 + M i_5$$

$$\lambda_5 = L_5 i_5 + M i_4$$

apply in reducing the state variable equations to the form

$$\dot{x} = f(x, t)$$

The resulting equations are

$$\dot{\lambda}_4 = \frac{q_7}{C_7} - \frac{R}{D} \left[L_5 \lambda_4 - M \lambda_5 \right] \quad (41)$$

$$\begin{aligned} \dot{\lambda}_5 = & \left[\frac{D}{D + L_{11} L_4} \right] \left[\frac{q_6}{C_6} - \left(\frac{R_9 + R_{10}}{D} \right) (L_4 \lambda_5 - M \lambda_4) \right. \\ & \left. - \frac{L_{11}}{D} (\lambda_5 \dot{L}_4 - M \dot{\lambda}_4 - \lambda_4 \dot{M}) - \frac{L_{11} \dot{D}}{D^2} (M \lambda_4 - L_4 \lambda_5) \right] \end{aligned} \quad (42)$$

$$\begin{aligned} \dot{q}_6 = & - \left[\frac{C_6}{C_6 + C_1} \right] \left[\frac{q_6}{C_6 R_2} + \frac{1}{R_{13}} \left(\frac{q_6}{C_6} - \frac{q_{12}}{C_{12}} \right) \right. \\ & \left. + \frac{1}{D} (L_4 \lambda_5 - M \lambda_4) \right] \end{aligned} \quad (43)$$

$$\dot{q}_7 = - \frac{q_7}{R C_7} - \frac{1}{D} (L_5 \lambda_4 - M \lambda_5) \quad (44)$$

$$\dot{q}_{12} = \frac{1}{R_{13}} \left(\frac{q_6}{C_6} - \frac{q_{12}}{C_{12}} \right) \quad (45)$$

where

$$D = L_4 L_5 - M^2$$

$$\dot{D} = L_4 \dot{L}_5 + L_5 \dot{L}_4 - 2M\dot{M}$$

c. Time-Varying Parameters

Note that the state variable equations are functions of the time-varying circuit elements L_4 , L_5 , R_4 , and R_5 and also \dot{L}_4 and \dot{L}_5 . To proceed with a solution, expressions must be obtained for each of these variables. An analysis of the physical model is necessary to determine these relationships.

A step stress and particle velocity and constant shock velocity are assumed for the physical input parameters. Figure 23 depicts the gage deformation, Δa , as a result of the particle velocity, u .

For typical gage designs, where the length is greater than five times the width, the self-inductance is essentially proportional to the length, and the inductance-per-unit-length is independent of gage length. Therefore, the self-inductance may be expressed as

$$L = L_0 \left(1 + \Delta a/a_0 \right), \quad \Delta a < 0 \quad (46)$$

where L_0 is the initial self-inductance, and a_0 is the initial gage length. L_0 is calculated by extrapolation of the data of reference 21 or by measurements on actual gages.

Differentiating equation (46) with respect to time gives

$$\dot{L} = L_0 \left[\dot{a}/a_0 \right] = -u \left[L_0/a_0 \right] \quad (47)$$

which is seen to be constant for a step velocity input.

The expression for resistance variations may be determined by considering the portion of the gage behind the shock exposed to high stress and the resistance change that is associated with that stress level. The situation is described in figure 24, where no consideration is given to gage deformation. For an initial undisturbed gage resistance of R_0 , length a , and width b , the resistance per unit length is

$$R_0/2(a + b)$$

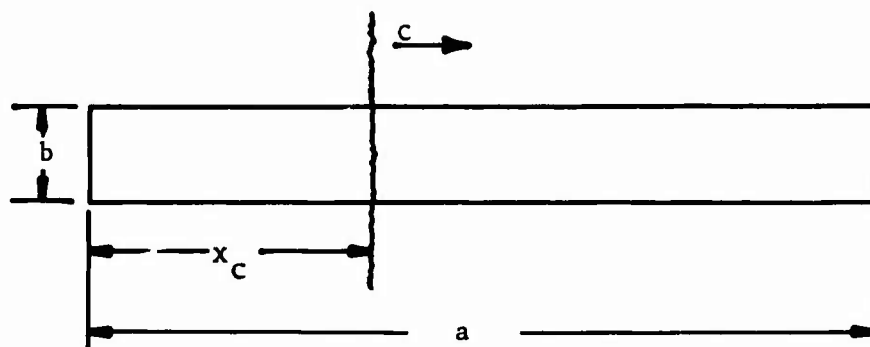


Figure 23. MIPV Undergoing Shock Deformation and Nomenclature for Determining $L(t)$ and $\dot{L}(t)$

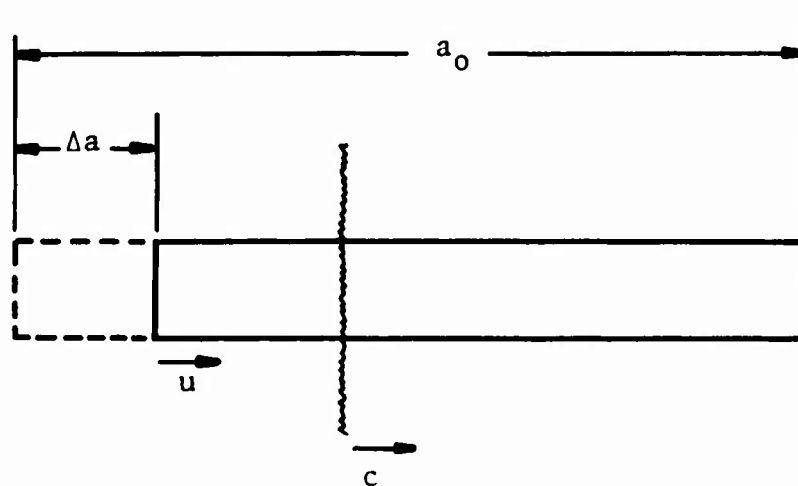


Figure 24. Nomenclature for Determining Gage $R(t)$

The length of the shocked portion of the gage is

$$b + 2 x_c$$

where x_c is the shock position relative to the position of the front of the gage prior to shock arrival. The remaining length is

$$b + 2 (a - x_c)$$

By assuming that behind the shock the gage resistance is changed by a factor K , the expression for the total gage resistance is seen to be

$$R = \frac{R_o}{2(a + b)} \left[b + 2(a - x_c) + K(b + 2 x_c) \right] \quad (48)$$

Equations (47) and (48) apply to both the primary and secondary loops in the gage.

Appendix C presents a study of various conductor materials as applied in the MIPV. Included in this study is information on the variation of resistance with stress level.

3. NUMERICAL RESULTS

Computer calculations were made to investigate this problem on an AFWL CDC 6600 utilizing a modified Rung-Kutta-Gill/Adams-Moulton method variable step size integration routine (ELMEK, appendix D). First, the program was run to simulate power supply turn-on and allow sufficient time for the transients induced in the gage secondary to decay. The shock was numerically positioned well away from the gage so that only the turn-on effects were present. Then the final conditions were input as initial conditions and runs made to observe the gage response to the shock.

The equations were found to be quite sensitive around the turn-on initial conditions, with the automatic step size feature converging to less than 10-nanosecond steps during start-up. A constant step size of 5 nanoseconds was selected and utilized for all subsequent calculations.

Because of the extremely wide range of stress and particle velocity environments in which the MIPV may be used and the different designs available, there are numerous test conditions which justify numerical investigation. Examples are

- Large-scale HE tests (such as MIXED COMPANY) with field-size gages (typically 2 inches wide by 30 to 40 inches long, 4 primary turns and 3 secondary turns) exposed to the 50- to 150-Kbar stress region.
- Large-scale HE tests, free-field measurements in stress region below 5 Kbar, field-size gages (same as above but with 10 primary and 9 secondary turns).
- High-pressure evaluation experiments (explosively driven flyer or gas gun) in 0.2- to 1.0-Mbar stress region with scaled gages (0.4 inch wide by 3 inches long, 3 primary and 2 secondary turns).
- Underground nuclear test, field-size gage in 0.2- to 2.0-Mbar stress region.

The two most severe conditions would be those in the megabar stress region--the high-pressure evaluation experiments and the underground nuclear test. These two conditions will be investigated and numerical results presented. Other test conditions may be investigated as the need arises.

a. High-Pressure Evaluation Experiments

The MIPV was evaluated in May and June 1974 on the Von Karman Gas Dynamics Facility Range G, two-stage light gas gun (ref. 22), located at Arnold Engineering Development Center (AEDC) near Tullahoma, Tennessee.

Two basic gage designs were evaluated at AEDC. The first consisted of 0.020-inch aluminum wires embedded in aluminum-oxide-loaded acrylic, as shown in figure 1. The second design, shown in figure 25, consisted of 0.020-inch titanium wires in 0.064-inch OD by 0.024-inch ID borosilicate glass tubing backfilled with C-7 epoxy resin. Titanium was utilized with the glass because it would

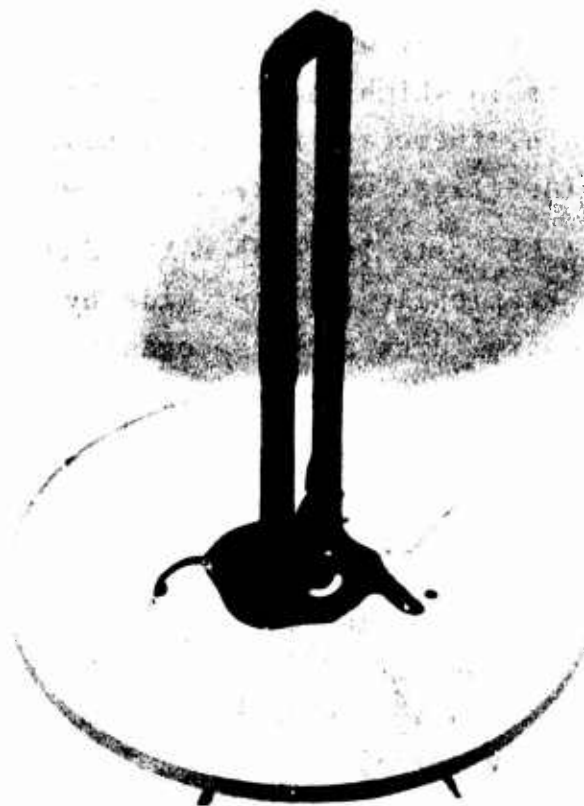


Figure 25. Glass Gage

better withstand the temperatures required for the glass forming. Both the aluminum and titanium wire designs were investigated but only the titanium gage will be discussed here since, as shown in appendix C, it presents a more severe perturbation to the gage response. The problem is further complicated by the fact that titanium, as a transition metal, undergoes an increase in electrical resistivity by a factor of 2 at high pressure. This condition must also be considered.

In preparing for the tests at AEDC an extensive investigation of the nonideal electrical behavior of the gage was made. Details of the gage design investigated which approximates the AEDC design are

Length	6.0 inches
Width	0.4 inch
Spacing between turns	0.050 inch

Primary turns	3
Secondary turns	2
Conductor material	0.020 titanium
Insulator	Borosilicate glass

This design resulted in the following electrical parameters:

$$\begin{aligned}
 R_{\text{pri}} &= 2.017 \text{ ohms} \\
 L_{\text{pri}} &= 1.68 \text{ } \mu\text{h} \\
 R_{\text{sec}} &= 1.345 \text{ ohms} \\
 L_{\text{sec}} &= 0.933 \text{ } \mu\text{h} \\
 M &= 0.655 \text{ } \mu\text{h} \\
 GF &= 4.179 \text{ mv/(amp mm/} \mu\text{sec)}
 \end{aligned}$$

The shock environment selected was

$$\begin{aligned}
 c &= 9.7 \text{ mm/} \mu\text{sec} \\
 u &= 5.25 \text{ mm/} \mu\text{sec} \\
 \sigma &= 1 \text{ Mbar} \\
 K &= 0.4/2.0
 \end{aligned}$$

The investigation was accomplished in two phases. In addition to determining suitable control parameters for this particular gage design and shock environment, there was a requirement to verify the code behavior, gain an understanding of how the nonideal electrical behavior affects the MIPV response, and determine the most effective means of controlling the induced errors.

In the first phase, several values of ballast inductance, L_{11} , and ballast resistance, R_{10} , were selected to observe their effect upon the shock-induced errors.

In the second phase, conditions were set up to observe the response for some extreme values of the control parameters while restricting the code to the following calculational modes:

- (1) Normal--inductance and resistance changes are permitted
- (2) Inductance changes only
- (3) Resistance changes only
- (4) No changes in inductance or resistance

Figures 26 and 27 show the effects of varying R_{10} and L_{11} upon gage response. For $K < 1$, the induced errors are negative; for $K > 1$, the induced errors are positive. The ballast inductance appears to have a strong effect in controlling the magnitude of the error while the ballast resistance has a relatively minor effect. The implication is that the errors can be adequately controlled solely with the ballast inductance. This result, which will be verified, is significant in that the amount of primary resistance has a direct effect upon the magnitude of the current in the primary and hence directly affects the gage sensitivity.

Now, it is of interest to determine the manner in which the errors are generated in the gage and verify the calculations of ELMEK.

Consider figure 28 where only inductance changes are permitted. Where no ballast inductance is provided, the rise time response is affected, but no error results in the magnitude. Where ballast inductance is included, the response is identical with the ideal response within the normal rise time capabilities of the system, regardless of whether or not there is ballast resistance.

In figure 29 only resistance changes are permitted. It will suffice to discuss the results for either of the values of the resistance change factor, K , since qualitatively the effects of one are, in a sense, reflected about the normalized voltage value of 1. Consider the case for $K = 0.4$ where the induced errors are negative. The first observation is that in no case is rise time degraded. Considering the result of the previous discussion of figure 28, it may then be concluded that the primary effect of self-inductance changes in the gage is to degrade the rise time of the gage output and that the ballast inductance is very effective in controlling this degradation.

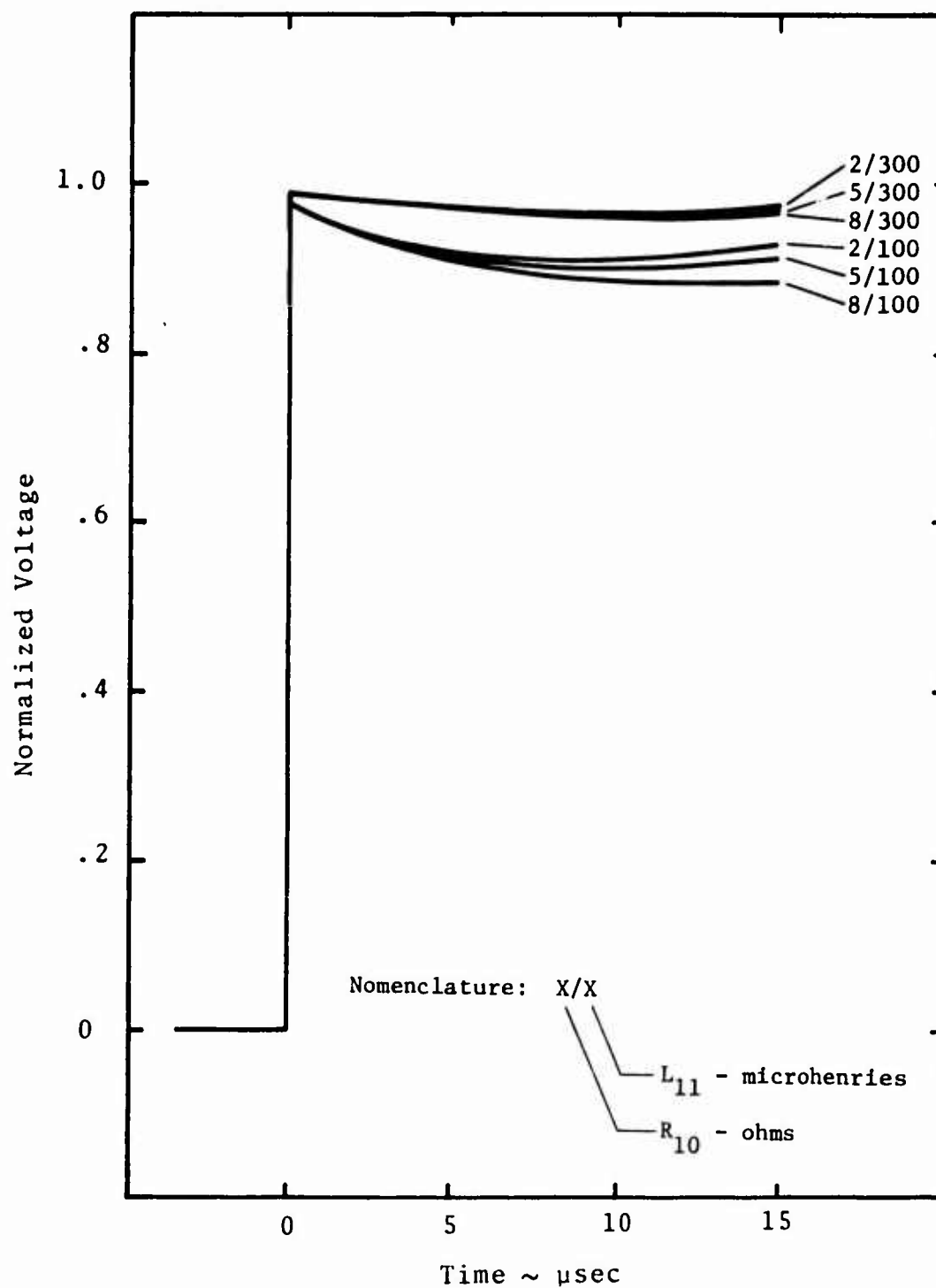


Figure 26. Shock Response of AEDC Gage as Calculated by ELMEK, $K = .4$

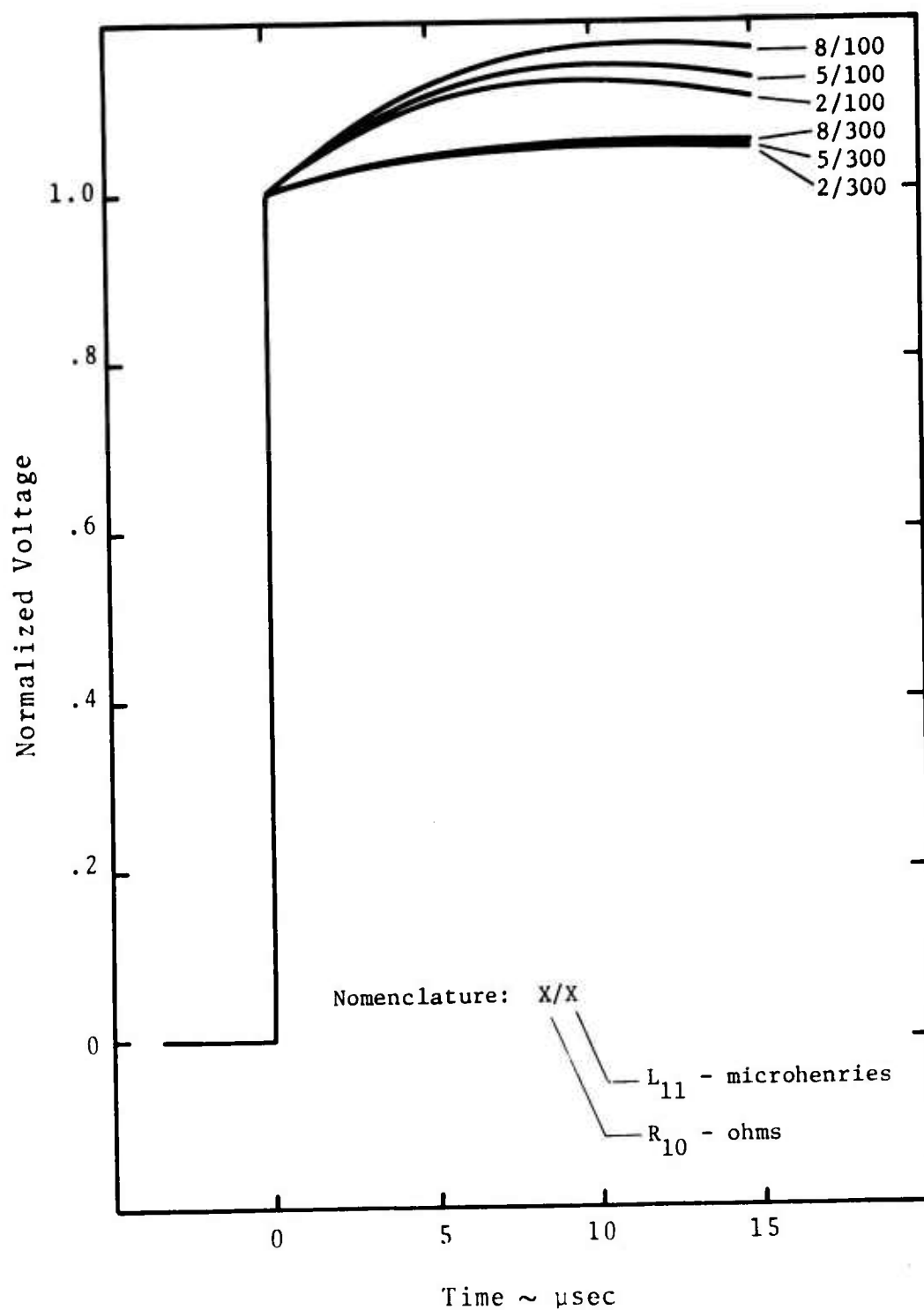


Figure 27. Shock Response of AEDC Gage as Calculated by ELMEK, $K = 2$

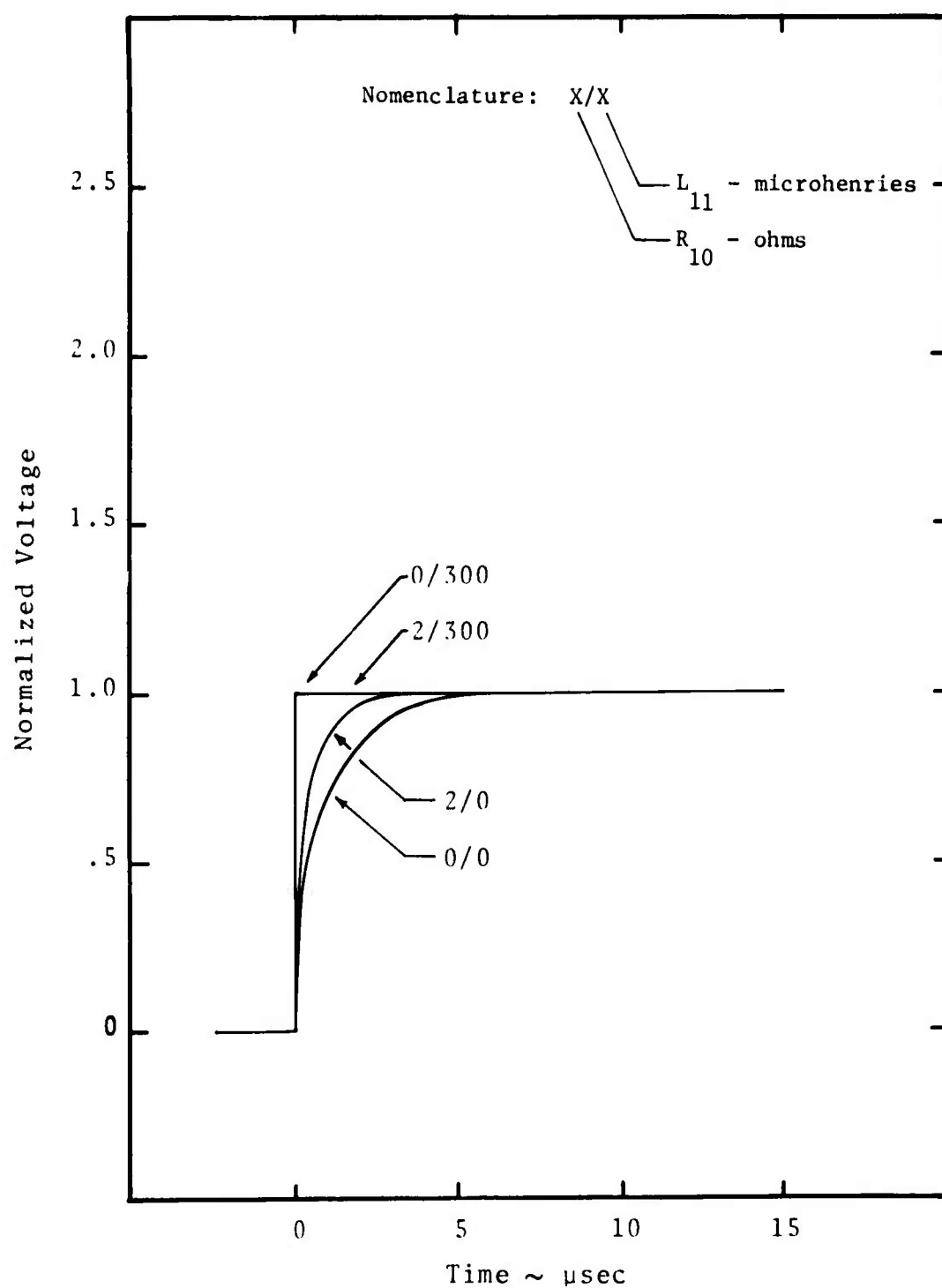


Figure 28. Calculated Gage Response Using ELMEK, Inductance Changes Only, AEDC Gage

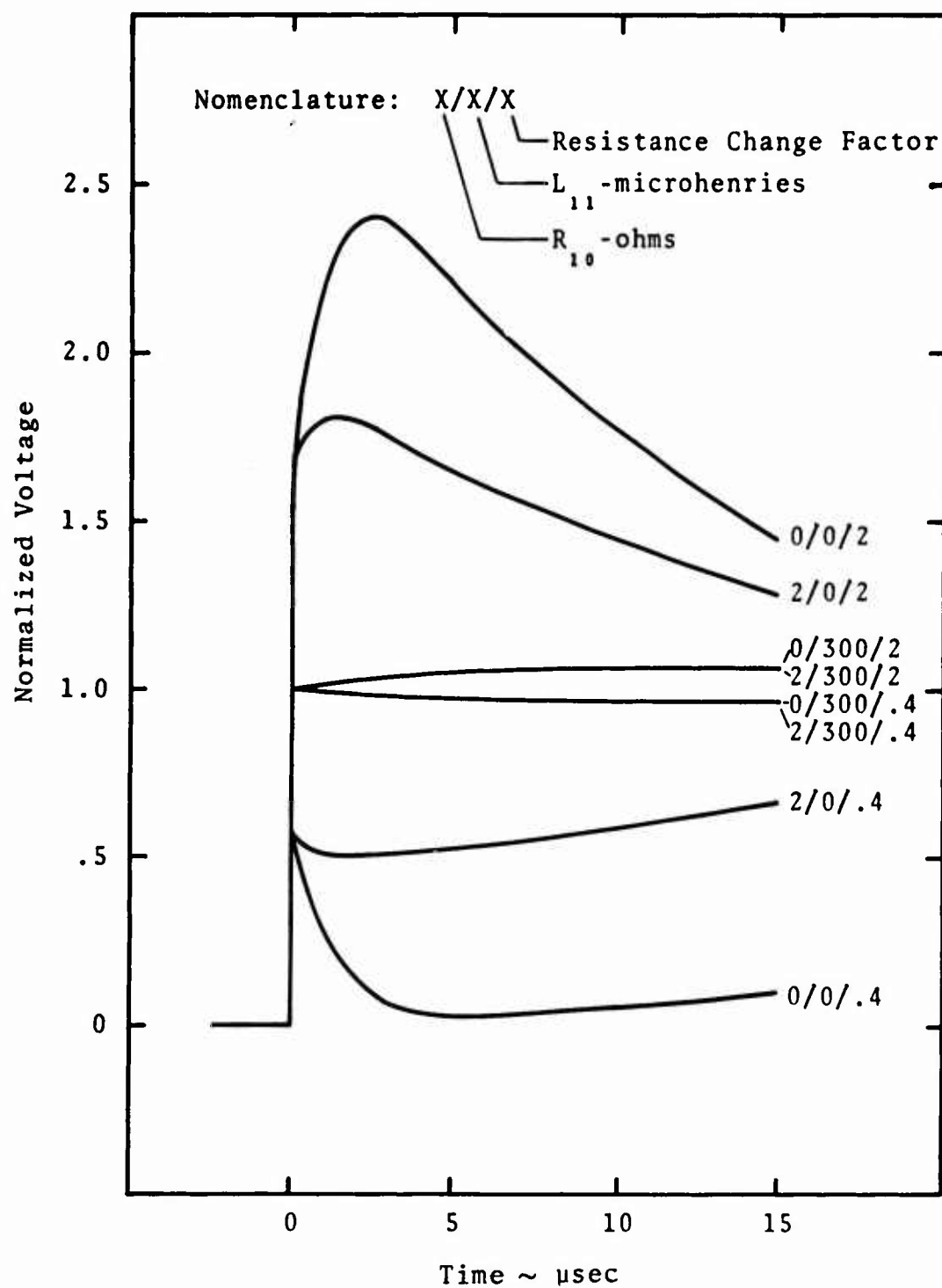


Figure 29. Calculated Gage Response Using ELMEK, Resistance Changes Only, AEDC Gage

The next observation is that where there is no ballast inductance, significant errors result which are only moderately affected by the ballast resistance. It is thus concluded that resistance changes in the gage produce large errors, but effective control is maintained with ballast inductance.

Now, consider figure 30 where normal resistance and inductance changes are permitted. Again, as in the discussion of figure 29, only the case where $K = 0.4$ is discussed. Applying the conclusions from before, it would be expected that in every case where there was no ballast inductance that the rise time would be degraded and large errors would result in the magnitude of the output. Likewise, where the ballast inductance is present, one would expect good rise-time performance and small errors in magnitude. The results in figure 30 confirm these expected behaviors.

An additional run was made where self-inductance and resistance changes were not permitted. This served as an additional check on the behavior of the model. In this case the model matched the ideal response within 0.20 to 0.05 percent.

b. Underground Nuclear Test

The primary difference in fielding a large gage in a field event as compared to the scaled gage previously discussed is that the electrical parameters are also larger. Also, for a field test, long lines on the order of 3000 to 5000 feet would be required. The large increase in secondary line capacitance could present a problem, at least in the lumped parameter model, in that there could be some undesirable oscillations due to the inductive and capacitive components in the circuit.

The possibility of an underdamped response was investigated by considering the secondary portion of the network in figure 21. If a step voltage is "inserted" into the network in place of the motion induced \dot{M} and the circuit parameters are assumed to be constant, the circuit can be modeled by the second order differential equation

$$\alpha \frac{d^2 Q}{dt^2} + \beta \frac{dQ}{dt} + \gamma Q = E(t)$$

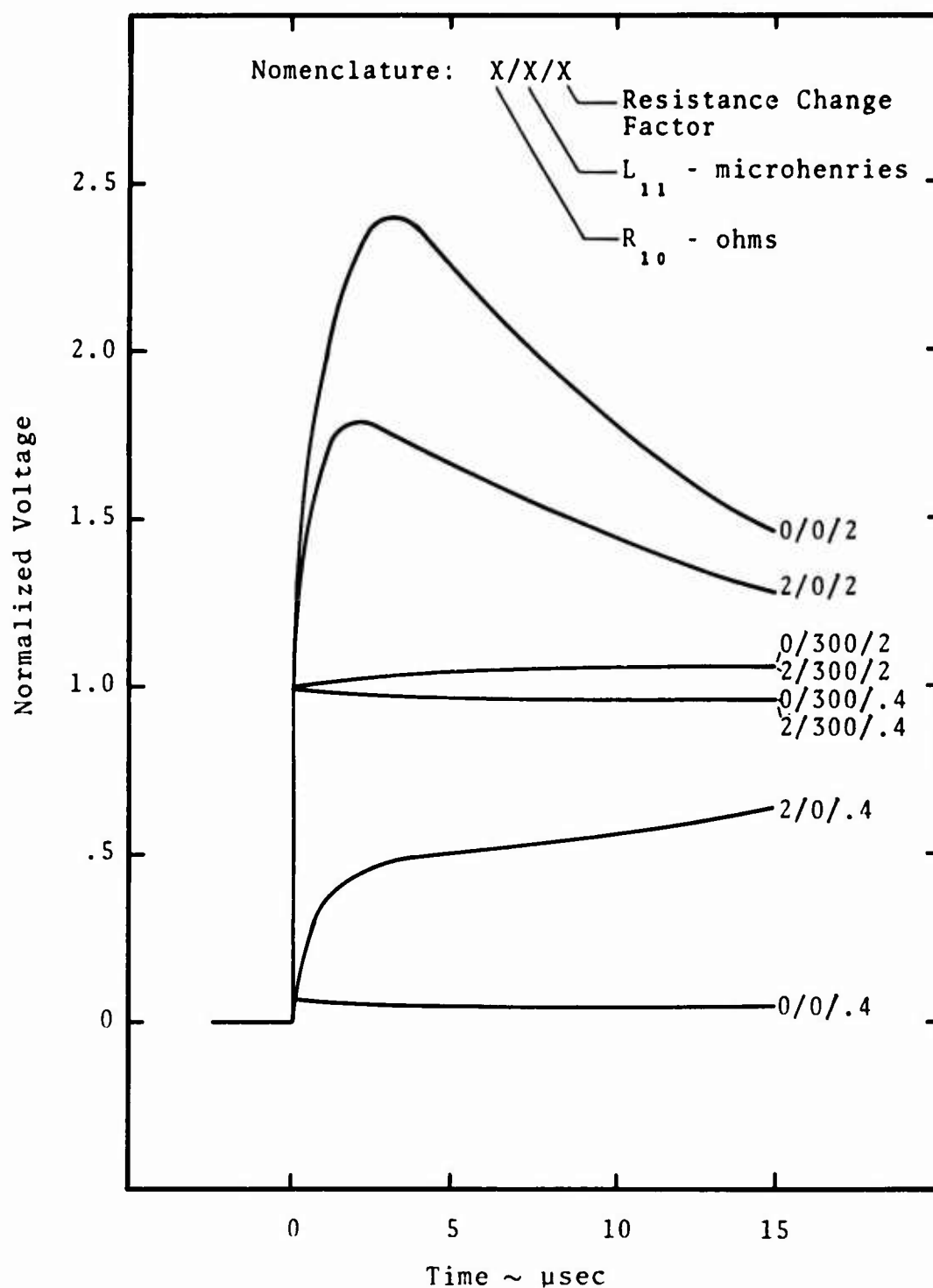


Figure 30. Calculated Gage Response Using ELMEK, Normal Resistance and Inductance Changes, AEDC Gage

where α , β , and γ are time invariant coefficients, $E(t)$ is the forcing function, and Q is the charge on C_7 . By lumping the long line capacitance and resistance for typical coaxial cable (RG-213 or RG-331) and for typical gage designs with L_4 on the order of 10 to 20 microhenries, damping ratios of 0.3 are obtained resulting in an underdamped response. Since the purpose of this analysis is to observe the response to self-inductance and resistance changes, a short length (100 feet) of cable was assumed for the secondary to avoid the underdamped response. The 5000 feet of RG-331 retained in the primary circuit presents no problem because of its relatively small magnitude in comparison with the other circuit components. In this case a damping ratio of 1.9 resulted for the problem investigated.

The effects of long-line capacitance are of great importance to the proper design of field gages, and this problem must be addressed in future analyses of the system. The approach anticipated is straightforward. First, an equivalent " π " or " T " network would be employed in the circuit to model the long line and the damping ratio calculated from the coefficients of the second order differential equation which describes the circuit. This would provide some insight into the range of permissible values of secondary self-inductance which would ensure an overdamped response. The next step would be to modify the complex model by inserting the equivalent network and observing the code response. This analysis is not presented here to ensure timely reporting of the present work.

The gage design selected is as follows:

Length	30 inches
Width	2 inches
Spacing between turns	0.140 inch
Primary turns	4
Secondary turns	3
Conductor material	0.060 beryllium

The resulting gage electrical parameters are

$$R_{\text{pri}} = 0.213 \text{ ohm}$$

$$L_{\text{pri}} = 14.3 \text{ } \mu\text{h}$$

$$R_{\text{sec}} = 0.160 \text{ ohm}$$

$$L_{\text{sec}} = 9.2 \text{ } \mu\text{h}$$

$$M = 19 \text{ } \mu\text{h}$$

$$GF = 9.81 \text{ mv/(amp}\cdot\text{mm}/\mu\text{sec)}$$

The shock environment is as before with $K = 0.2$ assumed for beryllium.

The results are shown in figure 31 for the only case investigated where $L_{11} = 500 \text{ } \mu\text{h}$.

As shown, the error is controlled to within approximately 3 percent. It is apparent that larger values of L_{11} could be employed to make the error negligible. It is worth noting that one reason for the effective error control here is that while the gage is considerably larger than that previously investigated, the resistances are significantly smaller because of the larger diameter and lower resistivity of the beryllium wire. As shown in appendix C, consideration must be given to a conductor's shock impedance, initial resistivity, and resistance-pressure characteristics to determine the magnitude of $\Delta R/\ell$, which directly causes the resistance-change-induced errors.

2. SUMMARY

The present mathematical model of the MIPV is adequate for investigating the effects of shock-induced self-inductance and resistance changes upon gage output.

The resulting error appears as essentially a level shift from the ideal, accompanied by a deterioration in rise-time performance. Both these effects are effectively controlled by employing a large ballast inductance in the primary circuit. Resistance in the primary external to the gage is relatively ineffective in controlling the errors. Therefore, the total primary resistance can be

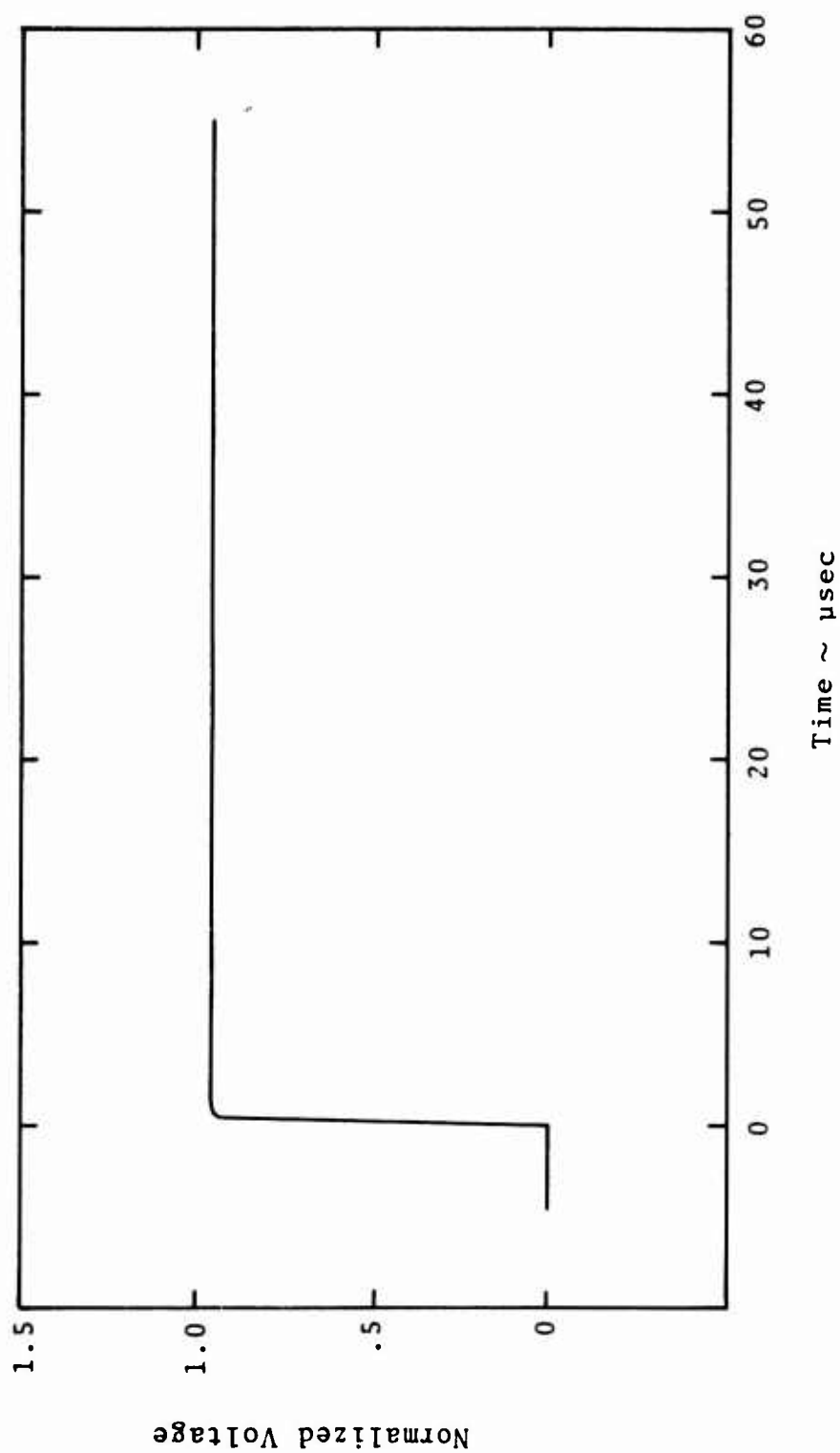


Figure 31. Shock Response of Field Design Gage as Calculated by ELMEK, $K = 0.2$, $L_{11} = 500 \mu h$

maintained at a reasonably small value to ensure maximum current and hence maximum sensitivity with no compromise to gage accuracy.

A major improvement to the present model would be to replace the lumped parameter model of the long lines with equivalent " π " or "T" networks. This would represent a more realistic model of a field installation of the system which would permit investigation of the possibility of an underdamped response and provide a manner in which to establish limitations upon gage secondary self-inductance. This work should be accomplished prior to fielding of the gage in a field event.

SECTION V

CONCLUSIONS AND RECOMMENDATIONS

These conclusions and recommendations are based upon the results of the three principal analytical investigations of the previous sections of this report and the conductor materials study of appendix C. The purpose of these analyses has been to provide improved understanding of how the MIPV responds to the shock environment. A direct consequence of this work, however, is the development of important analytical tools which are necessary for the proper design of a system to meet the requirements of a given test. Available also is the ability to study alternative designs and the nature and extent of resulting compromises which appear in the system performance.

1. CONCLUSIONS

As a result of the investigations of this report, the following conclusions are made.

a. To maintain a constant gage factor during gage deformation, the gage length-to-width ratio should be constrained such that $a/b \geq 5$ after shock transit through the gage. Generally, $a/b \geq 10$ prior to deformation would satisfy this requirement.

b. Gage factor may be increased significantly without affecting gage rise time by utilizing a Type II gage design instead of a Type I gage. The overall system design and specific experiment requirements must be considered to assess to overall benefits of the Type II design.

c. The MIPV is essentially insensitive to divergent flow effects for most anticipated experiments. Only when the source of spherical flow is within 1 meter of conventional gages ($b \leq 3$ inches) will significant errors in gage output occur.

d. The gage is relatively insensitive to off-axis flow in the x-y plane, the error induced being approximately equal to $1/2 (1 - \cos \gamma)$. However, off-axis flow in the x-z plane results in

much larger errors approximately equal to $3(1 - \cos \theta)$. An immediate result is that if in a field test there is a plane in which the uncertainty in shock propagation direction is a maximum, then the preferred orientation of the gage is with the x-y plane aligned with the plane of uncertainty.

e. The effects of pressure-induced resistance changes and motion-induced self-inductance changes upon the gage response are, respectively, to cause a level shift in the output voltage (positive for $K > 1$, negative for $K < 1$) and degrade the rise-time performance. Both of these effects are effectively controlled with a large ballast inductance in the primary circuit.

f. Three metals, aluminum, magnesium, and beryllium, all exhibit favorable shock impedance, electrical resistivity, and pressure-induced $\Delta R/\ell$ characteristics. Each presents a relatively low neutron cross section, with beryllium being the most favorable.

2. RECOMMENDATIONS

The conclusions above indicate that the MIPV has the basic characteristics of a desirable field gage; that is, it can be designed to produce a voltage level output and, with care in placement, small errors due to real flow can be maintained. Likewise, the effects of shock-induced resistance and inductance changes upon gage response have been shown to be effectively controlled with the ballast inductance. However, though based upon sound theoretical approaches, there is a need to verify these results. It is therefore recommended that these results be investigated experimentally in explosive testing. The approach would be to design an experiment, make calculations utilizing the appropriate code based upon that design, conduct the experiment, and compare the results.

As was noted in section IV, a requirement exists to modify the ELMEK code by providing an equivalent " π " or "T" network to properly model the secondary long lines. This will permit designing an overall system which will provide a desirable overdamped response. It is recommended that the model be modified accordingly and that experiments be conducted to ensure that the resulting model is suitable for actual design of field systems.

APPENDIX A

TABULATED NUMERICAL DATA FOR MIPV DESIGNS

The results of calculations utilizing two codes, DSIN1 for the Type I design and DSIN2 for the Type II design, are tabulated for several different applications of the MIPV. The codes are listed at the end of this appendix. The different applications are briefly discussed.

1. TYPE I GAGE DESIGN, FREE-FIELD MEASUREMENTS, LARGE HE TEST
(TABLE A-1)

This design would be suitable for free-field ground-motion measurements in the stress region below 10 Kbar, since large gage factors are available with the large number of primary and secondary turns. Results from this data are also presented in figures 6, 7, and 8.

2. TYPE I GAGE DESIGN, GAS GUN AND SMALL-SCALE EXPLOSIVE TESTS
(TABLE A-2)

Information is presented for scaled gage designs. Gage factors are considerably reduced; however, the smaller gage designs are more compatible with the gas gun and explosive experiments utilized in gage development and evaluation.

3. TYPES I AND II DESIGNS, GENERAL DESIGNS (TABLES A-3 AND A-4)

Data are presented for designs where gage parameters are varied over a wide range. These designs would be suitable for use in the high stress region close in to an explosive or nuclear source. The numerical results of figure 9 were obtained from this data.

TABLE A-1
TYPE I GAGE DESIGN, FREE-FIELD MEASUREMENTS, LARGE M- EVENT

LENGTH (INCHES)	WIDTH (INCHES)	LOOP SPACING (INCHES)	PRI TURNS	SEC TURNS	MUTUAL INDUCT (HENRIES)	GAGE FACTOR ($\frac{MV}{AMP \cdot MM/MUSEL}$)	ERROR TERM (PERCENT)
3.00000E+01	1.00000E+00	6.00000E-02	2	1	1.74905E-06	2.25245E+00	-1.93260E+00
3.00000E+01	1.00000E+00	6.00000E-02	3	2	4.96515E-06	5.85334E+00	-1.70463E+00
3.00000E+01	1.00000E+00	6.00000E-02	4	3	8.15605E-06	1.5251E+01	-1.09508E+00
3.00000E+01	1.00000E+00	6.00000E-02	5	4	1.23270E-05	1.59190E+01	-1.62402E+00
3.00000E+01	1.00000E+00	6.00000E-02	6	5	1.69566E-05	2.19097E+01	-1.56591E+00
3.00000E+01	1.00000E+00	6.00000E-02	7	6	2.19514E-05	2.53770E+01	-1.51732E+00
3.00000E+01	1.00000E+00	6.00000E-02	8	7	2.72442E-05	3.52335E+01	-1.47593E+00
3.00000E+01	1.00000E+00	6.00000E-02	9	8	3.27332E-05	4.24118E+01	-1.44029E+00
3.00000E+01	1.00000E+00	6.00000E-02	10	9	3.85205E-05	4.98597E+01	-1.40910E+00
3.00000E+01	1.00000E+00	6.00000E-02	11	10	4.44433E-05	5.75362E+01	-1.38154E+00
3.00000E+01	1.00000E+00	6.00000E-02	12	11	5.05174E-05	6.54083E+01	-1.35697E+00
3.00000E+01	1.00000E+00	7.00000E-02	2	1	1.65273E-06	2.12963E+00	-1.84333E+00
3.00000E+01	1.00000E+00	7.00000E-02	3	2	4.28287E-06	5.52541E+00	-1.72230E+00
3.00000E+01	1.00000E+00	7.00000E-02	4	3	7.59526E-06	9.50740E+00	-1.53190E+00
3.00000E+01	1.00000E+00	7.00000E-02	5	4	1.14123E-05	1.47466E+01	-1.56112E+00
3.00000E+01	1.00000E+00	7.00000E-02	6	5	1.56159E-05	2.01092E+01	-1.50307E+00
3.00000E+01	1.00000E+00	7.00000E-02	7	6	2.01217E-05	2.60274E+01	-1.45645E+00
3.00000E+01	1.00000E+00	7.00000E-02	8	7	2.48705E-05	3.21026E+01	-1.41041E+00
3.00000E+01	1.00000E+00	7.00000E-02	9	8	2.98168E-05	3.85903E+01	-1.36204E+00
3.00000E+01	1.00000E+00	7.00000E-02	10	9	3.49205E-05	4.52238E+01	-1.35213E+00
3.00000E+01	1.00000E+00	7.00000E-02	11	10	4.01732E-05	5.20309E+01	-1.32579E+00
3.00000E+01	1.00000E+00	7.00000E-02	12	11	4.55360E-05	5.89903E+01	-1.30236E+00
3.00000E+01	1.00000E+00	8.00000E-02	2	1	1.56945E-06	2.02344E+00	-1.78900E+00
3.00000E+01	1.00000E+00	8.00000E-02	3	2	4.03713E-06	5.21125E+00	-1.66003E+00
3.00000E+01	1.00000E+00	8.00000E-02	4	3	7.11444E-06	9.19171E+00	-1.57556E+00
3.00000E+01	1.00000E+00	8.00000E-02	5	4	1.06317E-05	1.37454E+01	-1.50653E+00
3.00000E+01	1.00000E+00	8.00000E-02	6	5	1.44735E-05	1.87292E+01	-1.44946E+00
3.00000E+01	1.00000E+00	8.00000E-02	7	6	1.85573E-05	2.43445E+01	-1.40337E+00
3.00000E+01	1.00000E+00	8.00000E-02	8	7	2.28305E-05	2.96226E+01	-1.36406E+00
3.00000E+01	1.00000E+00	8.00000E-02	9	8	2.73429E-05	3.54115E+01	-1.33158E+00
3.00000E+01	1.00000E+00	8.00000E-02	10	9	3.19375E-05	4.13735E+01	-1.30208E+00
3.00000E+01	1.00000E+00	8.00000E-02	11	10	3.66415E-05	4.74750E+01	-1.27765E+00
3.00000E+01	1.00000E+00	8.00000E-02	12	11	4.14388E-05	5.37075E+01	-1.25522E+00
3.00000E+01	1.00000E+00	9.00000E-02	2	1	1.49614E-06	1.92989E+00	-1.73865E+00
3.00000E+01	1.00000E+00	9.00000E-02	3	2	3.82170E-06	4.93565E+00	-1.61401E+00
3.00000E+01	1.00000E+00	9.00000E-02	4	3	6.69506E-06	8.55424E+00	-1.52470E+00
3.00000E+01	1.00000E+00	9.00000E-02	5	4	9.95469E-06	1.28764E+01	-1.45573E+00
3.00000E+01	1.00000E+00	9.00000E-02	6	5	1.34930E-05	1.74692E+01	-1.40102E+00
3.00000E+01	1.00000E+00	9.00000E-02	7	6	1.72506E-05	2.23435E+01	-1.35630E+00
3.00000E+01	1.00000E+00	9.00000E-02	8	7	2.11830E-05	2.74373E+01	-1.31091E+00
3.00000E+01	1.00000E+00	9.00000E-02	9	8	2.52431E-05	3.27064E+01	-1.26704E+00
3.00000E+01	1.00000E+00	9.00000E-02	10	9	2.94117E-05	3.81186E+01	-1.25943E+00
3.00000E+01	1.00000E+00	9.00000E-02	11	10	3.36702E-05	4.36475E+01	-1.23517E+00
3.00000E+01	1.00000E+00	9.00000E-02	12	11	3.80040E-05	4.92759E+01	-1.21360E+00

TABLE A-1 (CONT)
TYPE I GAGE DESIGN, FREE-FIELD MEASUREMENTS, LARGE HZ EVENT

LENGTH (INCHES)	WIDTH (INCHES)	LOOP SPACING (INCHES)	PRI TURNS	SEC TURNS	MUTUAL INDUCT (HENRIES)	GAGE FACTOR $\frac{HV}{AMP \cdot MM/USEL}$	ERROR TERM (PERCENT)
3.00000E+01	1.50000E+00	6.00000E-02	2	1	2.02316E-06	2.57635E+00	-3.0522E+00
3.00000E+01	1.50000E+00	6.00000E-02	3	2	5.37452E-06	6.5520E+00	-2.68004E+00
3.00000E+01	1.50000E+00	6.00000E-02	4	3	9.73918E-06	1.24378E+01	-2.75364E+00
3.00000E+01	1.50000E+00	6.00000E-02	5	4	1.49168E-05	1.90696E+01	-2.65464E+00
3.00000E+01	1.50000E+00	6.00000E-02	6	5	2.07643E-05	2.05079E+01	-2.50034E+00
3.00000E+01	1.50000E+00	6.00000E-02	7	6	2.71737E-05	3.47944E+01	-2.45000E+00
3.00000E+01	1.50000E+00	6.00000E-02	9	7	3.40602E-05	4.36403E+01	-2.42408E+00
3.00000E+01	1.50000E+00	6.00000E-02	9	8	4.13561E-05	5.30153E+01	-2.36662E+00
3.00000E+01	1.50000E+00	6.00000E-02	10	9	4.90002E-05	6.26574E+01	-2.31493E+00
3.00000E+01	1.50000E+00	6.00000E-02	11	10	5.69651E-05	7.30969E+01	-2.26068E+00
3.00000E+01	1.50000E+00	6.00000E-02	12	11	6.51950E-05	8.36943E+01	-2.22085E+00
3.00000E+01	1.50000E+00	7.00000E-02	2	1	1.92499E-06	2.45325E+00	-2.97503E+00
3.00000E+01	1.50000E+00	7.00000E-02	3	2	5.08230E-06	6.40773E+00	-2.90465E+00
3.00000E+01	1.50000E+00	7.00000E-02	4	3	9.16009E-06	1.17082E+01	-2.67263E+00
3.00000E+01	1.50000E+00	7.00000E-02	5	4	1.39022E-05	1.78648E+01	-2.56574E+00
3.00000E+01	1.50000E+00	7.00000E-02	6	5	1.93507E-05	2.47039E+01	-2.47653E+00
3.00000E+01	1.50000E+00	7.00000E-02	7	6	2.52227E-05	3.23246E+01	-2.40074E+00
3.00000E+01	1.50000E+00	7.00000E-02	9	7	3.14990E-05	4.03940E+01	-2.33513E+00
3.00000E+01	1.50000E+00	7.00000E-02	9	8	3.81173E-05	4.99987E+01	-2.27701E+00
3.00000E+01	1.50000E+00	7.00000E-02	10	9	4.50279E-05	5.78044E+01	-2.22736E+00
3.00000E+01	1.50000E+00	7.00000E-02	11	10	5.21904E-05	6.70209E+01	-2.18175E+00
3.00000E+01	1.50000E+00	7.00000E-02	12	11	5.95717E-05	7.55394E+01	-2.14090E+00
3.00000E+01	1.50000E+00	8.00000E-02	2	1	1.54311E-06	2.34069E+00	-2.90444E+00
3.00000E+01	1.50000E+00	8.00000E-02	3	2	4.82994E-06	6.17012E+00	-2.72901E+00
3.00000E+01	1.50000E+00	8.00000E-02	4	3	8.66121E-06	1.10790E+01	-2.55443E+00
3.00000E+01	1.50000E+00	8.00000E-02	5	4	1.31424E-05	1.53288E+01	-2.40033E+00
3.00000E+01	1.50000E+00	8.00000E-02	6	5	1.81406E-05	2.32492E+01	-2.35703E+00
3.00000E+01	1.50000E+00	8.00000E-02	7	6	2.35585E-05	3.02152E+01	-2.32157E+00
3.00000E+01	1.50000E+00	8.00000E-02	9	7	2.93224E-05	3.70316E+01	-2.25570E+00
3.00000E+01	1.50000E+00	8.00000E-02	9	8	3.53754E-05	4.54250E+01	-2.20033E+00
3.00000E+01	1.50000E+00	8.00000E-02	10	9	4.16727E-05	5.35372E+01	-2.15063E+00
3.00000E+01	1.50000E+00	8.00000E-02	11	10	4.83173E-05	6.19219E+01	-2.10642E+00
3.00000E+01	1.50000E+00	8.00000E-02	12	11	5.40037E-05	7.05417E+01	-2.06674E+00
3.00000E+01	1.50000E+00	9.00000E-02	2	1	1.76934E-06	2.25270E+00	-2.89906E+00
3.00000E+01	1.50000E+00	9.00000E-02	3	2	4.00307E-06	5.39907E+00	-2.69900E+00
3.00000E+01	1.50000E+00	9.00000E-02	4	3	6.22330E-06	1.05203E+01	-2.52322E+00
3.00000E+01	1.50000E+00	9.00000E-02	5	4	1.24253E-05	1.59224E+01	-2.41463E+00
3.00000E+01	1.50000E+00	9.00000E-02	6	5	1.79307E-05	2.19133E+01	-2.32562E+00
3.00000E+01	1.50000E+00	9.00000E-02	7	6	2.21145E-05	2.93020E+01	-2.25053E+00
3.00000E+01	1.50000E+00	9.00000E-02	9	7	2.74411E-05	3.52412E+01	-2.17044E+00
3.00000E+01	1.50000E+00	9.00000E-02	9	8	3.30145E-05	4.24210E+01	-2.13103E+00
3.00000E+01	1.50000E+00	9.00000E-02	10	9	3.87942E-05	4.99372E+01	-2.09331E+00
3.00000E+01	1.50000E+00	9.00000E-02	11	10	4.47400E-05	5.75514E+01	-2.05999E+00
3.00000E+01	1.50000E+00	9.00000E-02	12	11	5.08320E-05	6.54265E+01	-2.03136E+00

TABLE A-1 (CONT)
TYPE I GAGE DESIGN, FREE-FIELD MEASUREMENTS, LARGE HE EVENT

LENGTH (INCHES)	WIDTH (INCHES)	LOOP SPACING (INCHES)	PRI TURNS	SEC TURNS	MUTUAL INDUC (HENRIES)	GAGE FACTOR MV (AMP*MM/USEC)	ERROR TERM (PERCENT)
3.00000E+01	2.00000E+00	6.00000E-02	2	1	2.22910E-06	2.50661E+00	-4.22964E+00
3.00000E+01	2.00000E+00	6.00000E-02	3	2	5.97974E-06	7.54378E+00	-4.02512E+00
3.00000E+01	2.00000E+00	6.00000E-02	4	3	1.09285E-05	1.38085E+01	-3.86273E+00
3.00000E+01	2.00000E+00	6.00000E-02	5	4	1.68672E-05	2.13399E+01	-3.72800E+00
3.00000E+01	2.00000E+00	6.00000E-02	6	5	2.36443E-05	2.99479E+01	-3.61292E+00
3.00000E+01	2.00000E+00	6.00000E-02	7	6	3.11446E-05	3.94851E+01	-3.51280E+00
3.00000E+01	2.00000E+00	6.00000E-02	8	7	3.92732E-05	4.96331E+01	-3.42445E+00
3.00000E+01	2.00000E+00	6.00000E-02	9	8	4.79541E-05	6.08946E+01	-3.34564E+00
3.00000E+01	2.00000E+00	6.00000E-02	10	9	5.71235E-05	7.25882E+01	-3.27472E+00
3.00000E+01	2.00000E+00	6.00000E-02	11	10	6.67274E-05	8.48449E+01	-3.21043E+00
3.00000E+01	2.00000E+00	6.00000E-02	12	11	7.67198E-05	9.76059E+01	-3.15177E+00
3.00000E+01	2.00000E+00	7.00000E-02	2	1	2.12935E-06	2.68342E+00	-4.13682E+00
3.00000E+01	2.00000E+00	7.00000E-02	3	2	5.68202E-06	7.17522E+00	-3.92330E+00
3.00000E+01	2.00000E+00	7.00000E-02	4	3	1.03368E-05	1.30744E+01	-3.75494E+00
3.00000E+01	2.00000E+00	7.00000E-02	5	4	1.58883E-05	2.01231E+01	-3.61609E+00
3.00000E+01	2.00000E+00	7.00000E-02	6	5	2.21886E-05	2.81346E+01	-3.49634E+00
3.00000E+01	2.00000E+00	7.00000E-02	7	6	2.91248E-05	3.69660E+01	-3.39654E+00
3.00000E+01	2.00000E+00	7.00000E-02	8	7	3.66076E-05	4.65035E+01	-3.30725E+00
3.00000E+01	2.00000E+00	7.00000E-02	9	8	4.45645E-05	5.66548E+01	-3.22805E+00
3.00000E+01	2.00000E+00	7.00000E-02	10	9	5.29359E-05	6.73436E+01	-3.15713E+00
3.00000E+01	2.00000E+00	7.00000E-02	11	10	6.16720E-05	7.85061E+01	-3.09313E+00
3.00000E+01	2.00000E+00	7.00000E-02	12	11	7.07310E-05	9.00887E+01	-3.03499E+00
3.00000E+01	2.00000E+00	8.00000E-02	2	1	2.04303E-06	2.57674E+00	-4.05181E+00
3.00000E+01	2.00000E+00	8.00000E-02	3	2	5.42468E-06	6.55636E+00	-3.83063E+00
3.00000E+01	2.00000E+00	8.00000E-02	4	3	9.82611E-06	1.24402E+01	-3.65741E+00
3.00000E+01	2.00000E+00	8.00000E-02	5	4	1.50449E-05	1.90735E+01	-3.51552E+00
3.00000E+01	2.00000E+00	8.00000E-02	6	5	2.09369E-05	2.65738E+01	-3.39598E+00
3.00000E+01	2.00000E+00	8.00000E-02	7	6	2.73929E-05	3.48026E+01	-3.29325E+00
3.00000E+01	2.00000E+00	8.00000E-02	8	7	3.43278E-05	4.36511E+01	-3.20365E+00
3.00000E+01	2.00000E+00	8.00000E-02	9	8	4.16732E-05	5.30323E+01	-3.12456E+00
3.00000E+01	2.00000E+00	8.00000E-02	10	9	4.93739E-05	6.28749E+01	-3.05406E+00
3.00000E+01	2.00000E+00	8.00000E-02	11	10	5.73340E-05	7.31203E+01	-2.99068E+00
3.00000E+01	2.00000E+00	8.00000E-02	12	11	6.56656E-05	8.37196E+01	-2.93329E+00
3.00000E+01	2.00000E+00	9.00000E-02	2	1	1.96696E-06	2.48268E+00	-3.97309E+00
3.00000E+01	2.00000E+00	9.00000E-02	3	2	5.19321E-06	6.57552E+00	-3.74536E+00
3.00000E+01	2.00000E+00	9.00000E-02	4	3	9.37745E-06	1.18824E+01	-3.56824E+00
3.00000E+01	2.00000E+00	9.00000E-02	5	4	1.43056E-05	1.81522E+01	-3.42412E+00
3.00000E+01	2.00000E+00	9.00000E-02	6	5	1.98420E-05	2.52067E+01	-3.30346E+00
3.00000E+01	2.00000E+00	9.00000E-02	7	6	2.58819E-05	3.29124E+01	-3.20036E+00
3.00000E+01	2.00000E+00	9.00000E-02	8	7	3.23440E-05	4.11656E+01	-3.11088E+00
3.00000E+01	2.00000E+00	9.00000E-02	9	8	3.91645E-05	4.98843E+01	-3.03226E+00
3.00000E+01	2.00000E+00	9.00000E-02	10	9	4.62919E-05	5.90026E+01	-2.96243E+00
3.00000E+01	2.00000E+00	9.00000E-02	11	10	5.36844E-05	6.84665E+01	-2.89985E+00
3.00000E+01	2.00000E+00	9.00000E-02	12	11	6.13077E-05	7.82319E+01	-2.84333E+00

TABLE A-1 (CONT)
TYPE I GAGE DESIGN, FREE-FIELD MEASUREMENTS, LARGE HE EVENT

LENGTH (INCHES)	WIDTH (INCHES)	LOOP SPACING (INCHES)	PKI TURNS	SEC TURNS	MUTUAL INDUCT (HENRIES)	GAGE FACTOR MV (AMP*MM/USEC)	ERROR TERM (PERCENT)
3.00000E+01	2.50000E+00	6.00000E-02	2	1	2.39834E-06	2.38550E+00	-5.42371E+00
3.00000E+01	2.50000E+00	6.00000E-02	3	2	6.47257E-06	6.37343E+00	-5.18232E+00
3.00000E+01	2.50000E+00	6.00000E-02	4	3	1.19516E-05	1.48767E+01	-4.98910E+00
3.00000E+01	2.50000E+00	6.00000E-02	5	4	1.84620E-05	2.31137E+01	-4.32722E+00
3.00000E+01	2.50000E+00	6.00000E-02	6	5	2.60027E-05	3.25962E+01	-4.65777E+00
3.00000E+01	2.50000E+00	6.00000E-02	7	6	3.43995E-05	4.31727E+01	-4.56535E+00
3.00000E+01	2.50000E+00	6.00000E-02	8	7	4.35544E-05	5.47195E+01	-4.45639E+00
3.00000E+01	2.50000E+00	6.00000E-02	9	8	5.33555E-05	6.71337E+01	-4.35837E+00
3.00000E+01	2.50000E+00	6.00000E-02	10	9	6.38234E-05	8.13202E+01	-4.26946E+00
3.00000E+01	2.50000E+00	6.00000E-02	11	10	7.48089E-05	9.72279E+01	-4.18825E+00
3.00000E+01	2.50000E+00	6.00000E-02	12	11	8.62904E-05	1.18768E+02	-4.11363E+00
3.00000E+01	2.50000E+00	7.00000E-02	2	1	2.29700E-06	2.36226E+00	-5.31646E+00
3.00000E+01	2.50000E+00	7.00000E-02	3	2	6.17200E-06	7.71036E+00	-5.06362E+00
3.00000E+01	2.50000E+00	7.00000E-02	4	3	1.12990E-05	1.41400E+01	-4.88220E+00
3.00000E+01	2.50000E+00	7.00000E-02	5	4	1.74640E-05	2.18910E+01	-4.69433E+00
3.00000E+01	2.50000E+00	7.00000E-02	6	5	2.45130E-05	3.07732E+01	-4.59047E+00
3.00000E+01	2.50000E+00	7.00000E-02	7	6	3.23293E-05	4.06291E+01	-4.42482E+00
3.00000E+01	2.50000E+00	7.00000E-02	8	7	4.08145E-05	5.13478E+01	-4.31354E+00
3.00000E+01	2.50000E+00	7.00000E-02	9	8	4.98914E-05	6.28268E+01	-4.21391E+00
3.00000E+01	2.50000E+00	7.00000E-02	10	9	5.94932E-05	7.49028E+01	-4.12393E+00
3.00000E+01	2.50000E+00	7.00000E-02	11	10	6.95641E-05	8.77440E+01	-4.04203E+00
3.00000E+01	2.50000E+00	7.00000E-02	12	11	8.00563E-05	1.01152E+02	-3.96718E+00
3.00000E+01	2.50000E+00	8.00000E-02	2	1	2.20928E-06	2.75553E+00	-5.21823E+00
3.00000E+01	2.50000E+00	8.00000E-02	3	2	5.91090E-06	7.39092E+00	-4.99542E+00
3.00000E+01	2.50000E+00	8.00000E-02	4	3	1.07785E-05	1.35039E+01	-4.74711E+00
3.00000E+01	2.50000E+00	8.00000E-02	5	4	1.66024E-05	2.08349E+01	-4.57441E+00
3.00000E+01	2.50000E+00	8.00000E-02	6	5	2.32314E-05	2.91949E+01	-4.42716E+00
3.00000E+01	2.50000E+00	8.00000E-02	7	6	3.05493E-05	3.84304E+01	-4.29920E+00
3.00000E+01	2.50000E+00	8.00000E-02	8	7	3.84630E-05	4.84409E+01	-4.19640E+00
3.00000E+01	2.50000E+00	8.00000E-02	9	8	4.68987E-05	5.91308E+01	-4.08585E+00
3.00000E+01	2.50000E+00	8.00000E-02	10	9	5.57920E-05	7.04049E+01	-3.99543E+00
3.00000E+01	2.50000E+00	8.00000E-02	11	10	6.50911E-05	8.22043E+01	-3.91347E+00
3.00000E+01	2.50000E+00	8.00000E-02	12	11	7.47512E-05	9.44721E+01	-3.83871E+00
3.00000E+01	2.50000E+00	9.00000E-02	2	1	2.13197E-06	2.66141E+00	-5.12725E+00
3.00000E+01	2.50000E+00	9.00000E-02	3	2	5.68042E-06	7.10941E+00	-4.85563E+00
3.00000E+01	2.50000E+00	9.00000E-02	4	3	1.03207E-05	1.29479E+01	-4.64156E+00
3.00000E+01	2.50000E+00	9.00000E-02	5	4	1.58455E-05	1.99062E+01	-4.46495E+00
3.00000E+01	2.50000E+00	9.00000E-02	6	5	2.21072E-05	2.78125E+01	-4.31515E+00
3.00000E+01	2.50000E+00	9.00000E-02	7	6	2.89913E-05	3.65185E+01	-4.18559E+00
3.00000E+01	2.50000E+00	9.00000E-02	8	7	3.64103E-05	4.59130E+01	-4.07189E+00
3.00000E+01	2.50000E+00	9.00000E-02	9	8	4.42390E-05	5.59043E+01	-3.97095E+00
3.00000E+01	2.50000E+00	9.00000E-02	10	9	5.25737E-05	6.64170E+01	-3.88049E+00
3.00000E+01	2.50000E+00	9.00000E-02	11	10	6.12102E-05	7.73033E+01	-3.79377E+00
3.00000E+01	2.50000E+00	9.00000E-02	12	11	7.01509E-05	8.87660E+01	-3.72443E+00

TABLE A-1 (CONT)
TYPE I GAGE DESIGN, FREE-FIELD MEASUREMENTS, LARGE HE EVENT

LENGTH (INCHES)	WIDTH (INCHES)	LOOP SPACING (INCHES)	PRI TURNS	SEC TURNS	MUTUAL INDUC (HENRIES)	GAGE FACTOR ($\frac{MV}{AMP \cdot MM / JSEC}$)	ERROR TERM (PERCENT)
3.00000E+01	3.00000E+00	6.00000E-02	2	1	2.54471E-06	3.13191E+00	-6.62860E+00
3.00000E+01	3.00000E+00	6.00000E-02	3	2	6.90311E-06	8.51607E+00	-6.35262E+00
3.00000E+01	3.00000E+00	6.00000E-02	4	3	1.27332E-05	1.57524E+01	-6.13056E+00
3.00000E+01	3.00000E+00	6.00000E-02	5	4	1.98346E-05	2.45694E+01	-5.94347E+00
3.00000E+01	3.00000E+00	6.00000E-02	6	5	2.80269E-05	3.47730E+01	-5.75134E+00
3.00000E+01	3.00000E+00	6.00000E-02	7	6	3.71965E-05	4.62089E+01	-5.63617E+00
3.00000E+01	3.00000E+00	6.00000E-02	8	7	4.72346E-05	5.87507E+01	-5.50999E+00
3.00000E+01	3.00000E+00	6.00000E-02	9	8	5.80560E-05	7.22922E+01	-5.39401E+00
3.00000E+01	3.00000E+00	6.00000E-02	10	9	6.95932E-05	8.67425E+01	-5.28822E+00
3.00000E+01	3.00000E+00	6.00000E-02	11	10	8.17776E-05	1.02023E+02	-5.19106E+00
3.00000E+01	3.00000E+00	6.00000E-02	12	11	9.45543E-05	1.18064E+02	-5.1133E+00
3.00000E+01	3.00000E+00	7.00000E-02	2	1	2.44178E-06	3.00664E+00	-6.50772E+00
3.00000E+01	3.00000E+00	7.00000E-02	3	2	6.69543E-06	8.14673E+00	-6.21809E+00
3.00000E+01	3.00000E+00	7.00000E-02	4	3	1.21263E-05	1.50150E+01	-5.96588E+00
3.00000E+01	3.00000E+00	7.00000E-02	5	4	1.88179E-05	2.33435E+01	-5.79102E+00
3.00000E+01	3.00000E+00	7.00000E-02	6	5	2.65115E-05	3.29398E+01	-5.62267E+00
3.00000E+01	3.00000E+00	7.00000E-02	7	6	3.50837E-05	4.36517E+01	-5.47499E+00
3.00000E+01	3.00000E+00	7.00000E-02	8	7	4.44343E-05	5.53551E+01	-5.34313E+00
3.00000E+01	3.00000E+00	7.00000E-02	9	8	5.44802E-05	6.79466E+01	-5.22430E+00
3.00000E+01	3.00000E+00	7.00000E-02	10	9	6.51509E-05	8.13384E+01	-5.11633E+00
3.00000E+01	3.00000E+00	7.00000E-02	11	10	7.63860E-05	9.54547E+01	-5.01753E+00
3.00000E+01	3.00000E+00	7.00000E-02	12	11	8.81331E-05	1.10230E+02	-4.92660E+00
3.00000E+01	3.00000E+00	8.00000E-02	2	1	2.35263E-06	2.90188E+00	-6.39704E+00
3.00000E+01	3.00000E+00	8.00000E-02	3	2	6.32330E-06	7.82697E+00	-6.09535E+00
3.00000E+01	3.00000E+00	8.00000E-02	4	3	1.15967E-05	1.43771E+01	-5.85441E+00
3.00000E+01	3.00000E+00	8.00000E-02	5	4	1.79401E-05	2.22637E+01	-5.65305E+00
3.00000E+01	3.00000E+00	8.00000E-02	6	5	2.52030E-05	3.13565E+01	-5.49001E+00
3.00000E+01	3.00000E+00	8.00000E-02	7	6	3.32643E-05	4.14455E+01	-5.32846E+00
3.00000E+01	3.00000E+00	8.00000E-02	8	7	4.20262E-05	5.24294E+01	-5.19367E+00
3.00000E+01	3.00000E+00	8.00000E-02	9	8	5.14383E-05	6.42077E+01	-5.07305E+00
3.00000E+01	3.00000E+00	8.00000E-02	10	9	6.13430E-05	7.66957E+01	-4.96365E+00
3.00000E+01	3.00000E+00	8.00000E-02	11	10	7.17727E-05	8.98211E+01	-4.86383E+00
3.00000E+01	3.00000E+00	8.00000E-02	12	11	8.26479E-05	1.03521E+02	-4.77234E+00
3.00000E+01	3.00000E+00	9.00000E-02	2	1	2.27415E-06	2.80772E+00	-6.29454E+00
3.00000E+01	3.00000E+00	9.00000E-02	3	2	6.09492E-06	7.54711E+00	-5.98212E+00
3.00000E+01	3.00000E+00	9.00000E-02	4	3	1.11367E-05	1.38151E+01	-5.73363E+00
3.00000E+01	3.00000E+00	9.00000E-02	5	4	1.71637E-05	2.13510E+01	-5.52678E+00
3.00000E+01	3.00000E+00	9.00000E-02	6	5	2.40545E-05	2.99645E+01	-5.34979E+00
3.00000E+01	3.00000E+00	9.00000E-02	7	6	3.16695E-05	3.95034E+01	-5.19540E+00
3.00000E+01	3.00000E+00	9.00000E-02	8	7	3.99187E-05	4.98642E+01	-5.05861E+00
3.00000E+01	3.00000E+00	9.00000E-02	9	8	4.87243E-05	6.09345E+01	-4.93664E+00
3.00000E+01	3.00000E+00	9.00000E-02	10	9	5.80216E-05	7.26380E+01	-4.82633E+00
3.00000E+01	3.00000E+00	9.00000E-02	11	10	6.77560E-05	8.49058E+01	-4.72614E+00
3.00000E+01	3.00000E+00	9.00000E-02	12	11	7.78808E-05	9.76759E+01	-4.63441E+00

TABLE A-2
TYPE I GAGE DESIGN, GAS GUN AND SMALL SCALE EXPLOSIVE TESTS

LENGTH (INCHES)	WIDTH (INCHES)	LOOP SPACING (INCHES)	PRI TURNS	SEC TURNS	MUTUAL INDUCT (HENRIES)	GAGE FACTOR $\left(\frac{MV}{WHP \cdot MM/JSEC}\right)$	ERROR TERM (PERCENT)
5.00000E+00	4.00000E-01	4.00000E-02	2	1	2.90873E-07	1.04701E+00	-3.33505E+00
5.00000E+00	4.00000E-01	4.00000E-02	3	2	7.37160E-07	4.69261E+00	-3.07713E+00
5.00000E+00	4.00000E-01	4.00000E-02	4	3	1.28311E-06	0.10209E+00	-2.09016E+00
5.00000E+00	4.00000E-01	5.00000E-02	2	1	2.62563E-07	1.67071E+00	-3.12004E+00
5.00000E+00	4.00000E-01	5.00000E-02	3	2	6.55212E-07	4.17964E+00	-2.85263E+00
5.00000E+00	4.00000E-01	5.00000E-02	4	3	1.12625E-06	7.19738E+00	-2.67900E+00
5.00000E+00	4.00000E-01	6.00000E-02	2	1	2.39620E-07	1.52755E+00	-2.93347E+00
5.00000E+00	4.00000E-01	6.00000E-02	3	2	5.89716E-07	3.76050E+00	-2.67365E+00
5.00000E+00	4.00000E-01	6.00000E-02	4	3	1.00275E-06	6.41918E+00	-2.50146E+00
5.00000E+00	5.00000E-01	4.00000E-02	2	1	3.22000E-07	2.02461E+00	-4.33768E+00
5.00000E+00	5.00000E-01	4.00000E-02	3	2	8.27046E-07	5.21474E+00	-4.06664E+00
5.00000E+00	5.00000E-01	4.00000E-02	4	3	1.45554E-06	9.19670E+00	-3.32738E+00
5.00000E+00	5.00000E-01	5.00000E-02	2	1	2.93211E-07	1.54751E+00	-4.13766E+00
5.00000E+00	5.00000E-01	5.00000E-02	3	2	7.42636E-07	4.09410E+00	-3.80903E+00
5.00000E+00	5.00000E-01	5.00000E-02	4	3	1.29207E-06	6.18586E+00	-3.57079E+00
5.00000E+00	5.00000E-01	6.00000E-02	2	1	2.69767E-07	1.70339E+00	-3.91707E+00
5.00000E+00	5.00000E-01	6.00000E-02	3	2	5.74772E-07	4.27427E+00	-3.59330E+00
5.00000E+00	5.00000E-01	6.00000E-02	4	3	1.16213E-06	7.37020E+00	-3.35223E+00
5.00000E+00	6.00000E-01	4.00000E-02	2	1	3.48014E-07	2.17030E+00	-5.46020E+00
5.00000E+00	6.00000E-01	4.00000E-02	3	2	9.04149E-07	5.64599E+00	-5.05057E+00
5.00000E+00	6.00000E-01	4.00000E-02	4	3	1.60415E-06	1.00446E+01	-4.79213E+00
5.00000E+00	6.00000E-01	5.00000E-02	2	1	3.19422E-07	1.99277E+00	-5.17719E+00
5.00000E+00	6.00000E-01	5.00000E-02	3	2	8.17760E-07	5.12088E+00	-4.78435E+00
5.00000E+00	6.00000E-01	5.00000E-02	4	3	1.43366E-06	9.01041E+00	-4.49159E+00
5.00000E+00	6.00000E-01	6.00000E-02	2	1	2.95533E-07	1.54812E+00	-4.92757E+00
5.00000E+00	6.00000E-01	6.00000E-02	3	2	7.40062E-07	4.09593E+00	-4.52758E+00
5.00000E+00	6.00000E-01	6.00000E-02	4	3	1.30033E-06	6.10953E+00	-4.23444E+00

TABLE A-3
TYPE I GAGE, GENERAL DESIGNS

LENGTH (INCHES)	WIDTH (INCHES)	LOOP SPACING (INCHES)	PRI TURNS	SEC TURNS	MUTUAL INDUCT (HENRIES)	GAGE FACTOR ($\frac{MV}{AMP \cdot MM/USEL}$)	ERROR TERM (PERCENT)
2.00000E+01	2.00000E+00	8.00000E-02	2	1	1.38843E-06	2.57785E+00	-6.02347E+00
2.00000E+01	2.00000E+00	8.00000E-02	3	2	3.68283E-06	6.55969E+00	-5.66496E+00
2.00000E+01	2.00000E+00	8.00000E-02	4	3	6.66563E-06	1.24468E+01	-5.41905E+00
2.00000E+01	2.00000E+00	8.00000E-02	5	4	1.01991E-05	1.93346E+01	-5.20352E+00
2.00000E+01	2.00000E+00	8.00000E-02	6	5	1.41654E-05	2.65904E+01	-5.01577E+00
2.00000E+01	2.00000E+00	1.00000E-01	2	1	1.28964E-06	2.39968E+00	-5.79117E+00
2.00000E+01	2.00000E+00	1.00000E-01	3	2	3.38930E-06	6.32602E+00	-5.43337E+00
2.00000E+01	2.00000E+00	1.00000E-01	4	3	6.08535E-06	1.13917E+01	-5.15567E+00
2.00000E+01	2.00000E+00	1.00000E-01	5	4	9.24489E-06	1.73435E+01	-4.93058E+00
2.00000E+01	2.00000E+00	1.00000E-01	6	5	1.27754E-05	2.40098E+01	-4.74220E+00
2.00000E+01	2.00000E+00	1.20000E-01	2	1	1.20913E-06	2.25426E+00	-5.56577E+00
2.00000E+01	2.00000E+00	1.20000E-01	3	2	3.15048E-06	5.59516E+00	-5.21355E+00
2.00000E+01	2.00000E+00	1.20000E-01	4	3	5.61594E-06	1.05358E+01	-4.92843E+00
2.00000E+01	2.00000E+00	1.20000E-01	5	4	8.47667E-06	1.59374E+01	-4.69967E+00
2.00000E+01	2.00000E+00	1.20000E-01	6	5	1.16462E-05	2.19363E+01	-4.51017E+00
2.00000E+01	2.00000E+00	1.40000E-01	2	1	1.14125E-06	2.13145E+00	-5.40042E+00
2.00000E+01	2.00000E+00	1.40000E-01	3	2	2.95050E-06	5.53073E+00	-5.31743E+00
2.00000E+01	2.00000E+00	1.40000E-01	4	3	5.22341E-06	9.01812E+00	-4.72776E+00
2.00000E+01	2.00000E+00	1.40000E-01	5	4	7.83756E-06	1.47643E+01	-4.44756E+00
2.00000E+01	2.00000E+00	1.40000E-01	6	5	1.07121E-05	2.02158E+01	-4.36846E+00
2.00000E+01	2.00000E+00	1.60000E-01	2	1	1.08263E-06	2.02522E+00	-5.23078E+00
2.00000E+01	2.00000E+00	1.60000E-01	3	2	2.77826E-06	5.21657E+00	-4.84003E+00
2.00000E+01	2.00000E+00	1.60000E-01	4	3	4.88739E-06	9.20235E+00	-4.54774E+00
2.00000E+01	2.00000E+00	1.60000E-01	5	4	7.29353E-06	1.37631E+01	-4.31760E+00
2.00000E+01	2.00000E+00	1.60000E-01	6	5	9.92136E-06	1.87557E+01	-4.12978E+00
4.00000E+01	2.00000E+00	8.00000E-02	2	1	2.69746E-06	2.57635E+00	-3.05224E+00
4.00000E+01	2.00000E+00	8.00000E-02	3	2	7.16603E-06	6.55520E+00	-2.86804E+00
4.00000E+01	2.00000E+00	8.00000E-02	4	3	1.29856E-05	1.24373E+01	-2.75964E+00
4.00000E+01	2.00000E+00	8.00000E-02	5	4	1.98890E-05	1.90696E+01	-2.65464E+00
4.00000E+01	2.00000E+00	8.00000E-02	6	5	2.76855E-05	2.65673E+01	-2.56634E+00
4.00000E+01	2.00000E+00	1.00000E-01	2	1	2.50317E-06	2.39819E+00	-2.93903E+00
4.00000E+01	2.00000E+00	1.00000E-01	3	2	6.60241E-06	6.32353E+00	-2.76593E+00
4.00000E+01	2.00000E+00	1.00000E-01	4	3	1.18693E-05	1.13827E+01	-2.63258E+00
4.00000E+01	2.00000E+00	1.00000E-01	5	4	1.80503E-05	1.73285E+01	-2.52500E+00
4.00000E+01	2.00000E+00	1.00000E-01	6	5	2.49646E-05	2.39874E+01	-2.43566E+00
4.00000E+01	2.00000E+00	1.20000E-01	2	1	2.35379E-06	2.25276E+00	-2.83906E+00
4.00000E+01	2.00000E+00	1.20000E-01	3	2	6.14410E-06	5.59067E+00	-2.65960E+00
4.00000E+01	2.00000E+00	1.20000E-01	4	3	1.09651E-05	1.05268E+01	-2.52322E+00
4.00000E+01	2.00000E+00	1.20000E-01	5	4	1.65578E-05	1.59224E+01	-2.41468E+00
4.00000E+01	2.00000E+00	1.20000E-01	6	5	2.27822E-05	2.19138E+01	-2.32562E+00
4.00000E+01	2.00000E+00	1.40000E-01	2	1	2.22352E-06	2.12995E+00	-2.74899E+00
4.00000E+01	2.00000E+00	1.40000E-01	3	2	5.75567E-06	5.52624E+00	-2.56497E+00
4.00000E+01	2.00000E+00	1.40000E-01	4	3	1.02080E-05	9.00914E+00	-2.42707E+00
4.00000E+01	2.00000E+00	1.40000E-01	5	4	1.53328E-05	1.47493E+01	-2.31505E+00
4.00000E+01	2.00000E+00	1.40000E-01	6	5	2.09741E-05	2.11934E+01	-2.23061E+00
4.00000E+01	2.00000E+00	1.60000E-01	2	1	2.11043E-06	2.02372E+00	-2.66666E+00
4.00000E+01	2.00000E+00	1.60000E-01	3	2	5.42678E-06	5.21208E+00	-2.47954E+00
4.00000E+01	2.00000E+00	1.60000E-01	4	3	9.55915E-06	9.19336E+00	-2.34118E+00
4.00000E+01	2.00000E+00	1.60000E-01	5	4	1.42801E-05	1.37452E+01	-2.23362E+00
4.00000E+01	2.00000E+00	1.60000E-01	6	5	1.94417E-05	1.87333E+01	-2.14705E+00

TABLE A-3 (CONT)
TYPE I GAGE, GENERAL DESIGNS

LENGTH (INCHES)	WIDTH (INCHES)	LOOP SPACING (INCHES)	PRI TURNS	SEC TURNS	MUTUAL INDUCT (HENRIES)	GAGE FACTOR ($\frac{MV}{AMP \cdot MM/USEC}$)	ERROR TERM (PERCENT)
5.00000E+01	2.00000E+00	0.30000E-02	2	1	4.00617E-06	2.57607E+00	-2.04367E+00
5.00000E+01	2.00000E+00	0.00000E-02	3	2	1.06482E-05	6.85437E+00	-1.33531E+00
5.00000E+01	2.00000E+00	0.00000E-02	4	3	1.93035E-05	1.24362E+01	-1.85072E+00
5.00000E+01	2.00000E+00	0.00000E-02	5	4	2.95755E-05	1.30669E+01	-1.78167E+00
5.00000E+01	2.00000E+00	0.00000E-02	6	5	4.11810E-05	2.65638E+01	-1.72370E+00
5.00000E+01	2.00000E+00	1.00000E-01	2	1	3.72636E-06	2.39791E+00	-1.95884E+00
5.00000E+01	2.00000E+00	1.00000E-01	3	2	9.81451E-06	6.32270E+00	-1.85477E+00
5.00000E+01	2.00000E+00	1.00000E-01	4	3	1.76512E-05	1.13810E+01	-1.76702E+00
5.00000E+01	2.00000E+00	1.00000E-01	5	4	2.68523E-05	1.73257E+01	-1.69642E+00
5.00000E+01	2.00000E+00	1.00000E-01	6	5	3.71431E-05	2.33332E+01	-1.63796E+00
5.00000E+01	2.00000E+00	1.20000E-01	2	1	3.49910E-06	2.25248E+00	-1.90260E+00
5.00000E+01	2.00000E+00	1.20000E-01	3	2	9.13631E-06	5.88984E+00	-1.78463E+00
5.00000E+01	2.00000E+00	1.20000E-01	4	3	1.63122E-05	1.05251E+01	-1.69508E+00
5.00000E+01	2.00000E+00	1.20000E-01	5	4	2.46555E-05	1.59196E+01	-1.62402E+00
5.00000E+01	2.00000E+00	1.20000E-01	6	5	3.39132E-05	2.19097E+01	-1.56591E+00
5.00000E+01	2.00000E+00	1.40000E-01	2	1	3.30545E-06	2.12968E+00	-1.84333E+00
5.00000E+01	2.00000E+00	1.40000E-01	3	2	6.56575E-06	5.52541E+00	-1.72230E+00
5.00000E+01	2.00000E+00	1.40000E-01	4	3	1.51905E-05	9.60748E+00	-1.63190E+00
5.00000E+01	2.00000E+00	1.40000E-01	5	4	2.28246E-05	1.47466E+01	-1.56112E+00
5.00000E+01	2.00000E+00	1.40000E-01	6	5	3.12311E-05	2.01892E+01	-1.50387E+00
5.00000E+01	2.00000E+00	1.60000E-01	2	1	3.13889E-06	2.02344E+00	-1.78900E+00
5.00000E+01	2.00000E+00	1.60000E-01	3	2	8.07426E-06	5.21125E+00	-1.66608E+00
5.00000E+01	2.00000E+00	1.60000E-01	4	3	1.42289E-05	9.19171E+00	-1.57556E+00
5.00000E+01	2.00000E+00	1.60000E-01	5	4	2.12633E-05	1.37454E+01	-1.50553E+00
5.00000E+01	2.00000E+00	1.60000E-01	6	5	2.89570E-05	1.87292E+01	-1.44946E+00
2.00000E+01	2.50000E+00	0.30000E-02	2	1	1.50320E-06	2.75726E+00	-7.74708E+00
2.00000E+01	2.50000E+00	0.00000E-02	3	2	4.03314E-06	7.39611E+00	-7.34364E+00
2.00000E+01	2.50000E+00	0.00000E-02	4	3	7.34742E-06	1.35143E+01	-7.02299E+00
2.00000E+01	2.50000E+00	0.00000E-02	5	4	1.13086E-05	2.08522E+01	-6.75634E+00
2.00000E+01	2.50000E+00	0.00000E-02	6	5	1.58133E-05	2.32209E+01	-6.52830E+00
2.00000E+01	2.50000E+00	1.00000E-01	2	1	1.40809E-06	2.57697E+00	-7.47775E+00
2.00000E+01	2.50000E+00	1.00000E-01	3	2	3.73216E-06	6.56305E+00	-7.04826E+00
2.00000E+01	2.50000E+00	1.00000E-01	4	3	6.75091E-06	1.24535E+01	-6.71016E+00
2.00000E+01	2.50000E+00	1.00000E-01	5	4	1.03246E-05	1.30958E+01	-6.43166E+00
2.00000E+01	2.50000E+00	1.00000E-01	6	5	1.43539E-05	2.56072E+01	-6.19563E+00
2.00000E+01	2.50000E+00	1.20000E-01	2	1	1.32565E-06	2.43339E+00	-7.23943E+00
2.00000E+01	2.50000E+00	1.20000E-01	3	2	3.48740E-06	6.42652E+00	-6.75931E+00
2.00000E+01	2.50000E+00	1.20000E-01	4	3	6.26728E-06	1.15909E+01	-6.43837E+00
2.00000E+01	2.50000E+00	1.20000E-01	5	4	9.52952E-06	1.76717E+01	-6.15195E+00
2.00000E+01	2.50000E+00	1.20000E-01	6	5	1.31793E-05	2.44956E+01	-5.91120E+00
2.00000E+01	2.50000E+00	1.40000E-01	2	1	1.25612E-06	2.31039E+00	-7.02415E+00
2.00000E+01	2.50000E+00	1.40000E-01	3	2	3.28150E-06	6.56213E+00	-6.55753E+00
2.00000E+01	2.50000E+00	1.40000E-01	4	3	5.86173E-06	1.08656E+01	-6.19719E+00
2.00000E+01	2.50000E+00	1.40000E-01	5	4	8.86546E-06	1.64785E+01	-5.90563E+00
2.00000E+01	2.50000E+00	1.40000E-01	6	5	1.22024E-05	2.27333E+01	-5.66237E+00
2.00000E+01	2.50000E+00	1.60000E-01	2	1	1.19604E-06	2.20394E+00	-6.82685E+00
2.00000E+01	2.50000E+00	1.60000E-01	3	2	3.10410E-06	5.74575E+00	-6.34701E+00
2.00000E+01	2.50000E+00	1.60000E-01	4	3	5.51366E-06	1.02412E+01	-5.97989E+00
2.00000E+01	2.50000E+00	1.60000E-01	5	4	8.29771E-06	1.54554E+01	-5.68520E+00
2.00000E+01	2.50000E+00	1.60000E-01	6	5	1.13709E-05	2.12286E+01	-5.44390E+00

TABLE A-3 (CONT)
TYPE I GAGE, GENERAL DESIGNS

LENGTH (INCHES)	WIDTH (INCHES)	LOOP SPACING (INCHES)	PRI TURNS	SEC TURNS	MUTUAL INDUCT (HENRIES)	GAGE FACTOR $\left(\frac{MV}{AMP \cdot MM/JSEC}\right)$	ERROR TERM (PERCENT)
4.00000E+01	2.50000E+00	0.00000E-02	2	1	2.96310E-06	2.75492E+00	-3.93342E+00
4.00000E+01	2.50000E+00	0.00000E-02	3	2	7.76799E-06	7.38910E+00	-3.73859E+00
4.00000E+01	2.50000E+00	0.00000E-02	4	3	1.42079E-05	1.35003E+01	-3.58441E+00
4.00000E+01	2.50000E+00	0.00000E-02	5	4	2.16936E-05	2.08206E+01	-3.45077E+00
4.00000E+01	2.50000E+00	0.00000E-02	6	5	3.06490E-05	2.91059E+01	-3.34313E+00
4.00000E+01	2.50000E+00	1.00000E-01	2	1	2.71741E-06	2.97663E+00	-3.60277E+00
4.00000E+01	2.50000E+00	1.00000E-01	3	2	7.21622E-06	6.95634E+00	-3.59594E+00
4.00000E+01	2.50000E+00	1.00000E-01	4	3	1.30726E-05	1.24395E+01	-3.43402E+00
4.00000E+01	2.50000E+00	1.00000E-01	5	4	2.00173E-05	1.90724E+01	-3.30144E+00
4.00000E+01	2.50000E+00	1.00000E-01	6	5	2.76585E-05	2.95722E+01	-3.10979E+00
4.00000E+01	2.50000E+00	1.20000E-01	2	1	2.56102E-06	2.43105E+00	-3.68732E+00
4.00000E+01	2.50000E+00	1.20000E-01	3	2	6.75072E-06	6.42150E+00	-3.47117E+00
4.00000E+01	2.50000E+00	1.20000E-01	4	3	1.21507E-05	1.15769E+01	-3.30383E+00
4.00000E+01	2.50000E+00	1.20000E-01	5	4	1.84989E-05	1.76484E+01	-3.10827E+00
4.00000E+01	2.50000E+00	1.20000E-01	6	5	2.56113E-05	2.44606E+01	-3.05526E+00
4.00000E+01	2.50000E+00	1.40000E-01	2	1	2.42901E-06	2.30005E+00	-3.50317E+00
4.00000E+01	2.50000E+00	1.40000E-01	3	2	6.35869E-06	6.55511E+00	-3.35976E+00
4.00000E+01	2.50000E+00	1.40000E-01	4	3	1.13768E-05	1.08516E+01	-3.10871E+00
4.00000E+01	2.50000E+00	1.40000E-01	5	4	1.72287E-05	1.64552E+01	-3.05159E+00
4.00000E+01	2.50000E+00	1.40000E-01	6	5	2.37391E-05	2.25983E+01	-2.93831E+00
4.00000E+01	2.50000E+00	1.60000E-01	2	1	2.31485E-06	2.20161E+00	-3.48785E+00
4.00000E+01	2.50000E+00	1.60000E-01	3	2	6.02057E-06	5.73874E+00	-3.25803E+00
4.00000E+01	2.50000E+00	1.60000E-01	4	3	1.07115E-05	1.02272E+01	-3.00539E+00
4.00000E+01	2.50000E+00	1.60000E-01	5	4	1.61412E-05	1.54321E+01	-2.94770E+00
4.00000E+01	2.50000E+00	1.60000E-01	6	5	2.21432E-05	2.11936E+01	-2.83491E+00
5.00000E+01	2.50000E+00	0.00000E-02	2	1	4.30847E-06	2.75449E+00	-2.03529E+00
5.00000E+01	2.50000E+00	0.00000E-02	3	2	1.15413E-05	7.38730E+00	-2.50693E+00
5.00000E+01	2.50000E+00	0.00000E-02	4	3	2.10653E-05	1.34977E+01	-2.40549E+00
5.00000E+01	2.50000E+00	0.00000E-02	5	4	3.24733E-05	2.09249E+01	-2.32105E+00
5.00000E+01	2.50000E+00	0.00000E-02	6	5	4.54730E-05	2.91793E+01	-2.25042E+00
5.00000E+01	2.50000E+00	1.00000E-01	2	1	4.02020E-06	2.57020E+00	-2.54903E+00
5.00000E+01	2.50000E+00	1.00000E-01	3	2	1.06987E-05	6.95474E+00	-2.41293E+00
5.00000E+01	2.50000E+00	1.00000E-01	4	3	1.93911E-05	1.24369E+01	-2.30000E+00
5.00000E+01	2.50000E+00	1.00000E-01	5	4	2.97046E-05	1.90881E+01	-2.21966E+00
5.00000E+01	2.50000E+00	1.00000E-01	6	5	4.13551E-05	2.95657E+01	-2.14603E+00
5.00000E+01	2.50000E+00	1.20000E-01	2	1	3.79506E-06	2.43061E+00	-2.47293E+00
5.00000E+01	2.50000E+00	1.20000E-01	3	2	1.00124E-05	6.42023E+00	-2.33079E+00
5.00000E+01	2.50000E+00	1.20000E-01	4	3	1.90310E-05	1.15743E+01	-2.22103E+00
5.00000E+01	2.50000E+00	1.20000E-01	5	4	2.74629E-05	1.76440E+01	-2.13236E+00
5.00000E+01	2.50000E+00	1.20000E-01	6	5	3.90353E-05	2.44541E+01	-2.05065E+00
5.00000E+01	2.50000E+00	1.40000E-01	2	1	3.60137E-06	2.39702E+00	-2.40427E+00
5.00000E+01	2.50000E+00	1.40000E-01	3	2	9.43429E-06	6.95381E+00	-2.25722E+00
5.00000E+01	2.50000E+00	1.40000E-01	4	3	1.68886E-05	1.08490E+01	-2.14553E+00
5.00000E+01	2.50000E+00	1.40000E-01	5	4	2.55866E-05	1.64909E+01	-2.05601E+00
5.00000E+01	2.50000E+00	1.40000E-01	6	5	3.52679E-05	2.26918E+01	-1.93236E+00
5.00000E+01	2.50000E+00	1.60000E-01	2	1	3.43313E-06	2.21117E+00	-2.34140E+00
5.00000E+01	2.50000E+00	1.60000E-01	3	2	9.93545E-06	5.73744E+00	-2.19119E+00
5.00000E+01	2.50000E+00	1.60000E-01	4	3	1.99901E-05	1.02246E+01	-2.07750E+00
5.00000E+01	2.50000E+00	1.60000E-01	5	4	2.39793E-05	1.54277E+01	-1.93315E+00
5.00000E+01	2.50000E+00	1.60000E-01	6	5	3.29370E-05	2.11371E+01	-1.91500E+00

TABLE A-3 (CONT)
TYPE I GAGE, GENERAL DESIGNS

LENGTH (INCHES)	WIDTH (INCHES)	LOOP SPACING (INCHES)	PRI TURNS	SEC TURNS	MUTUAL INDUC (HENRIES)	GAGE FACTOR MV (AMP*MM/USEC)	ERROR TERM (PERCENT)
2.00000E+01	3.00000E+00	8.00000E-02	2	1	1.61535E-06	2.30437E+00	-9.46445E+00
2.00000E+01	3.00000E+00	8.00000E-02	3	2	4.33999E-06	7.63644E+00	-9.01993E+00
2.00000E+01	3.00000E+00	8.00000E-02	4	3	7.94342E-06	1.43920E+01	-8.64797E+00
2.00000E+01	3.00000E+00	8.00000E-02	5	4	1.22775E-05	2.23086E+01	-8.33623E+00
2.00000E+01	3.00000E+00	8.00000E-02	6	5	1.72347E-05	3.13930E+01	-8.06761E+00
2.00000E+01	3.00000E+00	1.00000E-01	2	1	1.51194E-06	2.72600E+00	-9.18007E+00
2.00000E+01	3.00000E+00	1.00000E-01	3	2	4.03186E-06	7.30262E+00	-8.68337E+00
2.00000E+01	3.00000E+00	1.00000E-01	4	3	7.33189E-06	1.33281E+01	-8.28854E+00
2.00000E+01	3.00000E+00	1.00000E-01	5	4	1.12669E-05	2.05436E+01	-7.96017E+00
2.00000E+01	3.00000E+00	1.00000E-01	6	5	1.57327E-05	2.87613E+01	-7.67425E+00
2.00000E+01	3.00000E+00	1.20000E-01	2	1	1.42761E-06	2.58034E+00	-8.91063E+00
2.00000E+01	3.00000E+00	1.20000E-01	3	2	3.78112E-06	6.56716E+00	-8.38767E+00
2.00000E+01	3.00000E+00	1.20000E-01	4	3	6.83544E-06	1.24618E+01	-7.97508E+00
2.00000E+01	3.00000E+00	1.20000E-01	5	4	1.04487E-05	1.91094E+01	-7.63449E+00
2.00000E+01	3.00000E+00	1.20000E-01	6	5	1.45204E-05	2.66277E+01	-7.34516E+00
2.00000E+01	3.00000E+00	1.40000E-01	2	1	1.35647E-06	2.45724E+00	-8.66725E+00
2.00000E+01	3.00000E+00	1.40000E-01	3	2	3.57003E-06	6.49969E+00	-8.12242E+00
2.00000E+01	3.00000E+00	1.40000E-01	4	3	6.41857E-06	1.17321E+01	-7.69590E+00
2.00000E+01	3.00000E+00	1.40000E-01	5	4	9.76373E-06	1.79046E+01	-7.34634E+00
2.00000E+01	3.00000E+00	1.40000E-01	6	5	1.35088E-05	2.48406E+01	-7.05132E+00
2.00000E+01	3.00000E+00	1.60000E-01	2	1	1.29498E-06	2.35068E+00	-8.44393E+00
2.00000E+01	3.00000E+00	1.60000E-01	3	2	3.38799E-06	6.18207E+00	-7.65095E+00
2.00000E+01	3.00000E+00	1.60000E-01	4	3	6.06009E-06	1.11029E+01	-7.44343E+00
2.00000E+01	3.00000E+00	1.60000E-01	5	4	9.17658E-06	1.88686E+01	-7.08742E+00
2.00000E+01	3.00000E+00	1.60000E-01	6	5	1.26447E-05	2.33083E+01	-6.75865E+00
4.00000E+01	3.00000E+00	8.00000E-02	2	1	3.08963E-06	2.90100E+00	-4.82503E+00
4.00000E+01	3.00000E+00	8.00000E-02	3	2	8.31748E-06	7.82635E+00	-4.60174E+00
4.00000E+01	3.00000E+00	8.00000E-02	4	3	1.52477E-05	1.43719E+01	-4.42365E+00
4.00000E+01	3.00000E+00	8.00000E-02	5	4	2.35989E-05	2.22750E+01	-4.27504E+00
4.00000E+01	3.00000E+00	8.00000E-02	6	5	3.31657E-05	3.13434E+01	-4.14753E+00
4.00000E+01	3.00000E+00	1.00000E-01	2	1	2.89561E-06	2.72264E+00	-4.67807E+00
4.00000E+01	3.00000E+00	1.00000E-01	3	2	7.73518E-06	7.29253E+00	-4.43993E+00
4.00000E+01	3.00000E+00	1.00000E-01	4	3	1.40958E-05	1.33080E+01	-4.25162E+00
4.00000E+01	3.00000E+00	1.00000E-01	5	4	2.16917E-05	2.05100E+01	-4.09586E+00
4.00000E+01	3.00000E+00	1.00000E-01	6	5	3.03264E-05	2.87133E+01	-3.90333E+00
4.00000E+01	3.00000E+00	1.20000E-01	2	1	2.73729E-06	2.57697E+00	-4.54818E+00
4.00000E+01	3.00000E+00	1.20000E-01	3	2	7.26622E-06	6.55707E+00	-4.29809E+00
4.00000E+01	3.00000E+00	1.20000E-01	4	3	1.31592E-05	1.24416E+01	-4.10208E+00
4.00000E+01	3.00000E+00	1.20000E-01	5	4	2.01440E-05	1.90758E+01	-3.94139E+00
4.00000E+01	3.00000E+00	1.20000E-01	6	5	2.80302E-05	2.65773E+01	-3.80588E+00
4.00000E+01	3.00000E+00	1.40000E-01	2	1	2.60361E-06	2.45388E+00	-4.43995E+00
4.00000E+01	3.00000E+00	1.40000E-01	3	2	6.86946E-06	6.48960E+00	-4.17115E+00
4.00000E+01	3.00000E+00	1.40000E-01	4	3	1.23717E-05	1.17113E+01	-3.96336E+00
4.00000E+01	3.00000E+00	1.40000E-01	5	4	1.88479E-05	1.78710E+01	-3.80536E+00
4.00000E+01	3.00000E+00	1.40000E-01	6	5	2.61108E-05	2.47933E+01	-3.66818E+00
4.00000E+01	3.00000E+00	1.60000E-01	2	1	2.48793E-06	2.34731E+00	-4.32358E+00
4.00000E+01	3.00000E+00	1.60000E-01	3	2	6.52500E-06	6.17199E+00	-4.15586E+00
4.00000E+01	3.00000E+00	1.60000E-01	4	3	1.16935E-05	1.10827E+01	-3.80378E+00
4.00000E+01	3.00000E+00	1.60000E-01	5	4	1.77345E-05	1.63350E+01	-3.63370E+00
4.00000E+01	3.00000E+00	1.60000E-01	6	5	2.44655E-05	2.32980E+01	-3.54583E+00

TABLE A-3 (CONT)
TYPE I GAGE, GENERAL DESIGNS

LENGTH (INCHES)	WIDTH (INCHES)	LOOP SPACING (INCHES)	PRI TURNS	SEC TURNS	MUTUAL INDUCT (HENRIES)	GAGE FACTOR $\left(\frac{MV}{AMP \cdot MM/JSEC}\right)$	ERROR TERM (PERCENT)
5.00000E+01	3.00000E+00	6.00000E-02	2	1	4.56315E-06	2.90038E+00	-3.23460E+00
5.00000E+01	3.00000E+00	6.00000E-02	3	2	1.22927E-05	7.62448E+00	-3.03771E+00
5.00000E+01	3.00000E+00	6.00000E-02	4	3	2.25475E-05	1.43681E+01	-2.97473E+00
5.00000E+01	3.00000E+00	6.00000E-02	5	4	3.45127E-05	2.22688E+01	-2.67326E+00
5.00000E+01	3.00000E+00	6.00000E-02	6	5	4.90553E-05	3.13340E+01	-2.75976E+00
5.00000E+01	3.00000E+00	1.00000E-01	2	1	4.27892E-06	2.72202E+00	-3.13773E+00
5.00000E+01	3.00000E+00	1.00000E-01	3	2	1.14422E-05	7.29066E+00	-2.95127E+00
5.00000E+01	3.00000E+00	1.00000E-01	4	3	2.08551E-05	1.33342E+01	-2.65774E+00
5.00000E+01	3.00000E+00	1.00000E-01	5	4	3.21099E-05	2.05035E+01	-2.75576E+00
5.00000E+01	3.00000E+00	1.00000E-01	6	5	4.49057E-05	2.87015E+01	-2.66922E+00
5.00000E+01	3.00000E+00	1.20000E-01	2	1	4.04620E-06	2.57635E+00	-3.05224E+00
5.00000E+01	3.00000E+00	1.20000E-01	3	2	1.07496E-05	6.5520E+00	-2.86904E+00
5.00000E+01	3.00000E+00	1.20000E-01	4	3	1.94754E-05	1.24378E+01	-2.75964E+00
5.00000E+01	3.00000E+00	1.20000E-01	5	4	2.98330E-05	1.90696E+01	-2.65904E+00
5.00000E+01	3.00000E+00	1.20000E-01	6	5	4.15266E-05	2.65679E+01	-2.56634E+00
5.00000E+01	3.00000E+00	1.40000E-01	2	1	3.84999E-06	2.45325E+00	-2.97508E+00
5.00000E+01	3.00000E+00	1.40000E-01	3	2	1.01646E-05	6.48773E+00	-2.80465E+00
5.00000E+01	3.00000E+00	1.40000E-01	4	3	1.83202E-05	1.17052E+01	-2.67268E+00
5.00000E+01	3.00000E+00	1.40000E-01	5	4	2.79245E-05	1.78648E+01	-2.56574E+00
5.00000E+01	3.00000E+00	1.40000E-01	6	5	3.87014E-05	2.47509E+01	-2.47659E+00
5.00000E+01	3.00000E+00	1.60000E-01	2	1	3.65023E-06	2.34689E+00	-2.90444E+00
5.00000E+01	3.00000E+00	1.60000E-01	3	2	9.65985E-06	6.17012E+00	-2.72901E+00
5.00000E+01	3.00000E+00	1.60000E-01	4	3	1.73224E-05	1.10790E+01	-2.59443E+00
5.00000E+01	3.00000E+00	1.60000E-01	5	4	2.62545E-05	1.68285E+01	-2.48633E+00
5.00000E+01	3.00000E+00	1.60000E-01	6	5	3.62811E-05	2.32492E+01	-2.39703E+00

TABLE A-4
TYPE II GAGE, GENERAL DESIGNS

LENGTH (INCHES)	WIDTH (INCHES)	LOOP SPACING (INCHES)	PRI/SEC PATTERN	MUTUAL INDUCT (HENRIES)	GAGE FACTOR MV (AMP*MM/USEC)	ERROR TERM (PERCENT)
2.00000E+01	2.00000E+00	8.00000E-02	00X00	2.47105E-06	4.60306E+00	-5.67471E+00
2.00000E+01	2.00000E+00	8.00000E-02	000X000	3.37703E-06	6.30706E+00	-5.40076E+00
2.00000E+01	2.00000E+00	8.00000E-02	0000X0000	4.15954E-06	7.78530E+00	-5.17344E+00
2.00000E+01	2.00000E+00	8.00000E-02	00X00X00	6.41301E-06	1.19897E+01	-5.29117E+00
2.00000E+01	2.00000E+00	8.00000E-02	000X000X000	8.60620E-06	1.61325E+01	-4.98999E+00
2.00000E+01	2.00000E+00	8.00000E-02	00X00X00X00	1.14037E-05	2.13794E+01	-4.99940E+00
2.00000E+01	2.00000E+00	8.00000E-02	000X000X000X000	1.50806E-05	2.83574E+01	-4.68579E+00
2.00000E+01	2.00000E+00	1.00000E-01	00X00	2.27474E-06	4.24781E+00	-5.41544E+00
2.00000E+01	2.00000E+00	1.00000E-01	000X000	3.08477E-06	5.77646E+00	-5.12290E+00
2.00000E+01	2.00000E+00	1.00000E-01	0000X0000	3.77317E-06	7.08175E+00	-4.88236E+00
2.00000E+01	2.00000E+00	1.00000E-01	00X00X00	5.83428E-06	1.09362E+01	-5.01609E+00
2.00000E+01	2.00000E+00	1.00000E-01	000X000X000	7.75275E-06	1.45761E+01	-4.70127E+00
2.00000E+01	2.00000E+00	1.00000E-01	00X00X00X00	1.02708E-05	1.93072E+01	-4.71766E+00
2.00000E+01	2.00000E+00	1.00000E-01	000X000X000X000	1.34290E-05	2.53220E+01	-4.39557E+00
2.00000E+01	2.00000E+00	1.20000E-01	00X00	2.11511E-06	3.95826E+00	-5.18755E+00
2.00000E+01	2.00000E+00	1.20000E-01	000X000	2.84772E-06	5.34490E+00	-4.88033E+00
2.00000E+01	2.00000E+00	1.20000E-01	0000X0000	3.46075E-06	6.51104E+00	-4.63032E+00
2.00000E+01	2.00000E+00	1.20000E-01	00X00X00	5.36656E-06	1.00823E+01	-4.77833E+00
2.00000E+01	2.00000E+00	1.20000E-01	000X000X000	7.06721E-06	1.33186E+01	-4.45419E+00
2.00000E+01	2.00000E+00	1.20000E-01	00X00X00X00	9.36211E-06	1.76395E+01	-4.47742E+00
2.00000E+01	2.00000E+00	1.20000E-01	000X000X000X000	1.21172E-05	2.29023E+01	-4.15043E+00
2.00000E+01	2.00000E+00	1.40000E-01	00X00	1.98082E-06	3.71417E+00	-4.98320E+00
2.00000E+01	2.00000E+00	1.40000E-01	000X000	2.64890E-06	4.98200E+00	-4.66427E+00
2.00000E+01	2.00000E+00	1.40000E-01	0000X0000	3.19961E-06	6.03260E+00	-4.40676E+00
2.00000E+01	2.00000E+00	1.40000E-01	00X00X00	4.97584E-06	9.36705E+00	-4.56829E+00
2.00000E+01	2.00000E+00	1.40000E-01	000X000X000	6.49830E-06	1.22719E+01	-4.23772E+00
2.00000E+01	2.00000E+00	1.40000E-01	00X00X00X00	8.60924E-06	1.62537E+01	-4.26763E+00
2.00000E+01	2.00000E+00	1.40000E-01	000X000X000X000	1.10412E-05	2.09112E+01	-3.93772E+00
2.00000E+01	2.00000E+00	1.60000E-01	00X00	1.86113E-06	3.50345E+00	-4.79734E+00
2.00000E+01	2.00000E+00	1.60000E-01	000X000	2.47816E-06	4.66959E+00	-4.46906E+00
2.00000E+01	2.00000E+00	1.60000E-01	0000X0000	2.97619E-06	5.62217E+00	-4.20629E+00
2.00000E+01	2.00000E+00	1.60000E-01	00X00X00	4.64176E-06	8.75391E+00	-4.37988E+00
2.00000E+01	2.00000E+00	1.60000E-01	000X000X000	6.01524E-06	1.13807E+01	-4.04479E+00
2.00000E+01	2.00000E+00	1.60000E-01	00X00X00X00	7.97099E-06	1.50757E+01	-4.08108E+00
2.00000E+01	2.00000E+00	1.60000E-01	000X000X000X000	1.01381E-05	1.92357E+01	-3.74926E+00

TABLE A-4 (CONT)
TYPE II GAGE, GENERAL DESIGNS

LENGTH (INCHES)	WIDTH (INCHES)	LOOP SPACING (INCHES)	PRI/SEC PATTERN	MUTUAL INDUCT (HENRIES)	GAGE FACTOR ($\frac{MW}{AMP \cdot MM/USEC}$)	ERROR TERM (PERCENT)
4.00000E+01	2.00000E+00	8.00000E-02	00X00	4.80839E-06	4.60007E+00	-2.88261E+00
4.00000E+01	2.00000E+00	8.00000E-02	000X000	6.57949E-06	6.30257E+00	-2.74983E+00
4.00000E+01	2.00000E+00	8.00000E-02	0000X0000	8.11244E-06	7.77931E+00	-2.64004E+00
4.00000E+01	2.00000E+00	8.00000E-02	00X00X00	1.25007E-05	1.19807E+01	-2.69756E+00
4.00000E+01	2.00000E+00	8.00000E-02	000X000X000	1.67988E-05	1.61227E+01	-2.55274E+00
4.00000E+01	2.00000E+00	8.00000E-02	00X00X00X00	2.22584E-05	2.13615E+01	-2.55786E+00
4.00000E+01	2.00000E+00	8.00000E-02	000X000X000X000	2.94776E-05	2.83304E+01	-2.40849E+00
4.00000E+01	2.00000E+00	1.00000E-01	00X00	4.43162E-06	4.24481E+00	-2.75667E+00
4.00000E+01	2.00000E+00	1.00000E-01	000X000	6.01769E-06	5.77197E+00	-2.61533E+00
4.00000E+01	2.00000E+00	1.00000E-01	0000X0000	7.36868E-06	7.07576E+00	-2.49957E+00
4.00000E+01	2.00000E+00	1.00000E-01	00X00X00	1.13868E-05	1.09272E+01	-2.56490E+00
4.00000E+01	2.00000E+00	1.00000E-01	000X000X000	1.51528E-05	1.45626E+01	-2.41446E+00
4.00000E+01	2.00000E+00	1.00000E-01	00X00X00X00	2.00727E-05	1.92892E+01	-2.42308E+00
4.00000E+01	2.00000E+00	1.00000E-01	000X000X000X000	2.62835E-05	2.52951E+01	-2.27104E+00
4.00000E+01	2.00000E+00	1.20000E-01	00X00	4.12489E-06	3.95526E+00	-2.64622E+00
4.00000E+01	2.00000E+00	1.20000E-01	000X000	5.56141E-06	5.34041E+00	-2.49829E+00
4.00000E+01	2.00000E+00	1.20000E-01	0000X0000	6.76634E-06	6.57506E+00	-2.37850E+00
4.00000E+01	2.00000E+00	1.20000E-01	00X00X00	1.04854E-05	1.00734E+01	-2.45071E+00
4.00000E+01	2.00000E+00	1.20000E-01	000X000X000	1.38285E-05	1.33051E+01	-2.29680E+00
4.00000E+01	2.00000E+00	1.20000E-01	00X00X00X00	1.83169E-05	1.76216E+01	-2.30888E+00
4.00000E+01	2.00000E+00	1.20000E-01	000X000X000X000	2.37425E-05	2.28754E+01	-2.15680E+00
4.00000E+01	2.00000E+00	1.40000E-01	00X00	3.86660E-06	3.71117E+00	-2.54741E+00
4.00000E+01	2.00000E+00	1.40000E-01	000X000	5.17823E-06	4.97751E+00	-2.39439E+00
4.00000E+01	2.00000E+00	1.40000E-01	0000X0000	6.26214E-06	6.02661E+00	-2.27178E+00
4.00000E+01	2.00000E+00	1.40000E-01	00X00X00	9.73126E-06	9.35807E+00	-2.35029E+00
4.00000E+01	2.00000E+00	1.40000E-01	000X000X000	1.27279E-05	1.22584E+01	-2.19436E+00
4.00000E+01	2.00000E+00	1.40000E-01	00X00X00X00	1.68600E-05	1.62357E+01	-2.20981E+00
4.00000E+01	2.00000E+00	1.40000E-01	000X000X000X000	2.16550E-05	2.08844E+01	-2.05711E+00
4.00000E+01	2.00000E+00	1.60000E-01	00X00	3.64387E-06	3.50046E+00	-2.45775E+00
4.00000E+01	2.00000E+00	1.60000E-01	000X000	4.84880E-06	4.66510E+00	-2.30084E+00
4.00000E+01	2.00000E+00	1.60000E-01	0000X0000	5.83023E-06	5.61618E+00	-2.17642E+00
4.00000E+01	2.00000E+00	1.60000E-01	00X00X00	9.08570E-06	8.74493E+00	-2.26060E+00
4.00000E+01	2.00000E+00	1.60000E-01	000X000X000	1.17921E-05	1.13673E+01	-2.10364E+00
4.00000E+01	2.00000E+00	1.60000E-01	00X00X00X00	1.56234E-05	1.50578E+01	-2.12231E+00
4.00000E+01	2.00000E+00	1.60000E-01	000X000X000X000	1.99007E-05	1.92089E+01	-1.97033E+00

TABLE A-4 (CONT)
TYPE II GAGE, GENERAL DESIGNS

LENGTH (INCHES)	WIDTH (INCHES)	LOOP SPACING (INCHES)	PRI/SEC PATTERN	MUTUAL INDUC (HENRIES)	GAGE FACTOR $\frac{MV}{(AMP \cdot MM/USEC)}$	ERROR TERM (PERCENT)
6.0000E+01	2.0000E+00	8.0000E-02	00X00	7.14506E-06	4.59951E+00	-1.93163E+00
6.0000E+01	2.0000E+00	8.0000E-02	000X000	9.78095E-06	6.30174E+00	-1.84434E+00
6.0000E+01	2.0000E+00	8.0000E-02	0000X0000	1.20640E-05	7.77820E+00	-1.77173E+00
6.0000E+01	2.0000E+00	8.0000E-02	00X00X00	1.85864E-05	1.19790E+01	-1.80975E+00
6.0000E+01	2.0000E+00	8.0000E-02	000X000X000	2.49884E-05	1.61202E+01	-1.71449E+00
6.0000E+01	2.0000E+00	8.0000E-02	00X00X00X00	3.31090E-05	2.13581E+01	-1.71798E+00
6.0000E+01	2.0000E+00	8.0000E-02	000X000X000X000	4.38673E-05	2.83254E+01	-1.62035E+00
6.0000E+01	2.0000E+00	1.0000E-01	00X00	6.58781E-06	4.24426E+00	-1.84849E+00
6.0000E+01	2.0000E+00	1.0000E-01	000X000	8.94960E-06	5.77114E+00	-1.67825E+00
6.0000E+01	2.0000E+00	1.0000E-01	0000X0000	1.09628E-05	7.07465E+00	-1.67927E+00
6.0000E+01	2.0000E+00	1.0000E-01	00X00X00	1.69374E-05	1.08056E+01	-1.72239E+00
6.0000E+01	2.0000E+00	1.0000E-01	000X000X000	2.25499E-05	1.45601E+01	-1.62364E+00
6.0000E+01	2.0000E+00	1.0000E-01	00X00X00X00	2.98707E-05	1.92859E+01	-1.62948E+00
6.0000E+01	2.0000E+00	1.0000E-01	000X000X000X000	3.91719E-05	2.52901E+01	-1.53012E+00
6.0000E+01	2.0000E+00	1.2000E-01	00X00	6.13399E-06	3.95471E+00	-1.77563E+00
6.0000E+01	2.0000E+00	1.2000E-01	000X000	8.27409E-06	5.33958E+00	-1.67825E+00
6.0000E+01	2.0000E+00	1.2000E-01	0000X0000	1.00706E-05	6.50395E+00	-1.59950E+00
6.0000E+01	2.0000E+00	1.2000E-01	00X00X00	1.56021E-05	1.00717E+01	-1.64731E+00
6.0000E+01	2.0000E+00	1.2000E-01	000X000X000	2.05867E-05	1.33026E+01	-1.54651E+00
6.0000E+01	2.0000E+00	1.2000E-01	00X00X00X00	2.72677E-05	1.76183E+01	-1.55467E+00
6.0000E+01	2.0000E+00	1.2000E-01	000X000X000X000	3.53617E-05	2.28704E+01	-1.45511E+00
6.0000E+01	2.0000E+00	1.4000E-01	00X00	5.75171E-06	3.71062E+00	-1.71050E+00
6.0000E+01	2.0000E+00	1.4000E-01	000X000	7.70655E-06	4.97667E+00	-1.60991E+00
6.0000E+01	2.0000E+00	1.4000E-01	0000X0000	9.32332E-06	6.02550E+00	-1.52954E+00
6.0000E+01	2.0000E+00	1.4000E-01	00X00X00	1.44847E-05	9.35641E+00	-1.58138E+00
6.0000E+01	2.0000E+00	1.4000E-01	000X000X000	1.89544E-05	1.22559E+01	-1.47951E+00
6.0000E+01	2.0000E+00	1.4000E-01	00X00X00X00	2.51068E-05	1.62324E+01	-1.48992E+00
6.0000E+01	2.0000E+00	1.4000E-01	000X000X000X000	3.22628E-05	2.08794E+01	-1.39086E+00
6.0000E+01	2.0000E+00	1.6000E-01	00X00	5.42194E-06	3.49990E+00	-1.65145E+00
6.0000E+01	2.0000E+00	1.6000E-01	000X000	7.21841E-06	4.86427E+00	-1.54845E+00
6.0000E+01	2.0000E+00	1.6000E-01	0000X0000	8.68291E-06	5.61507E+00	-1.46735E+00
6.0000E+01	2.0000E+00	1.6000E-01	00X00X00	1.35276E-05	8.74327E+00	-1.52259E+00
6.0000E+01	2.0000E+00	1.6000E-01	000X000X000	1.75659E-05	1.13648E+01	-1.42032E+00
6.0000E+01	2.0000E+00	1.6000E-01	00X00X00X00	2.32717E-05	1.50544E+01	-1.43288E+00
6.0000E+01	2.0000E+00	1.6000E-01	000X000X000X000	2.96573E-05	1.92039E+01	-1.33468E+00

TABLE A-4 (CONT)
TYPE II GAGE, GENERAL DESIGNS

LENGTH (INCHES)	WIDTH (INCHES)	LOOP SPACING (INCHES)	PRT/SEC PATTERN	MUTUAL INDUC (HENRIS)	GAGE FACTOR $\left(\frac{MV}{AMP \cdot MM/USEC}\right)$	ERROR TERM (PERCENT)
2.0000E+01	2.5000E+00	8.0000E-02	00X00	2.70524E-06	4.96120E+00	-7.33828E+00
2.0000E+01	2.5000E+00	8.0000E-02	000X000	3.7190E-06	6.84280E+00	-7.01453E+00
2.0000E+01	2.5000E+00	8.0000E-02	0000X0000	4.6076E-06	8.4976E+00	-6.74379E+00
2.0000E+01	2.5000E+00	8.0000E-02	00X00X00	7.0894E-06	1.30960E+01	-6.87490E+00
2.0000E+01	2.5000E+00	8.0000E-02	000X000X000	9.58921E-06	1.77224E+01	-6.51126E+00
2.0000E+01	2.5000E+00	8.0000E-02	00X00X00X00	1.2710E-05	2.34891E+01	-6.51609E+00
2.0000E+01	2.5000E+00	8.0000E-02	000X000X000X000	1.69679E-05	3.14716E+01	-6.13027E+00
2.0000E+01	2.5000E+00	1.0000E-01	00X00	2.5341E-06	4.60531E+00	-7.03583E+00
2.0000E+01	2.5000E+00	1.0000E-01	000X000	3.4201E-06	6.31042E+00	-6.68814E+00
2.0000E+01	2.5000E+00	1.0000E-01	0000X0000	4.21044E-06	7.76979E+00	-6.39913E+00
2.0000E+01	2.5000E+00	1.0000E-01	00X00X00	6.4932E-06	1.19964E+01	-6.54798E+00
2.0000E+01	2.5000E+00	1.0000E-01	000X000X000	8.70786E-06	1.61462E+01	-6.16410E+00
2.0000E+01	2.5000E+00	1.0000E-01	00X00X00X00	1.15387E-05	2.13929E+01	-6.17554E+00
2.0000E+01	2.5000E+00	1.0000E-01	000X000X000X000	1.52482E-05	2.83775E+01	-5.77427E+00
2.0000E+01	2.5000E+00	1.2000E-01	00X00	2.34039E-06	4.31498E+00	-6.76929E+00
2.0000E+01	2.5000E+00	1.2000E-01	000X000	3.17649E-06	5.87672E+00	-6.40194E+00
2.0000E+01	2.5000E+00	1.2000E-01	0000X0000	3.88852E-06	7.21458E+00	-6.09850E+00
2.0000E+01	2.5000E+00	1.2000E-01	00X00X00	6.01093E-06	1.11351E+01	-6.26377E+00
2.0000E+01	2.5000E+00	1.2000E-01	000X000X000	7.99699E-06	1.48700E+01	-5.86474E+00
2.0000E+01	2.5000E+00	1.2000E-01	00X00X00X00	1.05950E-05	1.96975E+01	-5.88299E+00
2.0000E+01	2.5000E+00	1.2000E-01	000X000X000X000	1.38728E-05	2.58920E+01	-5.47127E+00
2.0000E+01	2.5000E+00	1.4000E-01	00X00	2.2025E-06	4.06997E+00	-6.52957E+00
2.0000E+01	2.5000E+00	1.4000E-01	000X000	2.97181E-06	5.51132E+00	-6.14555E+00
2.0000E+01	2.5000E+00	1.4000E-01	0000X0000	3.6187E-06	6.73095E+00	-5.83090E+00
2.0000E+01	2.5000E+00	1.4000E-01	00X00X00	5.6068E-06	1.04113E+01	-6.01142E+00
2.0000E+01	2.5000E+00	1.4000E-01	000X000X000	7.40428E-06	1.38023E+01	-5.60088E+00
2.0000E+01	2.5000E+00	1.4000E-01	00X00X00X00	9.80911E-06	1.82808E+01	-5.62536E+00
2.0000E+01	2.5000E+00	1.4000E-01	000X000X000X000	1.27363E-05	2.38306E+01	-5.20696E+00
2.0000E+01	2.5000E+00	1.6000E-01	00X00	2.08366E-06	3.85821E+00	-6.31098E+00
2.0000E+01	2.5000E+00	1.6000E-01	000X000	2.79569E-06	5.19607E+00	-5.91312E+00
2.0000E+01	2.5000E+00	1.6000E-01	0000X0000	3.38715E-06	6.31468E+00	-5.58923E+00
2.0000E+01	2.5000E+00	1.6000E-01	00X00X00	5.26029E-06	9.78873E+00	-5.78395E+00
2.0000E+01	2.5000E+00	1.6000E-01	000X000X000	6.89851E-06	1.28883E+01	-5.36452E+00
2.0000E+01	2.5000E+00	1.6000E-01	00X00X00X00	9.13934E-06	1.70697E+01	-5.39635E+00
2.0000E+01	2.5000E+00	1.6000E-01	000X000X000X000	1.17754E-05	2.20820E+01	-4.97204E+00

TABLE A-4 (CONT)
TYPE II GAGE, GENERAL DESIGNS

LENGTH (INCHES)	WIDTH (INCHES)	LOOP SPACING (INCHES)	PRI/SEC PATTERN	MUTUAL INDUC (HENRIES)	GAGE FACTOR MV (AMP*MM/USEC)	ERROR TERM (PERCENT)
4.00000E+01	2.50000E+00	8.00000E-02	00X00	5.22395E-06	4.95653E+00	-3.73550E+00
4.00000E+01	2.50000E+00	8.00000E-02	000X000	7.19375E-06	6.83578E+00	-3.57932E+00
4.00000E+01	2.50000E+00	8.00000E-02	0000X0000	8.92095E-06	8.40771E+00	-3.44906E+00
4.00000E+01	2.50000E+00	8.00000E-02	00X00X00	1.37162E-05	1.30420E+01	-3.51285E+00
4.00000E+01	2.50000E+00	8.00000E-02	000X000X000	1.85851E-05	1.77014E+01	-3.33871E+00
4.00000E+01	2.50000E+00	8.00000E-02	00X00X00X00	2.46330E-05	2.34611E+01	-3.34162E+00
4.00000E+01	2.50000E+00	8.00000E-02	000X000X000X000	3.29412E-05	3.14298E+01	-3.15840E+00
4.00000E+01	2.50000E+00	1.00000E-01	00X00	4.84201E-06	4.60063E+00	-3.58925E+00
4.00000E+01	2.50000E+00	1.00000E-01	000X000	6.62342E-06	6.30341E+00	-3.42197E+00
4.00000E+01	2.50000E+00	1.00000E-01	0000X0000	8.16448E-06	7.78043E+00	-3.28352E+00
4.00000E+01	2.50000E+00	1.00000E-01	00X00X00	1.25826E-05	1.19824E+01	-3.35585E+00
4.00000E+01	2.50000E+00	1.00000E-01	000X000X000	1.69031E-05	1.61252E+01	-3.17300E+00
4.00000E+01	2.50000E+00	1.00000E-01	00X00X00X00	2.23968E-05	2.13648E+01	-3.17929E+00
4.00000E+01	2.50000E+00	1.00000E-01	000X000X000X000	2.96497E-05	2.83355E+01	-2.99025E+00
4.00000E+01	2.50000E+00	1.20000E-01	00X00	4.53082E-06	4.31030E+00	-3.46064E+00
4.00000E+01	2.50000E+00	1.20000E-01	000X000	6.15950E-06	5.86971E+00	-3.28439E+00
4.00000E+01	2.50000E+00	1.20000E-01	0000X0000	7.55036E-06	7.20524E+00	-3.13969E+00
4.00000E+01	2.50000E+00	1.20000E-01	00X00X00	1.16628E-05	1.11211E+01	-3.21987E+00
4.00000E+01	2.50000E+00	1.20000E-01	000X000X000	1.55438E-05	1.48490E+01	-3.03088E+00
4.00000E+01	2.50000E+00	1.20000E-01	00X00X00X00	2.05918E-05	1.96694E+01	-3.04064E+00
4.00000E+01	2.50000E+00	1.20000E-01	000X000X000X000	2.70117E-05	2.58500E+01	-2.84831E+00
4.00000E+01	2.50000E+00	1.40000E-01	00X00	4.26851E-06	4.06530E+00	-3.34521E+00
4.00000E+01	2.50000E+00	1.40000E-01	000X000	5.76919E-06	5.50431E+00	-3.16166E+00
4.00000E+01	2.50000E+00	1.40000E-01	0000X0000	7.03486E-06	6.72161E+00	-3.01219E+00
4.00000E+01	2.50000E+00	1.40000E-01	00X00X00	1.08911E-05	1.03973E+01	-3.09963E+00
4.00000E+01	2.50000E+00	1.40000E-01	000X000X000	1.44087E-05	1.37813E+01	-2.90632E+00
4.00000E+01	2.50000E+00	1.40000E-01	00X00X00X00	1.90863E-05	1.82528E+01	-2.91956E+00
4.00000E+01	2.50000E+00	1.40000E-01	000X000X000X000	2.48280E-05	2.37886E+01	-2.72556E+00
4.00000E+01	2.50000E+00	1.60000E-01	00X00	4.04205E-06	3.85354E+00	-3.24015E+00
4.00000E+01	2.50000E+00	1.60000E-01	000X000	5.43292E-06	5.18906E+00	-3.05062E+00
4.00000E+01	2.50000E+00	1.60000E-01	0000X0000	6.59185E-06	6.30534E+00	-2.89753E+00
4.00000E+01	2.50000E+00	1.60000E-01	00X00X00	1.02282E-05	9.77472E+00	-2.99168E+00
4.00000E+01	2.50000E+00	1.60000E-01	000X000X000	1.34387E-05	1.28674E+01	-2.79540E+00
4.00000E+01	2.50000E+00	1.60000E-01	00X00X00X00	1.78013E-05	1.70417E+01	-2.81206E+00
4.00000E+01	2.50000E+00	1.60000E-01	000X000X000X000	2.29789E-05	2.20401E+01	-2.61740E+00

TABLE A-4 (CONT)
TYPE II GAGE, GENERAL DESIGNS

LENGTH (INCHES)	WIDTH (INCHES)	LOOP SPACING (INCHES)	PRI/SEC PATTERN	MUTUAL INDUC (HENRIES)	GAGE FACTOR $\frac{MV}{(AMP \cdot MM/USEC)}$	ERROR TERM (PERCENT)
6.00000E+01	2.50000E+00	8.00000E-02	00X00	7.74160E-06	4.95566E+00	-2.50478E+00
6.00000E+01	2.50000E+00	8.00000E-02	000X000	1.06659E-05	6.83444E+00	-2.40190E+00
6.00000E+01	2.50000E+00	8.00000E-02	0000X0000	1.32322E-05	8.48598E+00	-2.31620E+00
6.00000E+01	2.50000E+00	8.00000E-02	00X00X00	2.03407E-05	1.30394E+01	-2.35833E+00
6.00000E+01	2.50000E+00	8.00000E-02	000X000X000	2.75762E-05	1.76975E+01	-2.24394E+00
6.00000E+01	2.50000E+00	8.00000E-02	00X00X00X00	3.65496E-05	2.34559E+01	-2.24599E+00
6.00000E+01	2.50000E+00	8.00000E-02	000X000X000X000	4.84052E-05	3.14220E+01	-2.12599E+00
6.00000E+01	2.50000E+00	1.00000E-01	00X00	7.17887E-06	4.59976E+00	-2.40837E+00
6.00000E+01	2.50000E+00	1.00000E-01	000X000	9.82516E-06	6.30211E+00	-2.29830E+00
6.00000E+01	2.50000E+00	1.00000E-01	0000X0000	1.21164E-05	7.77870E+00	-2.20734E+00
6.00000E+01	2.50000E+00	1.00000E-01	00X00X00	1.86689E-05	1.19798E+01	-2.25509E+00
6.00000E+01	2.50000E+00	1.00000E-01	000X000X000	2.50935E-05	1.61213E+01	-2.13521E+00
6.00000E+01	2.50000E+00	1.00000E-01	00X00X00X00	3.32485E-05	2.13596E+01	-2.13953E+00
6.00000E+01	2.50000E+00	1.00000E-01	000X000X000X000	4.40418E-05	2.83277E+01	-2.01608E+00
6.00000E+01	2.50000E+00	1.20000E-01	00X00	6.72019E-06	4.30944E+00	-2.32366E+00
6.00000E+01	2.50000E+00	1.20000E-01	000X000	9.14091E-06	5.86841E+00	-2.20781E+00
6.00000E+01	2.50000E+00	1.20000E-01	0000X0000	1.12101E-05	7.20350E+00	-2.11297E+00
6.00000E+01	2.50000E+00	1.20000E-01	00X00X00	1.73115E-05	1.11185E+01	-2.16581E+00
6.00000E+01	2.50000E+00	1.20000E-01	000X000X000	2.30859E-05	1.48451E+01	-2.04214E+00
6.00000E+01	2.50000E+00	1.20000E-01	00X00X00X00	3.05823E-05	1.95642E+01	-2.04879E+00
6.00000E+01	2.50000E+00	1.20000E-01	000X000X000X000	4.01411E-05	2.58422E+01	-1.92350E+00
6.00000E+01	2.50000E+00	1.40000E-01	00X00	6.33342E-06	4.06443E+00	-2.24769E+00
6.00000E+01	2.50000E+00	1.40000E-01	000X000	8.56498E-06	5.50301E+00	-2.12718E+00
6.00000E+01	2.50000E+00	1.40000E-01	0000X0000	1.04489E-05	6.71988E+00	-2.02929E+00
6.00000E+01	2.50000E+00	1.40000E-01	00X00X00	1.61721E-05	1.03947E+01	-2.08696E+00
6.00000E+01	2.50000E+00	1.40000E-01	000X000X000	2.14085E-05	1.37774E+01	-1.96075E+00
6.00000E+01	2.50000E+00	1.40000E-01	00X00X00X00	2.83571E-05	1.82476E+01	-1.96973E+00
6.00000E+01	2.50000E+00	1.40000E-01	000X000X000X000	3.69103E-05	2.37809E+01	-1.84387E+00
6.00000E+01	2.50000E+00	1.60000E-01	00X00	5.99938E-06	3.85267E+00	-2.17850E+00
6.00000E+01	2.50000E+00	1.60000E-01	000X000	8.06857E-06	5.18776E+00	-2.05432E+00
6.00000E+01	2.50000E+00	1.60000E-01	0000X0000	9.79444E-06	6.30361E+00	-1.95473E+00
6.00000E+01	2.50000E+00	1.60000E-01	00X00X00	1.51930E-05	9.77212E+00	-2.01628E+00
6.00000E+01	2.50000E+00	1.60000E-01	000X000X000	1.99741E-05	1.28635E+01	-1.88842E+00
6.00000E+01	2.50000E+00	1.60000E-01	00X00X00X00	2.64569E-05	1.70365E+01	-1.89970E+00
6.00000E+01	2.50000E+00	1.60000E-01	000X000X000X000	3.41729E-05	2.20323E+01	-1.77335E+00

TABLE A-4 (CONT)
TYPE II GAGE, GENERAL DESIGNS

LENGTH (INCHES)	WIDTH (INCHES)	LOOP SPACING (INCHES)	PRI/SEC PATTERN	MUTUAL INDUC (HENRIES)	GAGE FACTOR $\frac{MV}{AMP \cdot MM/USEC}$	ERROR TERM (PERCENT)
2.0000E+01	3.0000E+00	8.0000E-02	00X00	2.91033E-06	5.25504E+00	-9.01903E+00
2.0000E+01	3.0000E+00	8.0000E-02	000X000	4.01961E-06	7.26275E+00	-8.64678E+00
2.0000E+01	3.0000E+00	8.0000E-02	0000X0000	4.99846E-06	9.08227E+00	-8.33730E+00
2.0000E+01	3.0000E+00	8.0000E-02	00X00X00	7.67831E-06	1.39331E+01	-8.48089E+00
2.0000E+01	7.0000E+00	8.0000E-02	000X000X000	1.04467E-05	1.90307E+01	-8.05890E+00
2.0000E+01	3.0000E+00	8.0000E-02	00X00X00X00	1.38500E-05	2.52305E+01	-8.05931E+00
2.0000E+01	3.0000E+00	8.0000E-02	000X000X000X000	1.86159E-05	3.40554E+01	-7.60559E+00
2.0000E+01	3.0000E+00	1.0000E-01	00X00	2.70450E-06	4.89880E+00	-8.67598E+00
2.0000E+01	3.0000E+00	1.0000E-01	000X000	3.71248E-06	6.74941E+00	-8.27678E+00
2.0000E+01	3.0000E+00	1.0000E-01	0000X0000	4.59129E-06	8.37293E+00	-7.94265E+00
2.0000E+01	3.0000E+00	1.0000E-01	00X00X00	7.06790E-06	1.26700E+01	-8.10540E+00
2.0000E+01	3.0000E+00	1.0000E-01	000X000X000	9.54086E-06	1.74455E+01	-7.65685E+00
2.0000E+01	3.0000E+00	1.0000E-01	00X00X00X00	1.26454E-05	2.31206E+01	-7.66346E+00
2.0000E+01	3.0000E+00	1.0000E-01	000X000X000X000	1.68400E-05	3.09268E+01	-7.18727E+00
2.0000E+01	3.0000E+00	1.2000E-01	00X00	2.53689E-06	4.60804E+00	-8.37321E+00
2.0000E+01	3.0000E+00	1.2000E-01	000X000	3.46279E-06	6.31453E+00	-7.94967E+00
2.0000E+01	3.0000E+00	1.2000E-01	0000X0000	4.26083E-06	7.79525E+00	-7.59704E+00
2.0000E+01	3.0000E+00	1.2000E-01	00X00X00	6.57263E-06	1.20046E+01	-7.77768E+00
2.0000E+01	3.0000E+00	1.2000E-01	000X000X000	8.80844E-06	1.61585E+01	-7.30475E+00
2.0000E+01	3.0000E+00	1.2000E-01	00X00X00X00	1.16722E-05	2.14092E+01	-7.30475E+00
2.0000E+01	3.0000E+00	1.2000E-01	000X000X000X000	1.54135E-05	2.84020E+01	-6.82892E+00
2.0000E+01	3.0000E+00	1.4000E-01	00X00	2.39569E-06	4.36254E+00	-8.10044E+00
2.0000E+01	3.0000E+00	1.4000E-01	000X000	3.25278E-06	5.94774E+00	-7.65612E+00
2.0000E+01	3.0000E+00	1.4000E-01	0000X0000	3.98347E-06	7.30872E+00	-7.28817E+00
2.0000E+01	7.0000E+00	1.4000E-01	00X00X00	6.15701E-06	1.12760E+01	-7.48560E+00
2.0000E+01	3.0000E+00	1.4000E-01	000X000X000	8.19612E-06	1.50786E+01	-6.99965E+00
2.0000E+01	3.0000E+00	1.4000E-01	00X00X00X00	1.08593E-05	1.99745E+01	-7.01958E+00
2.0000E+01	3.0000E+00	1.4000E-01	000X000X000X000	1.42294E-05	2.62975E+01	-6.51476E+00
2.0000E+01	3.0000E+00	1.6000E-01	00X00	2.27383E-06	4.15020E+00	-7.85115E+00
2.0000E+01	3.0000E+00	1.6000E-01	000X000	3.07187E-06	5.63092E+00	-7.38888E+00
2.0000E+01	3.0000E+00	1.6000E-01	0000X0000	3.74496E-06	6.88917E+00	-7.00814E+00
2.0000E+01	7.0000E+00	1.6000E-01	00X00X00	5.79983E-06	1.06481E+01	-7.22139E+00
2.0000E+01	3.0000E+00	1.6000E-01	000X000X000	7.67204E-06	1.41512E+01	-6.72201E+00
2.0000E+01	3.0000E+00	1.6000E-01	00X00X00X00	1.01643E-05	1.87436E+01	-6.74875E+00
2.0000E+01	3.0000E+00	1.6000E-01	000X000X000X000	1.32235E-05	2.45029E+01	-6.23450E+00

TABLE A-4 (CONT)
TYPE II GAGE, GENERAL DESIGNS

LENGTH (INCHES)	WIDTH (INCHES)	LOOP SPACING (INCHES)	PRI/SEC PATTERN	MUTUAL INDUC (HENRIES)	GAGE FACTOR $\left(\frac{MV}{AMP \cdot MM/USEC}\right)$	ERROR TERM (PERCENT)
4.00000E+01	3.00000E+00	8.00000E-02	00X00	5.57762E-06	5.24832E+00	-4.60075E+00
4.00000E+01	3.00000E+00	8.00000E-02	000X000	7.71583E-06	7.27266E+00	-4.42289E+00
4.00000E+01	3.00000E+00	8.00000E-02	0000X0000	9.60770E-06	9.06882E+00	-4.27372E+00
4.00000E+01	3.00000E+00	8.00000E-02	00X00X00	1.47495E-05	1.39130E+01	-4.34328E+00
4.00000E+01	3.00000E+00	8.00000E-02	000X000X000	2.01041E-05	1.90003E+01	-4.14203E+00
4.00000E+01	3.00000E+00	8.00000E-02	00X00X00X00	2.66535E-05	2.51901E+01	-4.14287E+00
4.00000E+01	3.00000E+00	8.00000E-02	000X000X000X000	3.58956E-05	3.39949E+01	-3.92816E+00
4.00000E+01	3.00000E+00	1.00000E-01	00X00	5.19081E-06	4.89207E+00	-4.43563E+00
4.00000E+01	3.00000E+00	1.00000E-01	000X000	7.13777E-06	6.73932E+00	-4.24439E+00
4.00000E+01	3.00000E+00	1.00000E-01	0000X0000	8.84018E-06	8.35948E+00	-4.08497E+00
4.00000E+01	3.00000E+00	1.00000E-01	00X00X00	1.35990E-05	1.28499E+01	-4.16373E+00
4.00000E+01	3.00000E+00	1.00000E-01	000X000X000	1.83929E-05	1.74152E+01	-3.95086E+00
4.00000E+01	3.00000E+00	1.00000E-01	00X00X00X00	2.43770E-05	2.30803E+01	-3.95490E+00
4.00000E+01	3.00000E+00	1.00000E-01	000X000X000X000	3.25304E-05	3.08664E+01	-3.73119E+00
4.00000E+01	3.00000E+00	1.20000E-01	00X00	4.87550E-06	4.60132E+00	-4.29018E+00
4.00000E+01	3.00000E+00	1.20000E-01	000X000	6.66715E-06	6.30444E+00	-4.08787E+00
4.00000E+01	3.00000E+00	1.20000E-01	0000X0000	8.21626E-06	7.78181E+00	-3.92028E+00
4.00000E+01	3.00000E+00	1.20000E-01	00X00X00	1.26641E-05	1.19844E+01	-4.00758E+00
4.00000E+01	3.00000E+00	1.20000E-01	000X000X000	1.70067E-05	1.61283E+01	-3.78598E+00
4.00000E+01	3.00000E+00	1.20000E-01	00X00X00X00	2.25344E-05	2.13689E+01	-3.79339E+00
4.00000E+01	3.00000E+00	1.20000E-01	000X000X000X000	2.98213E-05	2.83417E+01	-3.56375E+00
4.00000E+01	3.00000E+00	1.40000E-01	00X00	4.60958E-06	4.35581E+00	-4.15942E+00
4.00000E+01	3.00000E+00	1.40000E-01	000X000	6.27082E-06	5.93766E+00	-3.94781E+00
4.00000E+01	3.00000E+00	1.40000E-01	0000X0000	7.69171E-06	7.29529E+00	-3.77365E+00
4.00000E+01	3.00000E+00	1.40000E-01	00X00X00	1.18784E-05	1.12559E+01	-3.86893E+00
4.00000E+01	3.00000E+00	1.40000E-01	000X000X000	1.58458E-05	1.50484E+01	-3.64072E+00
4.00000E+01	3.00000E+00	1.40000E-01	00X00X00X00	2.09928E-05	1.99343E+01	-3.65158E+00
4.00000E+01	3.00000E+00	1.40000E-01	000X000X000X000	2.75581E-05	2.62372E+01	-3.41811E+00
4.00000E+01	3.00000E+00	1.60000E-01	00X00	4.37985E-06	4.14344E+00	-4.04015E+00
4.00000E+01	3.00000E+00	1.60000E-01	000X000	5.92896E-06	5.62084E+00	-3.82068E+00
4.00000E+01	3.00000E+00	1.60000E-01	0000X0000	7.24012E-06	6.87574E+00	-3.64123E+00
4.00000E+01	3.00000E+00	1.60000E-01	00X00X00	1.12022E-05	1.06279E+01	-3.74398E+00
4.00000E+01	3.00000E+00	1.60000E-01	000X000X000	1.48506E-05	1.41210E+01	-3.51077E+00
4.00000E+01	3.00000E+00	1.60000E-01	00X00X00X00	1.96725E-05	1.87134E+01	-3.52511E+00
4.00000E+01	3.00000E+00	1.60000E-01	000X000X000X000	2.56506E-05	2.44427E+01	-3.28923E+00

TABLE A-4 (CONT)
TYPE II GAGE, GENERAL DESIGNS

LENGTH (INCHES)	WIDTH (INCHES)	LOOP SPACING (INCHES)	PRI/SEC PATTERN	MUTUAL INDUCT (HENRIES)	GAGE FACTOR MV (AMP*MM/USEC)	ERROR TERM (PERCENT)
6.00000E+01	3.00000E+01	6.00000E-02	00X00	8.24338E-06	5.24707E+00	-3.78694E+00
6.00000E+01	3.00000E+01	6.00000E-02	000X000	1.14098E-05	7.27079E+00	-2.96936E+00
6.00000E+01	3.00000E+01	6.00000E-02	0000X0000	1.42139E-05	9.06633E+00	-2.87137E+00
6.00000E+01	3.00000E+01	6.00000E-02	00X00X00	2.18162E-05	1.39092E+01	-2.91785E+00
6.00000E+01	3.00000E+01	6.00000E-02	000X000X000	2.97548E-05	1.89949E+01	-2.78533E+00
6.00000E+01	3.00000E+01	6.00000E-02	00X00X00X00	3.94478E-05	2.51826E+01	-2.78633E+00
6.00000E+01	3.00000E+01	6.00000E-02	000X000X000X000	5.31616E-05	3.39837E+01	-2.64608E+00
6.00000E+01	3.00000E+01	1.00000E-01	00X00	7.87560E-06	4.89082E+00	-2.97827E+00
6.00000E+01	3.00000E+01	1.00000E-01	000X000	1.05608E-05	6.77745E+00	-2.85262E+00
6.00000E+01	3.00000E+01	1.00000E-01	0000X0000	1.30960E-05	8.35699E+00	-2.74804E+00
6.00000E+01	3.00000E+01	1.00000E-01	00X00X00	2.01256E-05	1.28461E+01	-2.79935E+00
6.00000E+01	3.00000E+01	1.00000E-01	000X000X000	2.72381E-05	1.74096E+01	-2.66057E+00
6.00000E+01	3.00000E+01	1.00000E-01	00X00X00X00	3.60995E-05	2.30728E+01	-2.66342E+00
6.00000E+01	3.00000E+01	1.00000E-01	000X000X000X000	4.82071E-05	3.08552E+01	-2.51749E+00
6.00000E+01	3.00000E+01	1.20000E-01	00X00	7.21259E-06	4.60007E+00	-2.88251E+00
6.00000E+01	3.00000E+01	1.20000E-01	000X000	9.86924E-06	6.30257E+00	-2.74933E+00
6.00000E+01	3.00000E+01	1.20000E-01	0000X0000	1.21087E-05	7.77931E+00	-2.64014E+00
6.00000E+01	3.00000E+01	1.20000E-01	00X00X00	1.87511E-05	1.19807E+01	-2.69756E+00
6.00000E+01	3.00000E+01	1.20000E-01	000X000X000	2.51982E-05	1.61227E+01	-2.55274E+00
6.00000E+01	3.00000E+01	1.20000E-01	00X00X00X00	3.33876E-05	2.13615E+01	-2.55736E+00
6.00000E+01	3.00000E+01	1.20000E-01	000X000X000X000	4.42155E-05	2.93304E+01	-2.47849E+00
6.00000E+01	3.00000E+01	1.40000E-01	00X00	6.82196E-06	4.35457E+00	-2.79668E+00
6.00000E+01	3.00000E+01	1.40000E-01	000X000	9.28658E-06	5.93579E+00	-2.65794E+00
6.00000E+01	3.00000E+01	1.40000E-01	0000X0000	1.13970E-05	7.29279E+00	-2.54402E+00
6.00000E+01	3.00000E+01	1.40000E-01	00X00X00	1.75952E-05	1.12521E+01	-2.60677E+00
6.00000E+01	3.00000E+01	1.40000E-01	000X000X000	2.34897E-05	1.50428E+01	-2.45792E+00
6.00000E+01	3.00000E+01	1.40000E-01	00X00X00X00	3.11171E-05	1.99269E+01	-2.46537E+00
6.00000E+01	3.00000E+01	1.40000E-01	000X000X000X000	4.19932E-05	2.62260E+01	-2.31336E+00
6.00000E+01	3.00000E+01	1.60000E-01	00X00	6.48436E-06	4.14223E+00	-2.71836E+00
6.00000E+01	3.00000E+01	1.60000E-01	000X000	8.78378E-06	5.61897E+00	-2.57463E+00
6.00000E+01	3.00000E+01	1.60000E-01	0000X0000	1.07322E-05	6.87324E+00	-2.45743E+00
6.00000E+01	3.00000E+01	1.60000E-01	00X00X00	1.65001E-05	1.10624E+01	-2.52506E+00
6.00000E+01	3.00000E+01	1.60000E-01	000X000X000	2.27274E-05	1.41154E+01	-2.37327E+00
6.00000E+01	3.00000E+01	1.60000E-01	00X00X00X00	2.91715E-05	1.86959E+01	-2.38305E+00
6.00000E+01	3.00000E+01	1.60000E-01	000X000X000X000	3.80641E-05	2.44315E+01	-2.23057E+00

```

PROGRAM DSIN1(INPUT,OUTPUT,PUNCH,TAPE7=INPUT,TAPE8=OUTPUT)
DIMENSION QQ(50),ERR(50)
DIMENSION HD1(15),HD2(15),HD3(15),TIT(8),TAT(6)
PI=3.1415926
A4U=.00000125669
CV=.0254
READ 31,(HD1(I),I=1,12)
31 FORMAT (A6,A5,A4,A7,A3,A3,A6,A5,A4,A5,A5,A4)
READ 32,(HD2(I),I=1,6)
32 FORMAT (A6,A6,A6,A5,A5,A9,A2,A9)
READ 33,(HD3(I),I=1,2)
33 FORMAT (A4,A7)
1 CONTINUE
READ 4,(TAT(I),I=1,5)
READ 4,(TIT(I),I=1,8)
4 FORMAT (8A10)
READ 5,Y,X,R,DR
READ 6,IT,NMAX,ICR
5 FORMAT (4(F9.5,1X))
6 FORMAT (3(I2,1X))
IF(IT-1)1,16,99
10 CONTINUE
PRINT 20
20 FORMAT (1H1)
PRINT 44,(TAT(I),I=1,5)
PRINT 44,(TIT(I),I=1,8)
44 FORMAT (8A10)
PRINT 22
PRINT 22
22 FORMAT (* *)
PRINT 91,(HD1(I),I=1,12)
91 FORMAT (4X,A6,8X,A5,4X,A4,1X,A7,2X,A3,3X,A3,2X,A6,1X,A5,2X,A4,1X,A
16,2X,A5,1X,A4)
PRINT 92,(HD2(I),I=1,6)
92 FORMAT (3X,A6,5X,A6,5X,A6,3X,A5,1X,A5,2X,A9,6X,A2,7X,A9)
PRINT 93,(HD3(I),I=1,2)
93 FORMAT (66X,A4,A7)
PRINT 22
X=X*CV
Y=Y*CV
R=R*CV
DR=DR*CV
C IT - EXIT TEST
C NMAX - MAX NUMBER OF PRIMARY TURNS TO BE CONSIDERED
C ICR - MAX NUMBER OF TIMES DR IS ADDED TO R
C INTF - NUMBER OF PRIMARY/SECONDARY INTERFACES
C TAT - TABLE HEADING
C TIT - TABLE HEADING
C GAF - GAGE FACTOR IN MILLIVOLTS PER AMP*MM/MICROSECOND
C
C SET R
DO 100 I=1,ICR
PRINT 22
IF(I-1)16,15,17
17 R=R + DR
16 CONTINUE
C SET S AND CALCULATE Q2 AND ERR FOR EACH M
C

```

```

MM=NMAX-1
DO 80 M=1,MM
P=2*M-1
S=P*R
Z=R*(P+1.)
A=SQRT(X*X + Y*Y)
B=SQRT(X*X + S*S)
C=SQRT(Y*Y + S*S)
AA=SQRT(X*X + Y*Y + S*S)
QQ(M)=(AMU/PI)*(2.*S-2.*C-2.*B+2.*AA+X*ALOG(C*(X+B)/(S*(X+AA))) +
1 Y*ALOG(B*(Y+C)/(S*(Y+AA))))
PJQ=(AMU/PI)*(ALOG(C*(X+B)/(S*(X+AA))) + X*(AA-B)/(B*B))
QPL=QQ(M)/X
ERR(M)=(PJQ-QPL)/PJQ
80 CONTINUE

DO 200 N=2,NMAX
J=N-1
NP=N
NS=N-1
JC=N-1
INTF=2*(N-1)
QX=0.
QY=0.
COEF=INTF
DO 300 J=1,JC
QX=QX + COEF*QQ(J)
QY=QY + COEF*QQ(J)/(1.-ERR(J))
COEF=COEF-2.
300 CONTINUE
Q=QX
ER=1. - QX/QY
GAF=1000000.*Q/(X*(1.-ER))
ER=100.*ER
X=X/CV
Y=Y/CV
R=R/CV
PRINT 71,X,Y,R,NP,NS,Q,GAF,ER
71 FORMAT (1X,3(E12.5,1X),2X,I2,4X,I2,2X,3(E12.5,1X))
X=X*CV
Y=Y*CV
R=R*CV
200 CONTINUE
100 CONTINUE
GO TO 1
99 CONTINUE
CALL EXIT
END

```

```

PROGRAM DSIN2(INPUT,OUTPUT,PUNCH,TAPE7=INPUT,TAPE8=OUTPUT)
DIMENSION QQ(20),ERR(20)
DIMENSION HD1(15),HD2(15),HD3(15)
DIMENSION NPATT(10),PATT(10),TERNN(10),NMAXX(10)
DIMENSION TIT(8),TAT(8)
PI=3.1415926
AMU=.0000125669
CV=.0254
READ 31,(HD1(I),I=1,11)
31 FORMAT (A6,A5,A4,A7,A7,A6,A5,A4,A5,A4)
READ 32,(HD2(I),I=1,7)
32 FORMAT (A8,A8,A8,A7,A9,A2,A9)
READ 33,(HD3(I),I=1,2)
33 FORMAT (A4,A7)
READ 34,(NPATT(I),I=1,7)
34 FORMAT (8I10)
READ 35,(PATT(I),I=1,7)
35 FORMAT (7A9)
READ 36,(TERNN(I),I=1,7)
36 FORMAT (7A7)
READ 37,(NMAXX(I),I=1,7)
37 FORMAT (7I2)
READ 6,ICR
6 FORMAT (I2)
1 CONTINUE
READ 4,(TAT(I),I=1,8)
READ 4,(TIT(I),I=1,8)
4 FORMAT (6A10)
READ 5,Y,X,R,DR
5 FORMAT (4(F9.5,1X))
READ 7,IT
7 FORMAT (I2)
IF(IT-1)10,10,99
10 CONTINUE
PRINT 20
20 FORMAT (1H1)
PRINT 4,(TAT(I),I=1,8)
PRINT 4,(TIT(I),I=1,8)
PRINT 22
PRINT 22
22 FORMAT (* *)
PRINT 91,(HD1(I),I=1,11)
91 FORMAT (4X,A6,8X,A5,4X,A4,1X,A7,6X,A7,5X,A6,1X,A5,2X,A4,1X,A6,2X,A
15,1X,A4)
PRINT 92,(HD2(I),I=1,7)
92 FORMAT (3X,A8,5X,A6,5X,A8,8X,A7,7X,A9,8X,A2,7X,A9)
PRINT 93,(HD3(I),I=1,2)
93 FORMAT (71X,A4,A7)
PRINT 22
PRINT 22
X=X*CV
Y=Y*CV
R=R*CV
DR=DR*CV
IT - EXIT TEST
NMAX - NUMBER OF LOOP INTERFACES BETWEEN EXTREME PRI AND SEC TURNS
ICR - MAX NUMBER OF TIMES DR IS ADDED TO R
NPAT - PRI/SEC PATTERN

```



```

PAT,TERN - PRI/SEC PATTERN
TAT - TABLE HEADING
TIT - TABLE HEADING
GAF - GAGE FACTOR IN MILLIVOLTS PER AMP*MM/MICROSECOND

SET R
DO 100 I=1,ICR
  IF(I-1)16,16,17
17 R=R + JR
16 CONTINUE
  DO 200 J=1,7
    NPAT=NPATT(J)
    PAT=PATT(J)
    TERN=TERNN(J)
    NMAX=NMAXX(J)
  SET S AND CALCULATE QQ AND ERR FOR EACH M

  DO 60 M=1,NMAX
    P=M
    S=P*R
    A=SQRT(X*X + Y*Y)
    B=SQRT(X*X + S*S)
    C=SQRT(Y*Y + S*S)
    AA=SQRT(X*X + Y*Y + S*S)
    QQ(M)=(AMU/PI)*(2.*S-2.*C-2.*B+2.*AA+X*ALOG(C*(X+B)/(S*(X+AA))) +
1 Y*ALOG(B*(Y+C)/(S*(Y+AA))))
    PDQ=(AMU/PI)*(ALOG(C*(X+B)/(S*(X+AA))) + X*(AA-B)/(B*B))
    QPL=QQ(M)/X
    ERR(M)=(PDQ-QPL)/PDQ
  80 CONTINUE
    IF(212-NPAT)51,50,51
  51 IF(313-NPAT)53,52,53
  53 IF(414-NPAT)55,54,55
  55 IF(21212-NPAT)57,56,57
  57 IF(31313-NPAT)59,58,59
  59 IF(2121212-NPAT)61,60,61
  61 IF(3131313-NPAT)62,62,62
  50 Q=2.*(QQ(1) + QQ(2))
    ER=1.-(Q/2.)/(QQ(1)/(1.-ERR(1))+QQ(2)/(1.-ERR(2)))
    GO TO 70
  52 Q=2.*(QQ(1) + QQ(2) + QQ(3))
    ER=1.-(Q/2.)/(QQ(1)/(1.-ERR(1))+QQ(2)/(1.-ERR(2))+QQ(3)/(1.-ERR(3)
1))
    GO TO 70
  54 Q=2.*(QQ(1) + QQ(2) + QQ(3) + QQ(4))
    ER=1.-(Q/2.)/(QQ(1)/(1.-ERR(1))+QQ(2)/(1.-ERR(2))+QQ(3)/(1.-ERR(3)
1)+QQ(4)/(1.-ERR(4)))
    GO TO 70
  56 Q=4.*(QQ(1) + QQ(2)) + 2.*(QQ(4) + QQ(5))
    ER=1.-Q/(4.*(QQ(1)/(1.-ERR(1))+QQ(2)/(1.-ERR(2)))+2.*(QQ(4)/(1.-
1ERR(4))+QQ(5)/(1.-ERR(5))))
    GO TO 70
  58 Q=4.*(QQ(1) + QQ(2) + QQ(3)) + 2.*(QQ(5) + QQ(6) + QQ(7))
    ER=1.-Q/(4.*(QQ(1)/(1.-ERR(1))+QQ(2)/(1.-ERR(2))+QQ(3)/(1.-ERR(3)
1)+2.*(QQ(5)/(1.-ERR(5))+QQ(6)/(1.-ERR(6))+QQ(7)/(1.-ERR(7))))
    GO TO 70
  60 Q=6.*(QQ(1) + QQ(2)) + 4.*(QQ(4) + QQ(5)) + 2.*(QQ(7) + QQ(8))

```

```

      ER=1.-Q/(6.*(QQ(1)/(1.-ERR(1))+QQ(2)/(1.-ERR(2))+4.*(QQ(4)/(1.-
1ERR(4))+QQ(5)/(1.-ERR(5))+2.*(QQ(7)/(1.-ERR(7))+QQ(9)/(1.-ERR(9))
1))
      GO TO 70
62 Q=6.*(QQ(1) + QQ(2) + QQ(3)) + 4.*(QQ(5) + QQ(6) + QQ(7)) +
1 2.*(QQ(9) + QQ(10) + QQ(11))
      ER=1.-Q/(6.*(QQ(1)/(1.-ERR(1))+QQ(2)/(1.-ERR(2))+QQ(3)/(1.-ERR(3))
1)+4.*(QQ(5)/(1.-ERR(5))+QQ(6)/(1.-ERR(6))+QQ(7)/(1.-ERR(7)))+
22.*(QQ(9)/(1.-ERR(9))+QQ(10)/(1.-ERR(10))+QQ(11)/(1.-ERR(11))))
70 CONTINUE
      GAF=1000000.*Q/(X*(1.-ER))
      ER=100.*ER
      X=X/CV
      Y=Y/CV
      R=R/CV
      PRINT 71,X,Y,R,PAT,TERN,Q,GAF,ER
71 FORMAT (1X,3(E12.5,1X),1X,A8,A7,1X,3(E12.5,1X))
      X=X*CV
      Y=Y*CV
      R=R*CV
200 CONTINUE
      PRINT 22
100 CONTINUE
      GO TO 1
99 CONTINUE
      CALL EXIT
      END

```

APPENDIX B
COMPUTER CODE LISTING--DIVE

```

PROGRAM DIVE(INPUT,OUTPUT,PUNCH,TAPE7=INPUT,TAPE8=OUTPUT)
COMMON XX(1200),YY(1200),Q(600),ER(600),SR(600)
COMMON XCO(1200),YCO(1200),X(1200),Y(1200),ALFA(1200),SEGR(1200)
COMMON AY(1200),AX(1200),E(600),DMITA(600)
COMMON XC(1200),YC(1200),DSX(1200),DSY(1200)
COMMON J,CUR,PI,AMU,D,U,CV,C,DT,XS,YS,ZS,R,RAI)
COMMON N1,N2,N3,N4,N5,JMAX,NSHK,MSHK,T(600)
COMMON XXCO(1200),YYCO(1200),ZZCO(1200),ZCO(1200),Z(1200),ZZ(1200)
COMMON DSZ(1200),DSXX(1200),DSYY(1200),DSZZ(1200),ZC(1200)
COMMON XXC(1200),YYC(1200),ZZC(1200),AZ(1200)
COMMON ALFAA(1200),SEGAA(1200),BETAA(1200),BETA(1200)

```

THIS PROGRAM COMPUTES THE TOTAL RESPONSE OF THE MUTUAL INDUCTANCE PARTICLE VELOCIMETER IN A DIVERGENT, OFF-AXIS FLOW FIELD. THE IDEAL RESPONSE OF THE GAGE AS DEVELOPED THEORETICALLY IN THE DASA 1431 REPORTS CORRESPONDS TO ON-AXIS, ONE-DIMENSIONAL FLOW. THE IDEAL FLOW RESPONSE IS CALCULATED AND COMPARED WITH THE TOTAL GAGE RESPONSE AND PRESENTED AS A PERCENTAGE ERROR. INCLUDED IN THIS ERROR IS ALSO THE EFFECT OF THE CHANGE IN GAGE LENGTH UPON THE GAGE SENSITIVITY.

THE SHOCK SOURCE IS LOCATED AT THE POSITION (-XS,-YS,-ZS) AHEAD OF THE GAGE CENTER. THE SHOCKFRONT PROPAGATES SPHERICALLY FROM THIS SOURCE.

THE UNDISTURBED GAGE IS DIVIDED INTO N5 SEGMENTS. TIME IS STEPPED IN DT TIME INCREMENTS AND THE SHOCKFRONT POSITION CALCULATED. EACH GAGE SEGMENT POSITION IS CALCULATED AT EACH TIME STEP. PERIODICALLY THE TOTAL GAGE MUTUAL INDUCTANCE IS CALCULATED. THE GAGE RESPONSE IS THEN CALCULATED AS THE NEGATIVE TIME DERIVATIVE OF THE CURRENT TIMES THE MUTUAL INDUCTANCE.

C IS SHOCK VELOCITY
U IS PARTICLE VELOCITY

XCO, YCO, ZCO, XXCO, YYCO, AND ZZCO ARE INITIAL SEGMENT INTERSEC POSITIONS

GAMMA IS ANGLE OFF OF SOURCE IN THE X,Y PLANE RELATIVE TO THE GAGE CENTERLINE

THETA IS ANGLE OFF OF SOURCE IN THE X,Z PLANE RELATIVE TO THE GAGE CENTERLINE

THE ANGLES ALFA AND BETA DEFINE THE SHOCK PROPAGATION DIRECTION IN THE X,Y,Z LOOP

THE ANGLES ALFAA AND BETAA DEFINE THE SHOCK PROPAGATION DIRECTION IN THE XX,YY,ZZ LOOP

SUBSCRIPT I IDENTIFIES SEGMENT IN SECONDARY LOOP

SUBSCRIPT K IDENTIFIES SEGMENT IN PRIMARY LOOP

SUBSCRIPT J IDENTIFIES TIME INCREMENT

PDMX IS PARTIAL DERIVATIVE OF THE MUTUAL INDUCTANCE WRT X AS DERIVED IN DASA 1431 REPORTS

QQ IS MUTUAL INDUCTANCE DERIVED IN DASA 1431 REPORTS

```

C
C      DMITI IS DERIVATIVE OF MUTUAL INDUCTANCE WRT TIME - IDEAL FLOW
C
C      DMITA IS DERIVATIVE OF MUTUAL INDUCTANCE WRT TIME FOR ACTUAL
C      DIVERGENT/OFF-AXIS FLOW
C
C      ER IS PERCENTAGE ERROR IN GAGE RESPONSE DUE TO NON-IDEAL FLOW
C      OSO IS INITIAL SEGMENT LENGTH
C      YW IS INITIAL GAGE WIDTH, METERS
C      XL IS INITIAL GAGE LENGTH, METERS
C      YNSEG IS NUMBER OF SEGMENTS ACROSS GAGE WIDTH
C      XNSEG IS NUMBER OF SEGMENTS ALONG GAGE LENGTH
C      YNSEG MUST BE AN ODD WHOLE NUMBER
C      RATIO MUST BE AN ODD WHOLE NUMBER, TYPICALLY BETWEEN 7 AND 15
C      N1,N2,N3,N4 IDENTIFY CORNERS
C      N5 IS NUMBER OF GAGE SEGMENTS
C
C      JJ AND INT1 DETERMINE INITIAL VALUE AND INTERVAL IN J FOR
C      CALCULATING MVF
C
C
C
C
C
C
C
C
C
C
C
C
C      1 CONTINUE
C      READ 44,JEXIT
C      44 FORMAT (I1)
C
C      IF JEXIT = 1, READ DATA
C      IF JEXIT = 0, CALL EXIT
C
C      IF(JEXIT - 1)888,45,45
C      45 CONTINUE
C      READ 17,JDIAG
C      17 FORMAT (I1)
C
C      IF JDIAG = 1, PRINT OUT DIAGNOSTICS
C      IF JDIAG = 0, OMIT DIAGNOSTICS
C
C      PRINT 9
C      9 FORMAT (1H1)
C      READ 40,RS
C      40 FORMAT (4F10.0)
C      READ 41,YW,D,C,U,DT,GAMMA,THETA,RATIO
C      41 FORMAT (8F10.0)
C      READ 42,YNSEG,JMAX,JJ,INT1
C      42 FORMAT (F10.0,7I5)
C      READ 43,DATE
C      43 FORMAT (A9)
C
C      INITIALIZE
C
C      CV=1./0.0254
C      AMU=.00000125664
C      PI=3.1415926
C      CUR=1.
C      RAD=57.295779
C      DTS=DT*1000000.

```

JGRMF=JJ

C

```
PRINT 490
491 FORMAT (* DEVELOPMENT OF MUTUAL INDUCTANCE PARTICLE VELOCIMETER *)
PRINT 53
PRINT 491
491 FORMAT (* INVESTIGATION OF OFF-AXIS/DIVERGENT FLOW RESPONSE *)
PRINT 53
PRINT 492
492 FORMAT (* PROGRAM DIVE *)
PRINT 53
PRINT 493
493 FORMAT (* AFWL/DEX *)
PRINT 494,DATE
494 FORMAT (15H DATE OF RUN - ,A9)
PRINT 53
PRINT 53
PRINT 53
```

C

C

C

```
*****
XL=YH*RATIO
DSO=YH/YNSEG
XNSEG=(XL/YH)*YNSEG
NY=YNSEG
NX=XNSEG
N1=(NY + 1)/2
N2=N1 + NX
N3=N2 + NY
N4= N3 + NX
N5=N4 + (NY - 1)/2
GAMMA=GAMMA/RAD
THETA=THETA/RAD
DENOM=1 + (TAN(THETA))**2 + (TAN(GAMMA))**2
XS=SQRT((RS**2)/DENOM)
YS=SQRT((RS**2)*((TAN(GAMMA))**2)/DENOM)
ZS=SQRT((RS**2)*((TAN(THETA))**2)/DENOM)
GAMMA=GAMMA*RAD
THETA=THETA*RAD
```

C

```
XS=-XS
YS=-YS
ZS=-ZS
PRINT 500
500 FORMAT (* GAGE GEOMETRY *)
PRINT 53
PRINT 501,XL
501 FORMAT (5X,14H GAGE LENGTH =,F5.1,7H INCHES)
PRINT 502,YW
502 FORMAT (5X,13H GAGE WIDTH =,F4.1,7H INCHES)
PRINT 503,D
503 FORMAT (5X,15H LOOP SPACING =,F4.2,7H INCHES)
PRINT 514,N5
514 FORMAT (5X,21H NUMBER OF SEGMENTS =,I5)
PRINT 53
PRINT 53
PRINT 504
504 FORMAT (* SHOCK SOURCE POSITION *)
```

```

PRINT 53
PRINT 515,RS

515 FORMAT (5X,5H RS =,F9.4,7H METERS)
PRINT 505,XS
505 FORMAT (5X,5H XS =,F9.4,7H METERS)
PRINT 506,YS
506 FORMAT (5X,5H YS =,F9.4,7H METERS)
PRINT 507,ZS
507 FORMAT (5X,5H ZS =,F9.4,7H METERS)
PRINT 508,GAMMA
508 FORMAT (5X,8H GAMMA =,F5.1,8H DEGREES)
PRINT 509,THETA
509 FORMAT (5X,8H THETA =,F5.1,8H DEGREES)
PRINT 53
PRINT 53
PRINT 511

511 FORMAT (* SHOCK PARAMETERS *)
PRINT 53
PRINT 511,C
511 FORMAT (5X,17H SHOCK VELOCITY =,F6.1,11H METERS/SEC)
PRINT 512,U
512 FORMAT (5X,23H PARTICLE VELOCITY =,F6.1,11H METERS/SEC)
PRINT 53
PRINT 53
PRINT 513,DTS
513 FORMAT (2X,17H TIME INCREMENT =,F5.2,9H MICROSEC)
PRINT 53
PRINT 53
GAMMA=GAMMA/RAD
THETA=THETA/RAD
XL=XL/CV
YW=YW/CV
D=D/CV
DSO=DSO/CV
XS=-XS
YS=-YS
ZS=-ZS
DO 19 I=1,N1
19 XCO(I)=J.
YCO(1)=DSO/2.
NA=N1 - 1
DO 20 I=1,NA
IA=I + 1
20 YCO(IA)=YCO(I) + DSO
NA=N1 + 1
DO 21 I=NA,N2
21 YCO(I)=YCO(N1)
XCO(NA)=DSO
NB=N2 - 1
DO 22 I=NA,NB
IA=I + 1
22 XCO(IA)=XCO(I) + DSO
DO 23 I=1,N3
IP=N5 + 1 - I
XCO(IP)=XCO(I)
23 YCO(IP)=-YCO(I)
NC=N3 - 1

```

```

      DO 18 I=N2,NC
      IA=I + 1
      XCO(IA)=XCO(N2)
      YCO(IA)=YCO(I) - DSO
18  CONTINUE
      DO 25 I=1,N5
      XXCO(I)=XCO(I)
      YYCO(I)=YCO(I)
      ZCO(I)=D/2.
      ZZCO(I)=-D/2.
      ALFA(I)=ATAN((YCO(I) + YS)/(SQRT((XCO(I) + XS)**2 + (ZCO(I) + ZS)*
1*2)))
      ALFAA(I)=ATAN((YYCO(I) + YS)/(SQRT((XXCO(I) + XS)**2 + (ZZCO(I) +
1ZS)**2)))
      BETA(I)=ATAN((ZS + ZCO(I))/(XS + XCO(I)))
      BETAA(I)=ATAN((ZS + ZZCO(I))/(XS + XXCO(I)))
      SEGR(I)=SQRT((XS + XCO(I))**2 + (YS + YCO(I))**2 + (ZS + ZCO(I))*
1*2)
      SEGAA(I)=SQRT((XS + XXCO(I))**2 + (YS + YYCO(I))**2 + (ZS + ZZCO(I)
1)**2)
25  CONTINUE
      IF(YS + YCO(N+))89,89,90
89  CONTINUE
      SR(1)=SQRT(XS**2 + ZS**2) - .002
      GO TO 91
90  CONTINUE
      SR(1)=SQRT((YS + YCO(N+))**2 + XS**2 + ZS**2) - .002
91  CONTINUE
      T(1)=J.

C
C
C      * * * * *
      DO 20 J=1,JMAX
      JA=J+1
      JC=J-1
      T(JA)=T(J) + DTS
      SR(JA)=SR(J)+C*DT
      NQ=N3 + 2
      IF(SR(J) - SEGR(NQ))110,110,999
110 CONTINUE
      Q(J)=J.

C
      CALL COPOS
      IF(J - JJ)11,10,10
10  CONTINUE
      JJ=JJ + INT1

C
      CALL COMVP

C
      PRINT 9
      PRINT 239,T(J)
239 FORMAT (1X,4H T =,F6.1,9H MICROSEC)
      PRINT 2+J,NSHK
240 FORMAT (1X,7H NSHK =,I4)
      PRINT 241,MSHK
241 FORMAT (1X,7H MSHK =,I4)
      PRINT 53
      PRINT 53

```



```

      PRINT 231
231  FORMAT (*      I          XC          YC          ZC
      1      XXC          YYC          ZZC      *)
      PRINT 53

C
C
C      XC, YC, ZC, XXC, YYC, AND ZZC PRINTOUT IN INCHES

      DO 307 I=1,N5
      XC(I)=XC(I)*CV
      YC(I)=YC(I)*CV
      ZC(I)=ZC(I)*CV
      XXC(I)=XXC(I)*CV
      YYC(I)=YYC(I)*CV
307  ZZC(I)=ZZC(I)*CV
      DO 87 I=1,N1
      PRINT 86,I,XC(I),YC(I),ZC(I),XXC(I),YYC(I),ZZC(I)
      FORMAT (1X,I4,1X,7(E15.8,1X))
      IF(SR(J) - SEGRC(1))38,39,39
      CONTINUE
      NE=N1+1
      DO 88 I=NE,NSHK,5
      PRINT 86,I,XC(I),YC(I),ZC(I),XXC(I),YYC(I),ZZC(I)
      NF=NSHK-5
      NG=NSHK+5
      DO 30 I=NF,NG
      PRINT 86,I,XC(I),YC(I),ZC(I),XXC(I),YYC(I),ZZC(I)
30  CONTINUE
      NH=MSHK - 5
      NI=MSHK + 5
      DO 31 I=NH,NI
      PRINT 86,I,XC(I),YC(I),ZC(I),XXC(I),YYC(I),ZZC(I)
      DO 32 I=NI,N4,5
      PRINT 86,I,XC(I),YC(I),ZC(I),XXC(I),YYC(I),ZZC(I)
      DO 33 I=N4,N5
      PRINT 86,I,XC(I),YC(I),ZC(I),XXC(I),YYC(I),ZZC(I)
      IF(JOIAG)598,598,599
599  CONTINUE
      PRINT 9
      PRINT 601
601  FORMAT (*      I          ALFA(DEG)          ALFAA(DEG)          BETA(DEG)
      1      BETAA(DEG)      SEGRC(METERS)      SEGAA(METERS)      *)
      PRINT 53
      DO 601 I=1,N5
      ALFA(I)=ALFA(I)*RAD
      ALFAA(I)=ALFAA(I)*RAD
      BETA(I)=BETA(I)*RAD
      BETAA(I)=BETAA(I)*RAD
      PRINT 602,I,ALFA(I),ALFAA(I),BETA(I),BETAA(I),SEGRC(I),SEGAA(I)
602  FORMAT (1X,I5,2X,6(E14.7,2X))
      ALFA(I)=ALFA(I)/RAD
      ALFAA(I)=ALFAA(I)/RAD
      BETA(I)=BETA(I)/RAD
      BETAA(I)=BETAA(I)/RAD
601  CONTINUE
      PRINT 9
      PRINT 49
      FORMAT (*      PRINTOUT FROM CONVE      *)
      PRINT 53

```

```

53 FORMAT (* *)
   PRINT 233,T(J)
   PRINT 53
   PRINT 53
   PRINT 55
55 FORMAT (* I AX AY AZ *)
   PRINT 53
   DO 50 I=1,N5
50 PRINT 51,I,AX(I),AY(I),AZ(I)
51 FORMAT (1X,I+,1X,7(E14.7,1X))
598 CONTINUE
C
   DO 96 I=1,N5
96 Q(J)=Q(J) + AX(I)*DSX(I) + AY(I)*DSY(I) + AZ(I)*DSZ(I)
11 CONTINUE
23 CONTINUE
C
* * * * *
C
999 CONTINUE
   JD=INT1 + 1
   DO 300 J=JD,JC,INT1
   JA=J - INT1
   JB=J + INT1
   TINT1=INT1
   DTT=DT*2.*TINT1
   E(J)=-(Q(JB) - Q(JA))/DTT
   DMITA(J)=E(J)/CUR
   AA=SQRT(XL*XL + YW*YW)
   BB=SQRT(XL*XL + D*D)
   CC=SQRT(YW*YW + D*D)
   DD=SQRT(XL*XL + YW*YW + D*D)
   PDMX=(AMU/PI)*(ALOG(CC*(XL + BB)/(D*(XL + DD))) + XL*(DD - BB)/(BB
1*BB))
   DMITI=U*PDMX
   ER(J)=(DMITA(J) - DMITI)*100./DMITI
300 CONTINUE
   QQ=(AMU/PI)*(2.*J-2.*CC-2.*BB+2.*DD+XL*ALOG(CC*(XL+BB)/(D*(XL+DD))
1)+YW*ALOG(BB*(YW+CC)/(D*(YW+DD))))
   ERGAL=100.*(Q(1) - QQ)/QQ
   PRINT 9
   PRINT 788,QQ
788 FORMAT (1X,32H THEORETICAL MUTUAL INDUCTANCE =,1X,E14.7,1X,.H HENR
1IES)
   PRINT 53
   PRINT 786,ERGAL
786 FORMAT (1X,31H ERROR DUE TO FINITE ELEMENTS =,1X,E14.7,1X,8H PERCE
1NT)
   PRINT 53
   PRINT 53
   PRINT 790
790 FORMAT (* TIME MUTUAL IND *)
   PRINT 791
791 FORMAT (* (MICROSEC) (HENRIES) *)
   PRINT 53
   DO 792 J=JGRMP,JMAX,INT1
792 PRINT 891,T(J),Q(J)
   PRINT 53

```

```

PRINT 53
PRINT 53
PRINT 53
PRINT 53
PRINT 800
800 FORMAT (*      TIME      MUTUAL IND      ERROR      DM/DT A
1CTUAL      DM/DT IDEAL      NORMALIZED *)
PRINT 881
881 FORMAT (*      (MICROSEC)      (HENRIES)      (PERCENT)      (HENRIE
1S/SEC)      (HENRIES/SEC)      VELOCITY *)
PRINT 53
PRINT 53
DO 890 J=JD,JC,INT1
VNORM=DMITA(J)/DMITI
890 PRINT 891,T(J),Q(J),ER(J),DMITA(J),DMITI,VNORM
891 FORMAT (1X,6(E1+.7,2X))
998 CONTINUE
PRINT 9
GAMMA=GAMMA*RAD
THETA=THETA*RAD
YW=YW*CV
XL=XL*CV
D=D*CV
GO TO 1
880 CONTINUE
CALL EXIT
END

```

SUBROUTINE COPOS

COMMON XX(1200),YY(1200),Q(600),ER(600),SR(600)
 COMMON XCO(1200),YCO(1200),X(1200),Y(1200),ALFA(1200),SEGR(1200)
 COMMON AY(1200),AX(1200),E(600),DMITA(600)
 COMMON XC(1200),YC(1200),DSX(1200),DSY(1200)
 COMMON J,CUR,PI,AMU,D,U,CV,C,DT,XS,YS,ZS,R,RAJ
 COMMON N1,N2,N3,N4,N5,JMAX,NSHK,MSHK,T(600)
 COMMON XXCN(1200),YYCO(1200),ZZCO(1200),ZCO(1200),Z(1200),ZZ(1200)
 COMMON DSZ(1200),DSXX(1200),DSYY(1200),DSZZ(1200),ZC(1200)
 COMMON XXC(1200),YYC(1200),ZZC(1200),AZ(1200)
 COMMON ALFAA(1200),SEGAA(1200),BETAA(1200),BETA(1200)

NSHK INDICATES FIRST INTERSECTION POSITION IN UPPER HALF WHICH
 IS UNSHOCKED

MSHK INDICATES FIRST INTERSECTION POSITION IN LOWER HALF WHICH
 IS UNSHOCKED

MX=J
 MY=0
 MSHK=N-2J

HIGH SIDE CALCULATIONS OF XC, YC, AND ZC

NA=N2 - 1
 DO 55 I=1,NA
 IF(SR(J) - SEGR(I))60,60,61
 61 CONTINUE
 SEGR(I)=SEGR(I) + U*DT
 XC(I)=SEGR(I)*COS(ALFA(I))*COS(BETA(I)) - XS
 YC(I)=SEGR(I)*SIN(ALFA(I)) - YS
 ZC(I)=SEGR(I)*COS(ALFA(I))*SIN(BETA(I)) - ZS
 GO TO 67
 60 YC(I)=YCO(I)
 XC(I)=XCO(I)
 ZC(I)=ZCO(I)
 MX=MX + 1
 IF(MX - 1)80,80,81
 80 NSHK=I
 81 CONTINUE
 67 CONTINUE
 55 CONTINUE
 XC(N2)=XCO(N2)
 YC(N2)=YCO(N2)
 ZC(N2)=ZCO(N2)

HIGH SIDE CALCULATIONS OF XXC, YYC, AND ZXC

NA=N2-1
 DO 155 I=1,NA
 IF(SR(J) - SEGAA(I))160,160,161
 161 CONTINUE
 SEGAA(I)=SEGAA(I) + U*DT
 XXC(I)=SEGAA(I)*COS(ALFAA(I))*COS(BETAA(I)) - XS
 YYC(I)=SEGAA(I)*SIN(ALFAA(I)) - YS

```

      ZYC(I)=SEGAA(I)*COS(ALFAA(I))*SIN(BETAA(I)) - ZS
      GO TO 167
165 YYC(I)=YYCO(I)
      XXC(I)=XXCO(I)
      ZYC(I)=ZYCO(I)
167 CONTINUE
155 CONTINUE
      XXC(N2)=XXCO(N2)
      YYC(N2)=YYCO(N2)
      ZYC(N2)=ZYCO(N2)

```

C
C
C

LOW AND RIGHT SIDE CALCULATIONS OF XC, YC, AND ZC

```

      NB=N2 + 1
      DO 70 I=NB,N5
      IF(SR(J) - SEGRG(I)) 71,71,72
71 XC(I)=XCO(I)
      YC(I)=YCO(I)
      ZC(I)=ZCO(I)
      GO TO 77
72 CONTINUE
      SEGRG(I)=SEGRG(I) + U*DT
      XC(I)=SEGRG(I)*COS(ALFA(I))*COS(BETA(I)) - XS
      YC(I)=SEGRG(I)*SIN(ALFA(I)) - YS
      ZC(I)=SEGRG(I)*COS(ALFA(I))*SIN(BETA(I)) - ZS
      MY=MY + 1
      IF(MY - 1) 90,90,91
90 MSHK=I-1
91 CONTINUE
77 CONTINUE
70 CONTINUE

```

C
C
C

LOW AND RIGHT SIDE CALCULATIONS OF XXC, YYC, AND ZYC

```

      NB=N2 - 1
      DO 170 I=NB,N5
      IF(SR(J) - SEGAA(I)) 171,171,172
171 XXC(I)=XXCO(I)
      YYC(I)=YYCO(I)
      ZYC(I)=ZYCO(I)
      GO TO 177
172 CONTINUE
      SEGAA(I)=SEGAA(I) + U*DT
      XXC(I)=SEGAA(I)*COS(ALFAA(I))*COS(BETAA(I)) - XS
      YYC(I)=SEGAA(I)*SIN(ALFAA(I)) - YS
      ZYC(I)=SEGAA(I)*COS(ALFAA(I))*SIN(BETAA(I)) - ZS
177 CONTINUE
170 CONTINUE

```

C
C
C

CALCULATIONS OF X, Y, AND Z

```

      NC=N5 - 1
      DO 57 I=1,NC
      IA=I + 1
      X(IA)=(XC(IA) + XC(I))/2.
      Z(IA)=(ZC(IA) + ZC(I))/2.
57 Y(IA)=(YC(IA) + YC(I))/2.
      X(1)=(XC(1) + XC(N5))/2.

```

```

Y(1)=(YC(1) + YC(N5))/2.
Z(1)=(ZC(1) + ZC(N5))/2.

C
C
C   CALCULATIONS OF DSX, DSY, AND DSZ

DSX(1)=XC(1) - XC(N5)
DSY(1)=YC(1) - YC(N5)
DSZ(1)=ZC(1) - ZC(N5)
DO 50 I=1,NC
IA=I + 1
DSX(IA)=XC(IA) - XC(I)
DSZ(IA)=ZC(IA) - ZC(I)
50 DSY(IA)=YC(IA) - YC(I)

C
C
C   CALCULATIONS OF XX, YY, AND ZZ

NC=N5 - 1
DO 157 I=1,NC
IA=I + 1
XX(IA)=(XXC(IA) + XXC(I))/2.
YY(IA)=(YYC(IA) + YYC(I))/2.
157 ZZ(IA)=(ZZC(IA) + ZZC(I))/2.
XX(1)=(XXC(1) + XXC(N5))/2.
YY(1)=(YYC(1) + YYC(N5))/2.
ZZ(1)=(ZZC(1) + ZZC(N5))/2.

C
C
C   CALCULATIONS OF DSXX, DSY, AND DSZZ

DSXX(1)=XXC(1) - XXC(N5)
DSYY(1)=YYC(1) - YYC(N5)
DSZZ(1)=ZZC(1) - ZZC(N5)
DO 150 I=1,NC
IA=I + 1
DSXX(IA)=XXC(IA) - XXC(I)
DSYY(IA)=YYC(IA) - YYC(I)
150 DSZZ(IA)=ZZC(IA) - ZZC(I)
RETURN
END

```

SUBROUTINE COMVP

```
COMMON XX(1200),YY(1200),Q(600),ER(600),SR(600)
COMMON XCO(1200),YCO(1200),X(1200),Y(1200),ALFA(1200),SEGR(1200)
COMMON AY(1200),AX(1200),E(600),DMITA(600)
COMMON XC(1200),YC(1200),DSX(1200),DSY(1200)
COMMON J,CUR,PI,AMU,D,U,CV,C,DT,XS,YS,ZS,R,RAD
COMMON N1,N2,N3,N4,N5,JMAX,NSHK,MSHK,T(600)
COMMON XXCO(1200),YYCO(1200),ZZCO(1200),ZCO(1200),Z(1200),7Z(1200)
COMMON DSZ(1200),DSXX(1200),DSYY(1200),DSZZ(1200),ZC(1200)
COMMON XXC(1200),YYC(1200),ZZC(1200),AZ(1200)
COMMON ALFAA(1200),SEGAA(1200),BETAA(1200),BETA(1200)
```

THIS SUBROUTINE CALCULATES THE MAGNETIC VECTOR POTENTIAL AT EACH
SEGMENT IN THE X,Y,Z LOOP

AX IS X COMPONENT OF MVP
AY IS Y COMPONENT OF MVP
AZ IS Z COMPONENT OF MVP
A IS MAGNETIC VECTOR POTENTIAL (MVP)

```
FAT=(AMU*CUR)/(4.*PI)
DO 90 I=1,N5
  AX(I)=0.
  AY(I)=0.
  AZ(I)=0.
DO 91 K=1,N5
  P=SQRT((X(I) - XX(K))**2 + (Y(I) - YY(K))**2 + (Z(I) - ZZ(K))**2)
  AXX=FAT*DSXX(K)/R
  AYY=FAT*DSYY(K)/R
  AZZ=FAT*DSZZ(K)/R
  AX(I)=AX(I) + AXX
  AY(I)=AY(I) + AYY
  AZ(I)=AZ(I) + AZZ
90 CONTINUE
91 CONTINUE
RETURN
END
```

APPENDIX C

SELECTION OF OPTIMUM GAGE CONDUCTOR

The analysis in section IV identified the manner in which the shock-induced resistance changes cause errors in the gage output. As indicated in section IV, these errors are controlled with a large ballast inductance in the primary circuit. It was also evident that these errors were influenced by the ballast resistance, though not to the same extent as the ballast inductance. Since there are many metals which can be used as conductors in the MIPV and each has its own resistivity, resistance-pressure, and shock impedance characteristics, it is of interest to compare these characteristics. This information is required for gage design and must be considered along with other factors such as radiation cross section and the practical aspects of availability, cost (beryllium cost: approximately \$2000 per pound), and compatibility with fabrication techniques in selecting the optimum conductor material.

1. THE IDEAL CONDUCTOR

The characteristics of the ideal conductor are identified by considering the total gage environment. The gage must rapidly equilibrate with the shock-loaded geology in which it is embedded, and it will be exposed to extreme pressures and an intense radiation environment. The ideal conductor would, therefore, have a low resistivity and exhibit little or no change in resistance with change in pressure, have a shock Hugoniot which is identical to that of the media in which it is embedded, present a low neutron cross section, and present no insurmountable fabrication problems in its use. Several metals and their alloys have some of these characteristics, but none exhibit all.

For the moment, if the radiation cross-section characteristics are ignored, and it is assumed that no fabrication problems will be encountered, the criteria for selecting the most favorable gage

conductor material is reduced to that of determining which material would result in the minimum resistance change while meeting equilibration time requirements. The materials under consideration may be ordered in this respect and the radiation and fabrication characteristics considered separately.

2. CANDIDATE CONDUCTORS

The candidate conductor materials and their important characteristics are listed in table C-1. For the analysis, a shock pressure of 200 Kbar will be assumed. It is further assumed that the results obtained at 200 Kbar would not differ in terms of which conductor material was most favorable from results obtained at higher pressures. Three columns in table C-1 require comments.

The resistivity data assumes a high purity metal. Alloying and impurities will increase the resistivity in varying amounts. For instance, several magnesium alloys have a resistivity of $12.5 \mu\Omega \cdot \text{cm}$, a 300 percent increase over the pure metal, while both aluminum and copper alloy systems exhibit increases in resistivity of only a few percent over that of the pure metals. If a pure metal is not used, the particular alloy should be considered. For this analysis, a pure metal is assumed.

The column headed " (R/R_0) 200 Kbar" indicates the resistance of the material at 200 Kbar pressure relative to the resistance at zero pressure. The data is based upon the extrapolation of Bridgeman's static data (ref. 23) shown in figure C-1. Since Bridgeman's data above $30,000 \text{ kg/cm}^2$ is itself corrected, it must be recognized that some uncertainty exists in the table C-1 data. However, the relative magnitudes in R/R_0 between materials are preserved, and the results are probably affected insignificantly by the uncertainties. Nevertheless, until high-pressure dynamic resistance-pressure data become available, the R/R_0 data must be considered, at best, an estimate for pressures to 1 Mbar.

The column headed " $(\rho_0 c)$ 200 Kbar" is the slope of the shock loading path in the stress-particle velocity plane at 200 Kbar. The intent of this column is simply to indicate the relative magnitudes of the shock impedances.

Table C-1
CHARACTERISTICS OF CANDIDATE CONDUCTOR MATERIALS

<u>Material</u>	<u>Resistivity ($\mu\Omega \cdot \text{cm}$)</u>	<u>(R/R_o) 200 Kbar</u>	<u>Density (g/cm^3)</u>	<u>($\rho_o C$) 200 Kbar ($\text{Kb}/\text{mm}/\mu\text{sec}$)</u>	<u>Remarks</u>
Magnesium	4.46	0.675	1.740	115	
Beryllium	5.9	0.798	1.850	170	Toxic
Aluminum	2.65	0.673	2.785	187	
Titanium	42.0	0.850	4.517	256	Transition metal
Copper	1.673	0.787	8.930	405	

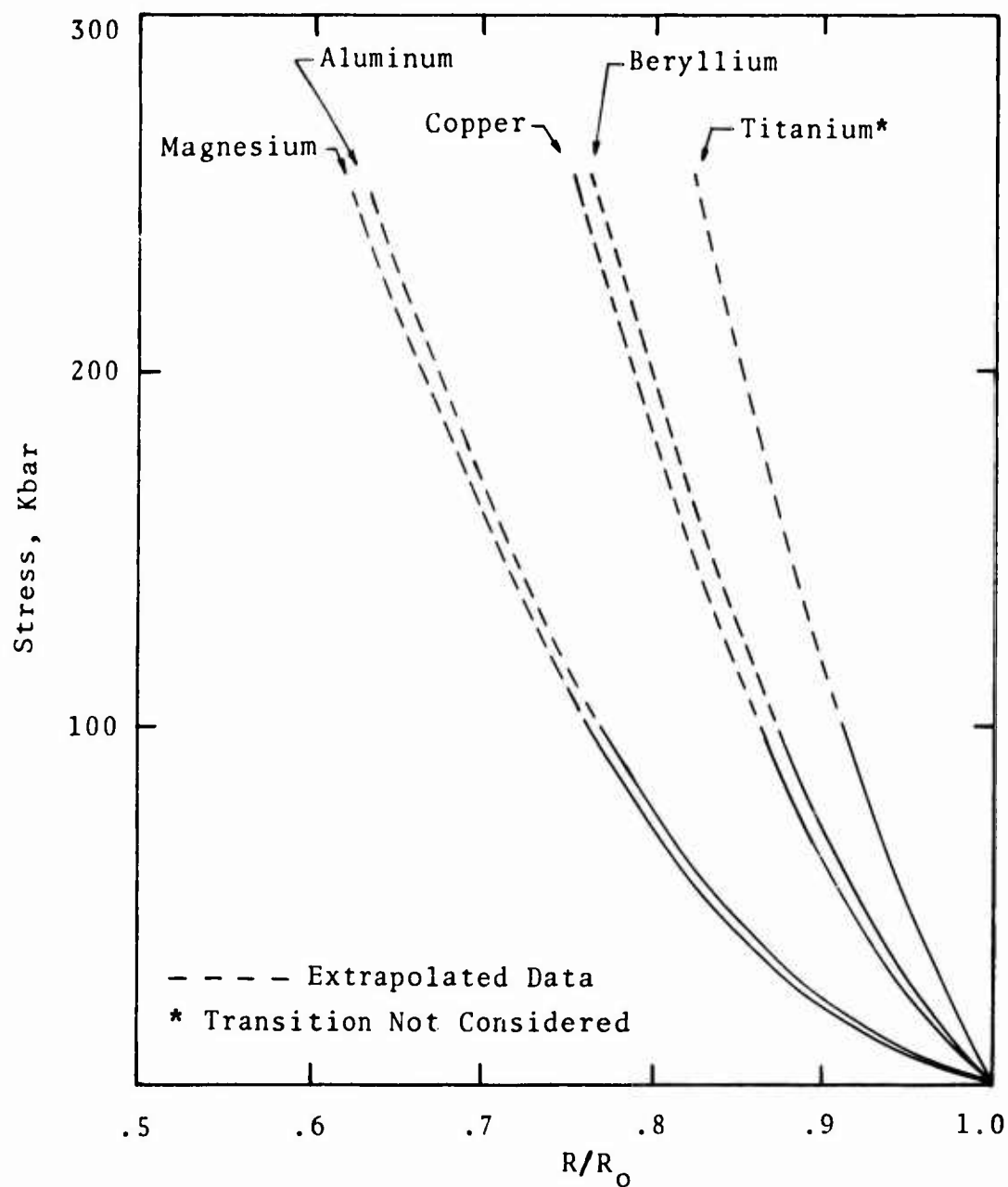


Figure C-1. Change in Resistance as a Function of Stress for Several Metals (Bridgeman, ref. 23)

3. COMPARISON OF CANDIDATE CONDUCTORS

The conductor material characteristics listed in table C-1 interact in a straightforward manner to influence the change in conductor resistance per unit length, $\Delta R/\ell$. The problem begins with a specified equilibration time, t_e , and concludes with a calculated $\Delta R/\ell$.

A one-dimensional analysis of the conductor shock response is performed to determine the minimum cross-sectional area that is required for circular conductors to meet the equilibration time requirements. The geometry is shown in figure C-2. In general, the conductor will be stiffer than most geologies; therefore, for this analysis it is not necessary to consider many geologies, only a representative one. The chosen Hugoniot approximates a saturated tuff with a density of 1.96. The Hugoniot in the stress-particle velocity plane is shown in figure C-3. The states in the conductor during equilibration with the geology are determined by the interactions at the conductor-geology boundaries. (In reality, an insulating material electrically isolates the conductor from the geology. Here it is assumed that the insulation and geology Hugoniots are identical to simplify the one-dimensional analysis.) In figure C-3 the equilibration of copper is shown. Due to the large difference in Hugoniot between copper and the geology, a large number of transits are required, seven in this case, to reach a conductor particle velocity of 0.99 times that of the geology. A lesser number of transits is required for the other conductor materials; five for titanium, three for aluminum, three for beryllium, and two for magnesium.

Having defined the number of transits required for equilibration, the conductor thickness, or diameter, may be determined if the time required for equilibration, t_e , is defined. Several cases will be considered to observe the variation of $\Delta R/\ell$ with t_e . The conductor diameter may be determined from the expression for the equilibration time

$$t_e = d \left(\frac{1}{c_1} + \frac{1}{c_2} + \dots + \frac{1}{c_n} \right)$$

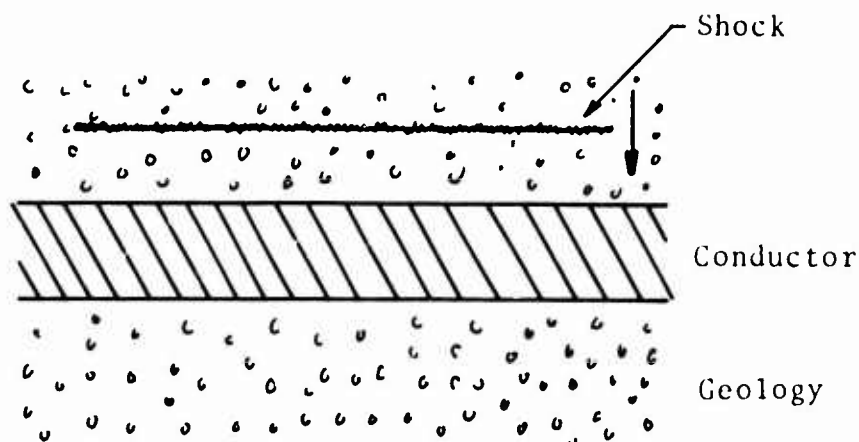


Figure C-2. Geometry for One-Dimensional Shock Response Analysis

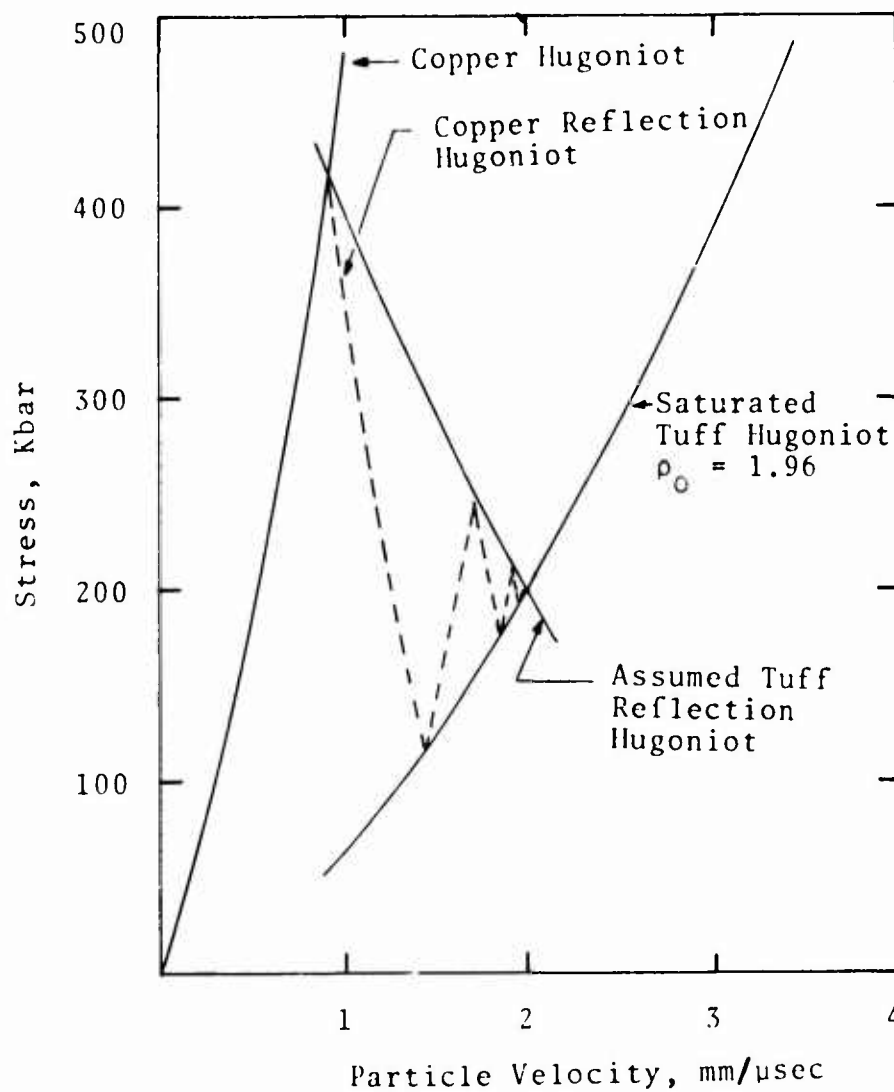


Figure C-3. Shock Equilibration of Copper in Tuff

where

d is the conductor thickness, mm

n is the number of shock transits required for equilibration

c is the shock velocity for the first, second, ... n th shock transit

The cross-sectional area is determined from the diameter. The resistivity and area provide the resistance-per-unit-length, and from R/R_0 data of table C-1, $\Delta R/\ell$ may be determined. The results are summarized in table C-2 and presented in figure C-4 on a semi-log plot.

In figure C-4 magnesium, beryllium, and aluminum all indicate values of $\Delta R/\ell$ an order of magnitude less than copper and two orders of magnitude less than titanium. They also are more favorable with respect to radiation cross section with beryllium being the obvious choice because of its low atomic number.

4. SUMMARY

The results of this study identify the relative merits of several conductors and provides insight into how they would respond in the problem of section IV.

Magnesium, beryllium, and aluminum are the most favorable of the materials considered. Aluminum would be the preferred choice in the high explosive environment due to its availability and ease of use. However, at low pressures copper has been shown (ref. 16) to exhibit better survivability characteristics. In the nuclear environment beryllium would be preferable due to its low thermal neutron cross section (0.0085-Be, 0.22-Al, 0.063-Mg) (Ref. 24). Also, beryllium's relative high melting temperature of 1278°C is more compatible with the softening temperature of glass systems under consideration for use as insulators.

Table C-2

SUMMARY OF CONDUCTOR RESPONSES

<u>Mtl</u>	<u>Transits</u>	<u>t_e</u> (μ sec)	<u>d</u> (in)	<u>R/l</u> (m Ω /in)	<u>$\Delta R/l$</u> (m Ω /in)
Mg	2	0.5	0.067	0.4980	0.1618
		1.0	0.134	0.1250	0.0406
		2.0	0.269	0.0310	0.0101
		5.0	0.672	0.0049	0.0016
Be	3	0.5	0.061	0.7950	0.1606
		1.0	0.122	0.1990	0.0402
		2.0	0.244	0.0500	0.0101
		5.0	0.611	0.0079	0.0016
Al	3	0.5	0.045	0.6560	0.2145
		1.0	0.089	0.1680	0.0549
		2.0	0.178	0.0420	0.0137
		5.0	0.446	0.0067	0.0022
Ti	5	0.5	0.023	39.8	5.970
		1.0	0.045	10.4	1.560
		2.0	0.091	2.54	0.381
		5.0	0.228	0.405	0.0607
Cu	7	0.5	0.013	4.96	0.1056
		1.0	0.026	1.24	0.2641
		2.0	0.052	0.310	0.0660
		5.0	0.130	0.0496	0.0105

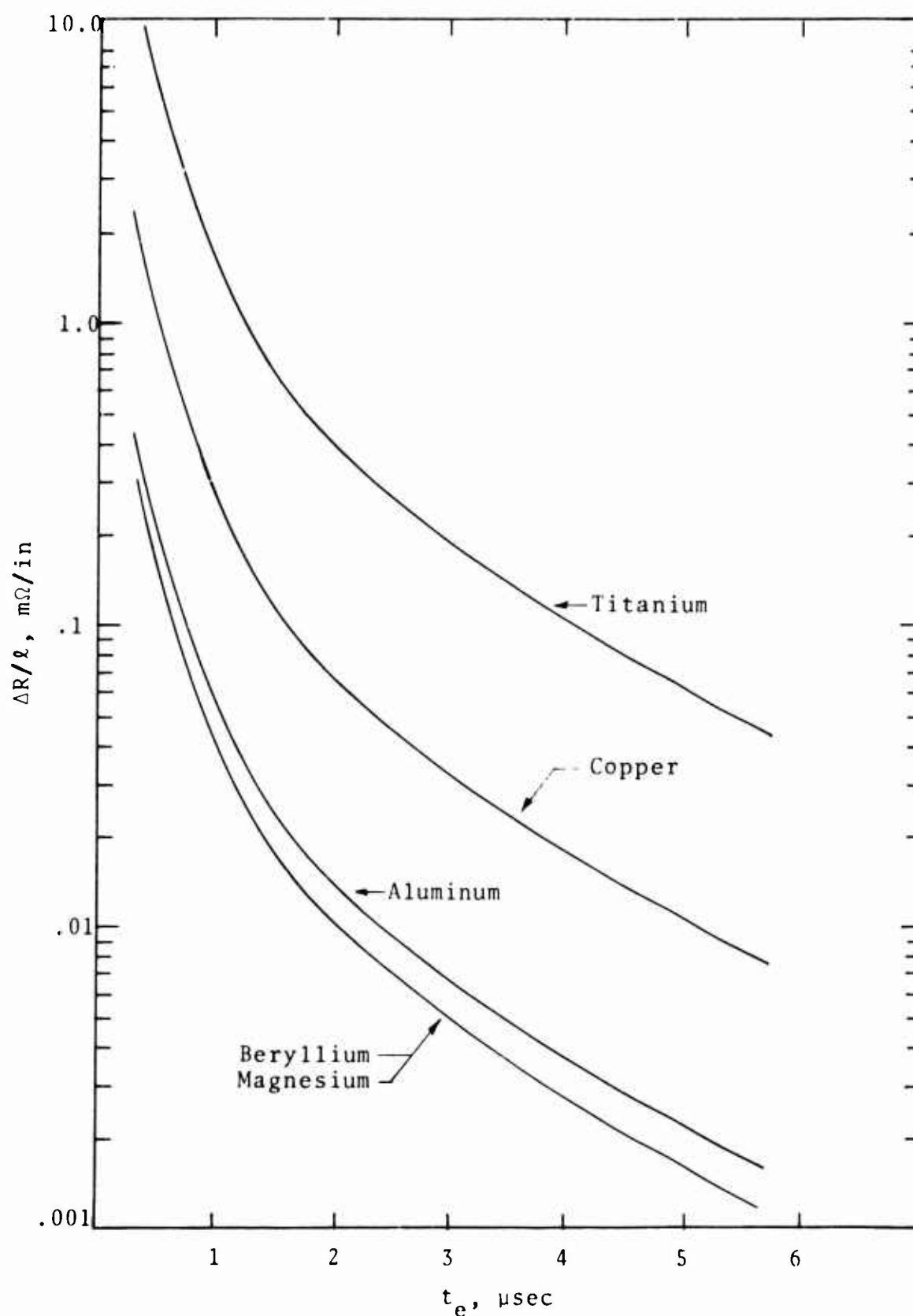


Figure C-4. Resistance Change Per-Unit-Length as a Function of Equilibration Time, t_e , for Several Conductor Materials, 200 Kbar

APPENDIX D
COMPUTER CODE LISTING--ELMEK

PROGRAM ELMEK(INPUT,OUTPUT,PUNCH,TAPE7=INPUT,TAPE8=OUTPUT)

DIFFERENTIAL EQUATIONS INTEGRATION ROUTINE

RUNGE-KUTTA-GILL / ADAMS-MOULTON METHOD
VARIABLE STEP-SIZE INTEGRATION ROUTINE

N SIMUTANEOUS EQUATIONS

MAIN PROGRAM OF THE SUBROUTINE /OR DRIVER

COMMON Y(24), Y1(24), Y2(24), Y3(24), Y4(24), Z(24), Z1(24)
COMMON Z2(24), Z3(24), Z4(24), YI(24), E(24), XI, XC, X, X1, X2
COMMON X3, X4, DXI, DX, DXH, EMIN, EMAX, KONT, LC, MP, MC, M1, M2
COMMON M3, M4, N, MT
COMMON CP0, R80, R90, XQ, YQ, R, AK, AM, AL40, AL50, CP, AL11, NZ, OMDX, V
COMMON U, CAP1, R2, R3, CAP6, CAP7, R10, CAP12, R13, NMAX
COMMON U0, C0, CURRI, NCI, ZAP, RSEC
COMMON RMK1(8), RMK2(8)

READ INITIAL CONDITIONS AND CONTROL DATA

1 READ 100, N, XI, XC, DXI, DXH, EMIN, EMAX, MP, MC, MT, NZ

100 FORMAT (I3, 6E10.3, 3I2, I3)

IF(N-990)3,3,50

2 IF N GREATER THAN 990, CALL EXIT

3 READ 101, (YI(I), I=1, N)

101 FORMAT (5E14.7)

READ 300, C0, U0, AK, CP0

300 FORMAT (4F10.0)

READ 310, NMAX, XQ, YQ, R

310 FORMAT (I2, 8X, 3F10.0)

READ 320, CAP1, R2, R3, AL40, AL50, CAP6, CAP7

READ 320, R80, R90, CAP12, R13, RSEC

READ 320, R10, AL11, XPRT

320 FORMAT (8E10.3)

READ 330, CONO

330 FORMAT (A10)

READ 340, (RMK1(I), I=1, 8)

READ 340, (RMK2(I), I=1, 8)

340 FORMAT (8A10)

READ 440, ZAP

440 FORMAT (F5.0)

NCI=0

C0=C0/1000.

U0=U0/1000.

CP0 INITIAL SHOCK POSITION, METERS (-10 METERS FOR TURN-ON)

CP SHOCK POSITION

C, C0 SHOCK VELOCITY, METERS/SECOND

U, U0 PARTICLE VELOCITY, METERS/SECOND

AK RESISTANCE CHANGE FACTOR

NMAX NUMBER OF PRIMARY TURNS

XQ INITIAL GAGE LENGTH, INCHES

YQ INITIAL GAGE WIDTH, INCHES

C R SPACING BETWEEN LOOPS, INCHES
 C UP GAGE DEFORMATION
 C V DEFORMED GAGE LENGTH
 C
 C C1 PRIMARY LINE CAPACITANCE (CAP1)
 C R2 POWER SUPPLY SHUNT RESISTANCE
 C R3 SECONDARY LINE TERMINATION, 50 OHMS
 C AL40 INITIAL SECONDARY SELF INDUCTANCE
 C AL50 INITIAL PRIMARY SELF INDUCTANCE
 C C6 POWER SUPPLY CAPACITANCE (CAP6)
 C C7 SECONDARY LINE CAPACITANCE (CAP7)
 C R80 INITIAL RESISTANCE, GAGE SECONDARY
 C RS=C SECONDARY LINE RESISTANCE, LUMPED WITH R8
 C R90 INITIAL RESISTANCE, GAGE PRIMARY
 C R10 PRIMARY LINE RESISTANCE
 C AL11 BALLAST INDUCTANCE IN PRIMARY
 C C12 POWER SUPPLY CONTROL CAPACITANCE (CAP12)
 C R13 POWER SUPPLY CONTROL RESISTANCE
 C
 C N NUMBER OF STATE EQUATIONS
 C XI INITIAL TIME
 C XC CUTOFF TIME
 C DX TIME INCREMENT
 C NZ NUMBER OF Y VALUES TO BE PRINTED OUT
 C XPRT PRINTOUT CONTROL, TIME INTERVAL
 C
 C MP=0 PRINT COMPLETE OUTPUT
 C MP=1 PRINT INITIAL AND FINAL RESULTS ONLY
 C MC=0 AUTOMATIC STEP SIZE CONTROL
 C MC=1 NO STEP SIZE CONTROL
 C MT=0 RKG PLUS A-M METHOD
 C MT=1 RKG METHOD ONLY
 C
 C CURRI INITIAL VALUE OF CURRENT
 C NCI COUNTER IN DERV, CURRI CALCULATION
 C ZAP DETERMINES CALCULATIONAL MODE
 C ZAP= -1. INDUCTANCE CHANGES ONLY
 C ZAP= 0. NORMAL
 C ZAP= +1. RESISTANCE CHANGES ONLY
 C

NPRI=NMAX
 NS=C=NPRI - 1
 DO 777 LU=1,2
 PRINT 501
 501 FORMAT (1H1)
 PRINT 395
 395 FORMAT (* MUTUAL INDUCTANCE PARTICLE VELOCIMETER DEVELOPMENT *)
 PRINT 496
 496 FORMAT (* AFWL/DEX *)
 PRINT 500
 500 FORMAT (* *)
 PRINT 400
 400 FORMAT (* GAGE DESIGN *)
 PRINT 401,XQ
 401 FORMAT (5X,9H LENGTH =,F7.3,1X,7H INCHES)
 PRINT 402,YQ
 402 FORMAT (5X,8H WIDTH =,F7.3,1X,7H INCHES)
 PRINT 403,R

```

403 FORMAT (5X,15H LOOP SPACING =,F5.3,1X,7H INCHES)
PRINT 404,NPRI
404 FORMAT (6X,I1,1X,14H PRIMARY TURNS)
PRINT 405,NSEC
405 FORMAT (6X,I1,1X,15H SECONDARY TURNS)
PRINT 430,COND
430 FORMAT (5X,21H CONDUCTOR MATERIAL -,A10)
PRINT 500
PRINT 406
406 FORMAT (* SHOCK PARAMETERS *)
PRINT 407,C0
407 FORMAT (5X,17H SHOCK VELOCITY =,F6.3,1X,15H MM/MICROSECOND)
PRINT 408,U0
408 FORMAT (5X,20H PARTICLE VELOCITY =,F6.3,1X,15H MM/MICROSECOND)
PRINT 409,AK
409 FORMAT (5X,27H RESISTANCE CHANGE FACTOR =,F4.2)
PRINT 410,CP0
410 FORMAT (5X,25H INITIAL SHOCK POSITION =,F9.5,1X,7H METERS)
PRINT 500
PRINT 411
411 FORMAT (* ELECTRICAL PARAMETERS *)
PRINT 412,CAP1
412 FORMAT (5X,4H C1=,1X,E14.7)
PRINT 413,R2
413 FORMAT (5X,4H R2=,1X,E14.7)
PRINT 414,R3
414 FORMAT (5X,4H R3=,1X,E14.7)
PRINT 415,AL40
415 FORMAT (5X,6H AL40=,1X,E14.7)
PRINT 416,AL50
416 FORMAT (5X,6H AL50=,1X,E14.7)
PRINT 417,CAP6
417 FORMAT (5X,4H C6=,1X,E14.7)
PRINT 418,CAP7
418 FORMAT (5X,4H C7=,1X,E14.7)
PRINT 419,R80
419 FORMAT (5X,5H R80=,1X,E14.7)
PRINT 420,RSEC
420 FORMAT (5X,6H RSEC=,1X,E14.7)
PRINT 420,R90
420 FORMAT (5X,5H R90=,1X,E14.7)
PRINT 421,CAP12
421 FORMAT (5X,5H C12=,1X,E14.7)
PRINT 422,R13
422 FORMAT (5X,5H R13=,1X,E14.7)
PRINT 500
PRINT 423
423 FORMAT (* TIME PARAMETERS *)
PRINT 424,XI
424 FORMAT (5X,13H START TIME =,E14.7,1X,8H SECONDS)
PRINT 425,XC
425 FORMAT (5X,14H CUTOFF TIME =,E14.7,1X,8H SECONDS)
PRINT 426,DXI
426 FORMAT (5X,11H TIME STEP =,E14.7,1X,8H SECONDS)
PRINT 500
PRINT 427
427 FORMAT (* VARIABLES *)
PRINT 428,R10

```

```

428 FORMAT (5X,5H R10=,1X,E14.7)
      PRINT 429,AL11
429 FORMAT (5X,6H AL11=,1X,E14.7)
      PRINT 500
      PRINT 500
      PRINT 500
      PRINT 500
      PRINT 431,(RMK1(I),I=1,8)
      PRINT 431,(RMK2(I),I=1,8)
431 FORMAT (1X,8A10)
777 CONTINUE
      XQ=XQ*.0254
      YQ=YQ*.0254
      R=R*.0254
      U0=U0*1000.
      C0=C0*1000.
      IRK=N + 1
      DO 17 I=IRK,NZ
        Z(I)=J.
17 E(I)=0.
C      INITIALIZE FOR START-UP
2 KONT = 1
  M1 = J
  M2 = 0
  M3 = 0
  M4 = 0
  LC = 0
  EF = 1.0E11
C
C      CHECK ALL INPUT OPTIONS
10 IF (DXM) 11,10,11
11 DXM = 10.0 * DXI
12 IF (EMAX) 13,12,13
13 EMAX = 10.0E-06
14 IF (EMIN) 15,14,15
15 EMIN = EMAX / 100.0
  X = XI
  DO 16 I = 1, N
    Y(I) = YI(I)
16 CONTINUE
  DX = DXI
  XXX=XI + XPRT - DX
C
C      OBTAIN THE DERIVATIVE OF FUNCTION AT INITIAL CONDITIONS
      CALL DERV
C
C      PROVIDE OUTPUT OPTION ON INITIAL CONDITIONS
      CALL PRNT (1)
C
C      * * * * *
C
C      MOVE DATA IN ARRAY PRIOR TO NEXT POINT
20 CALL MOVE
C
C      TEST CONDITION OF SYSTEM
      RKG ON START-UP (4 POINTS) AND AFTER CHANGE IN INTERVAL
      A-M ON ALL OTHER

```

```

IF (MT) 22,21,22
21 KONT = KONT + 1
   IF (KONT - 4) 22,22,23
C
C     PERFORM RKG INTEGRATION TO PICK UP POINT N+1 FROM N
22 CALL RKGI
   DO 24 I = 1, N
   E(I) = 0.0
24 CONTINUE
   GO TO 25
C
C     PERFORM A-M INTEGRATION FOR POINT N+1 USING N THRU N-3
23 CALL ADMI
   CHECK FOR START UP ERROR
   IF (Z2(1) - EF) 25,25,40
C
C
C
C
C     * * * * *
C     PROVIDE OUTPUT OPTION FOR PRINT N
25 CONTINUE
   IF (X-XXX) 77,88,88
88 CALL PRNT(2)
   XXX=XXX + XPRT
77 CONTINUE
C
C     STEP INDEPENDENT VARIABLE X AND INTERROGATE CUT-OFF
   CALL ITRO (MCO)
   IF (MCO) 30,20,30
C
C
C
C
C     * * * * *
C     OUTPUT FINAL VALUES FROM INTEGRATION AND REINITIALIZE
30 CALL PRNT (3)
   GO TO 1
40 PRINT 200
   PRINT 201, (E(I), I = 1, N)
   PRINT 202
   DXI = DXI / 2.0
   GO TO 2
C
50 PRNT 203
   GO TO 51
C
200 FORMAT (35H INITIAL INCREMENT UNSATISFACTORY/10X15HERROR RANGE W
1AS)
201 FORMAT (8E15.7)
202 FORMAT (3X21HHALVING THE INCREMENT/)
203 FORMAT (14H^1^+END DIFFEQ)
51 CALL EXIT
   END

```

SUBROUTINE DERV

```
COMMON Y(24), Y1(24), Y2(24), Y3(24), Y4(24), Z(24), Z1(24)
COMMON Z2(24), Z3(24), Z4(24), YI(24), E(24), XI, XC, X, X1, X2
COMMON X3, X4, DXI, DX, DXM, EMIN, EMAX, KONT, LC, MP, MC, M1, M2
COMMON M3, M4, N, MT
COMMON CPJ, P80, R90, XQ, YQ, R, AK, AM, AL40, AL50, CP, AL11, NZ, DMOX, V
COMMON U, CAP1, R2, R3, CAP6, CAP7, R10, CAP12, R13, NMAX
COMMON U0, C0, CURRI, NCI, ZAP, RSEC
COMMON RMK1(8), RMK2(8)
```

PARAMETER LIST

```
Y(1) - LAMDA 4
Y(2) - LAMDA 5
Y(3) - Q6
Y(4) - Q7
Y(5) - Q12
Y(6) - I5
Y(7) - AM
Y(8) - L4
Y(9) - L5
Y(10) - R8
Y(11) - R9
Y(12) - CP
Y(13) - UP
Y(14) - I5 DOT
Y(15) - E3 (ABSOLUTE VALUE)
Y(16) - E3 IDEAL (ABSOLUTE VALUE), INCLUDES SECONDARY ATTENUATION
AND IS CALCULATED UTILIZING THE CALCULATED VALUE OF CURRENT, Y(6),
AT EACH TIME STEP
Y(17) - E3 IDEAL (ABSOLUTE VALUE), INCLUDES SECONDARY ATTENUATION
AND IS CALCULATED UTILIZING THE INITIAL VALUE OF CURRENT, CURRI,
PRIOR TO SHOCK ARRIVAL
Y(18) - NORMALIZED E3, E3/E3 IDEAL, BASED ON Y(6)
Y(19) - NORMALIZED E3, E3/E3 IDEAL, BASED ON CURRI
Y(20) - AMOUNT OF CURRENT CHANGE DURING SHOCK TRANSIT
```

C=C0

C1=CAP1

C6=CAP6

C7=CAP7

C12=CAP12

CHECK ON SHOCK POSITION

CP=CPJ + C*(X - XI)

IF(CP)22,33,33

22 CONTINUE

V=XQ

CALL MUTI

DMOX0=DMOX

U=0.

DMDT=0.

AL4=AL40

AL5=AL50

DLOT4=0.

DLOT5=0.

R8=R80 + RSEC

R9=R90

UP=0.

```

GO TO 99
33 CONTINUE
U=U0
DT=CP/C
UP=U*DT
V=XQ - UP

C
CALL MUTI
DMOT=-DMOX*U
DLOX4=AL40/XQ
DLOX5=AL50/XQ
AL4=AL40 - DLOX4*UP
AL5=AL50 - DLOX5*UP
DLOT4=-DLOX4*U
DLOT5=-DLOX5*U
R8=(R80/(2.*(XQ + YQ)))*(YQ + 2.*(XQ - CP) + AK*(YQ + 2.*CP))+RSEC
R9=(R90/(2.*(XQ + YQ)))*(YQ + 2.*(XQ - CP) + AK*(YQ + 2.*CP))

C
C CHECK CALCULATIONAL MODE
IF(ZAP)44,99,66
44 CONTINUE

C
C INDUCTANCES CHANGES ONLY
C
R8=R80 + RSEC
R9=R90
GO TO 99
66 CONTINUE

C
C RESISTANCE CHANGES ONLY
C
AL4=AL40
AL5=AL50
DLOT4=0.
DLOT5=0.
99 CONTINUE
DET=AL4*AL5 - AM*AM
DETDI=AL4*DLOT5 + AL5*DLOT4 - 2.*AM*DMOT
Z(1)=Y(4)/C7 -(R8/DET)*(AL5*Y(1) - AM*Y(2))
Z(2)=(DET/(DET + AL11*AL4))*(Y(3)/C6 - ((R9 + R10)/DET)*(AL4*Y(2)-
1AM*Y(1)) - (AL11/DET)*(Y(2)*DLOT4 - AM*Z(1) - Y(1)*DMOT) - ((AL11*
2DETDI)/(DET*DET))*(AM*Y(1) - AL4*Y(2)))
Z(3)=- (C6/(C6 + C1))*(Y(3)/(R2*C6) + (1./R13)*(Y(3)/C6 - Y(5)/C12)
1 + (1./DET)*(AL4*Y(2) - AM*Y(1)))
Z(4)= - Y(4)/(R3*C7) - (AL5*Y(1) - AM*Y(2))/DET
Z(5)=(1./R13)*(Y(3)/C6 - Y(5)/C12)
Y(6)=(AL4*Y(2) - AM*Y(1))/DET
IF(NCI)50,50,51
50 ,URRI=Y(6)
51 CONTINUE
NCI=NCI + 1
Y(7)=AM
Y(8)=AL4
Y(9)=AL5
Y(10)=R8
Y(11)=R9
Y(12)=CP
Y(13)=UP

```



```

Y(14)=(1./DET)*(AL4*Z(2) + Y(2)*DLOT4 - AM*Z(1) - Y(1)*DMDT) +
1 (DETOT/(DET*DET))*(AM*Y(1) - AL4*Y(2))
Y(15)=Y(4)/C7
Y(15)=ABS(Y(15))
Y(16)=Y(6)*DMDX*U*(R3/(R3 + R80 + RSEC))
Y(16)=ABS(Y(16))
IF(Y(16))101,102,101
101 CONTINUE
Y(17)=CURRI*DMDX*U*(R3/(R3 + R80 + RSEC))
Y(17)=ABS(Y(17))
Y(18)=Y(15)/Y(16)
Y(19)=Y(15)/Y(17)
GO TO 103
102 CONTINUE
Y(16)=0.
Y(17)=0.
Y(18)=0.
Y(19)=0.
103 CONTINUE
Y(20)=Y(6)/CURRI
RETURN
END

```

SUBROUTINE MUTI

```

COMMON Y(24), Y1(24), Y2(24), Y3(24), Y4(24), Z(24), Z1(24)
COMMON Z2(24), Z3(24), Z4(24), YI(24), E(24), XI, XC, X, X1, X2
COMMON X3, X4, DXI, DX, DXM, EMIN, EMAX, KONT, LC, MP, MC, M1, M2
COMMON M3, M4, N, MT
COMMON CPJ, R80, R90, XQ, YQ, R, AK, AM, AL40, AL50, CP, AL11, NZ, DMDX, V
COMMON U, CAP1, R2, R3, CAP6, CAP7, R10, CAP12, R13, NMAX
COMMON UG, C0, CURRI, NCI, ZAP, RSEC
COMMON RMK1(8), RMK2(8)
DIMENSION QQ(50), ERR(50)
PI=3.1415926
AMU=.00000125569
Z=YQ
MM=NMAX-1
DO 80 M=1, MM
P=2*M-1
S=P*R
A=SQRT(V*V + Z*Z)
B=SQRT(V*V + S*S)
C=SQRT(Z*Z + S*S)
AA=SQRT(V*V + Z*Z + S*S)
QQ(M)=(AMU/PI)*(2.*S-2.*C-2.*B+2.*AA+V*ALOG(C*(V+B)/(S*(V+AA))) +
1 Z*ALOG(B*(Z+C)/(S*(Z+AA))))
PQQ=(AMU/PI)*(ALOG(C*(V+B)/(S*(V+AA))) + V*(AA-B)/(B*B))
QPL=QQ(M)/V
ERR(M)=(PQQ-QPL)/PQQ
80 CONTINUE
JC=NMAX-1
INTF=2*(NMAX-1)
QX=0.
QY=0.
COEF=INTF
DO 300 J=1, JC
QX=QX + COEF*QQ(J)
QY=QY + COEF*QQ(J)/(1.-ERR(J))
COEF=COEF-2.
300 CONTINUE
AM=QY
ER=1 - QX/QY
DMDX = V*(1.-ER)
RETURN
END

```

```

SUBROUTINE PRNT (K)
C   PROVIDE OUTPUT AS REQUESTED BY OPTIONS
COMMON Y(24), Y1(24), Y2(24), Y3(24), Y4(24), Z(24), Z1(24)
COMMON Z2(24), Z3(24), Z4(24), YI(24), E(24), XI, XC, X, X1, X2
COMMON X3, X4, DXI, DX, DXM, EMIN, EMAX, KONT, LC, MP, MC, M1, M2
COMMON M3, M4, N, NT
COMMON CP0, R00, R90, XQ, YQ, R, AK, AM, AL40, AL50, CP, AL11, NZ, DMGX, V
COMMON U, CAP1, R2, R3, CAP6, CAP7, R10, CAP12, R13, NMAX
COMMON U0, C0, CURRI, NCI, ZAP, RSEC
COMMON RMK1(8), RMK2(8)
C   TEST PRINT ON INITIAL AND INTERMEDIATE POINTS
IF (K - 3) 50,3,80
50 IF (K - 1) 52,1,52
52 IF (MP) 60,51,60
51 IF (K-1) 1,1,2
1 IF (MT) 10,10,11
C
C   * * * * *
C
10 PRINT 200
PRINT 206
PRINT 206
LF = 1
12 PRINT 201, XI, DXI, DXM, XC, EMIN, EMAX
DO 6 I = 1, NZ
PRINT 208, I, Y(I), I, Z(I)
5 CONTINUE
PRINT 209
LC=11+NZ
GO TO 60
11 PRINT 202
PRINT 206
PRINT 206
LF = 2
GO TO 12
2 IF (LC + NZ - 58) 20,20,70
20 PRINT 203, X, DX
DO 4 I=1,NZ
PRINT 205, I, Y(I), I, Z(I), I, E(I)
4 CONTINUE
PRINT 206
LC = LC + 2 + NZ
GO TO 60
3 IF (LC + NZ - 58) 30,30,73
30 PRINT 204, XC
DO 5 I=1,NZ
PRINT 206, I, Y(I), I, Z(I)
5 CONTINUE
PRINT 207
60 RETURN
70 GO TO (71, 72), LF
71 PRINT 200
PRINT 209
LC = 6
GO TO 20
72 PRINT 202
LC = 6
PRINT 209

```

```

      GO TO 20
73   GO TO ( 74, 75), LF
74   PRINT 200
      GO TO 30
75   PRINT 202
      GO TO 30
80   GO TO (81, 82), LF
81   PRINT 200
      PRINT 209
      LC = 6
      GO TO 60
82   PRINT 202
      PRINT 209
      LC = 6
      GO TO 60

C
C
C      *      *      *      *      *      *      *      *      *      *
200  FORMAT (50H1  RUNGE-KUTTA-GILL / ADAMS-MOULTON INTEGRATION ROUTIN
1E)
201  FORMAT (20H  INITIAL CONDITIONS/16X1HX,17X5HDEL X,12X9HMAX DEL X,
113X,5HOUT X,12X,9HMIN ERROR,10X,9HMAX ERROR/5X,6E19.7)
202  FORMAT (40H1  RUNGE-KUTTA-GILL INTEGRATION ROUTINE)
203  FORMAT (2E15.7)
204  FORMAT (/34H  FINAL RESULT AT A CUT-OFF X OF,E15.7)
205  FORMAT (10X,2HY(,I2,4H) = ,E15.7,4X5HDERV(,I2,4H) = ,E15.7,4X,
15HERROR(,I2,4H) = ,E15.7)
206  FORMAT (1H )
207  FORMAT (1H1/1H1)
208  FORMAT (9X,3HYI(,I2,4H) = ,E15.7,3X,6HDERVI(,I2,4H) = ,E15.7)
209  FORMAT (/12X19HINTEGRATION RESULTS/ 8X,1HX,13X,5HDEL X/20X,4HY(1),
123X,7HDERV(I),23X,8HERROR(I)/)
210  FORMAT (10X,2HY(,I2,4H) = ,E15.7,4X5HDERV(,I2,4H) = ,E15.7)
      END

SUBROUTINE MOVE
C      TO REPOSITION DATA ARRAY FOR NEXT POINT
COMMON Y(24), Y1(24), Y2(24), Y3(24), Y4(24), Z(24), Z1(24)
COMMON Z2(24), Z3(24), Z4(24), YI(24), E(24), XI, XC, X, X1, X2
COMMON X3, X4, DXI, DX, DXM, EMIN, EMAX, KONT, LC, MF, MC, M1, M2
COMMON M3, M4, N, NT
COMMON CP0,R00,R90,X0,Y0,R,AK,AM,AL40,AL50,CP,AL11,NZ,DMOX,V
COMMON U,CAP1,R2,R3,CAP6,CAP7,R10,CAP12,R13,NMAX
COMMON UG,C,CURRI,NCI,ZAP,RSEC
COMMON RMK1(6),RMK2(8)
C
      X4 = X3
      X3 = X2
      X2 = X1
      X1 = X
      DO 1 I = 1, N
      Y4(I) = Y3(I)
      Y3(I) = Y2(I)
      Y2(I) = Y1(I)
      Y1(I) = Y(I)
      Z4(I) = Z3(I)
      Z3(I) = Z2(I)
      Z2(I) = Z1(I)
      Z1(I) = Z(I)
1    CONTINUE
      RETURN
      END

```

SUBROUTINE RKGI

```

C      OBTAIN VALUE OF NEXT POINT VIA RUNGE-KUTTA-GILL INTEGRATION
COMMON Y(24), Y1(24), Y2(24), Y3(24), Y4(24), Z(24), Z1(24)
COMMON Z2(24), Z3(24), Z4(24), YI(24), E(24), XI, XC, X, X1, X2
COMMON X3, X4, DXI, DX, DXH, EMIN, EMAX, KONT, LC, MP, MC, M1, M2
COMMON M3, M4, N, MT
COMMON CPJ, R80, R90, XU, YQ, R, AK, AM, AL40, AL50, CP, AL11, NZ, DMDX, V
COMMON U, CAP1, R2, R3, CAP6, CAP7, R10, CAP12, R13, NMAX
COMMON U0, C0, CURRI, NCI, ZAP, RSEC
COMMON RMK1(8), RMK2(8)
DIMENSION A(24)

```

C
C
C

RKG INTEGRATION CONSTANTS

```

D1 = SQRT (0.5000)
D2 = SQRT (2.0000)
D3 = 3.0 * D1
C1 = 1.0 - D1
C2 = 2.0 - D2
C3 = 2.0 - D3
C4 = 1.0 + D1
C5 = 2.0 + D2
C6 = 2.0 + D3
DO 10 I = 1, N
A(I) = Z(I)

```

1)

CONTINUE

C
C
C

```

DO 1 I = 1, N
Y(I) = Y(I) + DX * Z(I) / 2.0
CONTINUE
X = X1 + DX / 2.0
CALL DERV
DO 2 I = 1, N
Y(I) = Y(I) + C1 * DX * (Z(I) - A(I))
A(I) = C2 * Z(I) - C3 * A(I)
CONTINUE
CALL DERV
DO 3 I = 1, N
Y(I) = Y(I) + C4 * DX * (Z(I) - A(I))
A(I) = C5 * Z(I) - C6 * A(I)
CONTINUE
X = X1 + DX
CALL DERV
DO 4 I = 1, N
Y(I) = Y(I) + DX * Z(I) / 6.0 - DX * A(I) / 3.0
CONTINUE
CALL DERV
RETURN
END

```

SUBROUTINE ITRO (K)

TO INTERROGATE CURRENT VALUE OF X FOR CUT-OFF X

```

COMMON Y(24), Y1(24), Y2(24), Y3(24), Y4(24), Z(24), Z1(24)
COMMON Z2(24), Z3(24), Z4(24), YI(24), E(24), XI, XC, X, X1, X2
COMMON X3, X4, DXI, DX, DXM, EMIN, EMAX, KONT, LC, MP, MC, M1, M2
COMMON M3, M4, N, MT
COMMON CP0, R80, R90, XQ, YQ, R, AK, AM, AL40, AL50, CP, AL11, NZ, DMDX, V
COMMON U, CAP1, R2, R3, CAP6, CAP7, R10, CAP12, R13, NMAX
COMMON U0, C0, CUKRI, NCI, ZAP, RSEC
COMMON RMK1(8), RMK2(8)
IF (X + DX - XC) 2,1,1
1 IF (M4) 4,5,4
2 K = 0
3 RETURN
C
C      *      *      *      *      *      *      *      *      *      *
C
5 DX = XC - X
  KONT = 1
  M4 = 1
  GO TO 3
4 K = 1
  GO TO 3
END

```

```

SUBROUTINE ADMI
C      OBTAIN TENTATIVE VALUE OF NEXT POINT VIA ADAMS-MOULTON INTEGRATI
C      CHECK ERROR FOR POSSIBLE CHANGE IN STEP-SIZE
COMMON Y(24), Y1(24), Y2(24), Y3(24), Y4(24), Z(24), Z1(24)
COMMON Z2(24), Z3(24), Z4(24), YI(24), E(24), XI, XC, X, X1, X2
COMMON X3, X4, DXI, DX, DXM, EMIN, EMAX, KONT, LC, MP, MC, M1, M2
COMMON M3, M4, N, MT
COMMON CPJ,RBJ,K90,XQ,YQ,R,AK,AM,AL40,AL50,CP,AL11,NZ,DMDX,V
COMMON U,CAP1,R2,R3,CAP6,CAP7,R10,CAP12,R13,NMAX
COMMON UO,CJ,CURRI,NCI,ZAP,RSEC
COMMON RMK1(8),RMK2(8)
DIMENSION YY(24)

C      IF (KF) 50,51,50
50      IF (KFF) 52,53,52
52      KF = 0
      KFF = 0
      GO TO 51
53      KFF = 1
51      CONTINUE
      * * * * *

C      STEP X AND PREDICT A Y
C      X = X1 + DX
      MM = 0
      D1 = DX/24.0
      D2 = 19.0/270.0
      DO 5 I = 1, N
      Y(I) = Y1(I)+D1*(55.0*Z1(I)-59.0*Z2(I)+37.0*Z3(I)-9.0*Z4(I))
      YY(I) = Y(I)
5      CONTINUE
      CALL DERV

C      CORRECT Y AND PREDICT CHECK ON ERROR
C      DO 6 I = 1, N
      Y(I) = Y1(I) + D1*(9.0*Z(I)+19.0*Z1(I)-5.0*Z2(I)+Z3(I) )
5      CONTINUE
      CALL DERV
      * * * * *

C      DO 7 I = 1, N
      E(I) = ABS (D2 * (Y(I) - YY(I) ))
C      CHECK ERROR RANGE
      IF (EMAX - E(I) ) 45,1,1
1      IF (E(I) - EMIN ) 8,7,7
45      MM = MM + 1
      GO TO 7
8      M3 = M3 + 1
7      CONTINUE
      IF (MM) 46,46,3
46      IF ( M3 - N ) 10,2,2
      * * * * *

C      ERROR LESS THAN MINIMUM - DOUBLE THE STEP-SIZE
2      IF (MC) 10,21,10
21      IF (X + 4.0 *DX - XC) 22,22,10
22      IF (DX+DX -DXM) 23,23,10
23      CALL PRNT (2)

```

```

DX = DX + DX
IF (LC + N - 58) 230,230,231
231 CALL PRNT(4)
230 PRINT 201
DO 24 I = 1, N
PRINT 203, I, E(I)
24 CONTINUE
PRINT 204
LC = LC + 2 + N
X1 = X
DO 25 I = 1, N
Z3(I) = Z4(I)
Z1(I) = Z(I)
Y1(I) = Y(I)
25 CONTINUE
* * * * *
CALL RKGI
DO 26 I = 1, N
E(I) = 0.0
26 CONTINUE
M1 = 1
GO TO 13
* * * * *
C
C
C
      ERROR GREATER THAN MAXIMUM - HALVE THE STEP-SIZE
3 IF (M2) 30,40,30
30 IF (M0) 10,31,10
31 IF (M1) 34,32,34
32 IF (X + DX + DX - XC) 33,33,10
33 IF (KFF) 36,35,36
* * * * *
C
35 DX = DX / 2.0
IF (LC + N - 58) 350,350,351
351 CALL PRNT(4)
350 PRINT 202
DO 37 I = 1, N
PRINT 203, I, E(I)
37 CONTINUE
PRINT 204
LC = LC + 2 + N
DO 42 I = 1, N
Y(I) = Y1(I)
Z(I) = Z1(I)
42 CONTINUE
CALL RKGI
DO 38 I = 1, N
F(I) = 0.0
38 CONTINUE
KONT = 2
KF = 1
KFF = 0
GO TO 13
* * * * *
C
34 X1 = X2
M1 = 0
DO 39 I = 1, N
Y(I) = Y2(I)
Y1(I) = Y2(I)

```

```

      Z(I) = Z2(I)
      Z1(I) = Z2(I)
35  CONTINUE
      GO TO 35
10  M2 = 1
      IF (M1) 11,13,11
11  M1 = 0
13  M3 = J
      RETURN
C   * * * * *
36  KFF = 0
      X1 = X4
      DO 41 I = 1, N
          Y(I) = Y4(I)
          Y1(I) = Y4(I)
          Z(I) = Z4(I)
          Z1(I) = Z4(I)
41  CONTINUE
      GO TO 35
40  Z2(1) = 1.0E12
      GO TO 13
C   * * * * *
201 FORMAT (51H      DOUBLING THE INTERVAL,      ERROR ARRAY AS FOLLOWS)
202 FORMAT (50H      HALVING THE INTERVAL,      ERROR ARRAY AS FOLLOWS)
203 FORMAT (8X,6HERROR(,I2,5H) = ,E15.9)
204 FORMAT (1H )
      END

```


REFERENCES

1. Bunker, R. B., Doran, J. A., Impedance-Mismatch High Stress Transducer (IMHST), AFWL-TR-73-45, AF Weapons Laboratory, Kirtland AFB, NM, March 1973.
2. Baum, N., Shunk, R., Bunker, R. B., Thermoelectric Thermopile Transducer (T³) Development, AFWL-TR-73-24, AF Weapons Laboratory, Kirtland AFB, NM, April 1973.
3. Danek, W. L., Jr., Schooley, D. L., Jerozal, F. A., Particle Velocimeter for Use Close-In to Underground Explosions, DASA Report 1431-3, Defense Atomic Support Agency, Wash, DC 12 October 1967.
4. Liberman, P., Newell, D., Piezoresistive Dielectric/Dielectric Microwave Waveguide, AFWL-TR-73-37, AF Weapons Laboratory, Kirtland AFB, NM, February 1973.
5. Specification Sheet for Velocity Transducer, Crescent Engineering and Research Company, 15 November 1964.
6. Perret, W. R., Wistor, J. W., Hansen, G. J., Palmer, D. G., "DX Pendulum Velocity Gage," in Four Papers Concerning Recent Work on Ground Motion Measurements, SC-R-65-905, Sandia Corp., Albuquerque, NM, pp 25-28, July 1965.
7. Liberman, P., Theory and Operation of the IITRI Pressure-Time Gages in the 20-200 Kilobar Region, DASA Report 2161, Defense Atomic Support Agency, Wash, DC, November 1968.
8. Barker, L. M., Laser Interferometry in Shock-Wave Research, SC-DC-70-5465, Sandia Laboratories, Albuquerque, NM, December 1970.
9. Danek, W. L., Jr., Reily, D. M., Cushing, V. J., Particle Velocimeter for Use Close-In to Underground Explosions, Phase I, DASA Report 1431, Defense Atomic Support Agency, Wash, DC, 30 November 1963.
10. Danek, W. L., Jr., Particle Velocimeter for Use Close-In to Underground Explosions, Phases II and III, DASA Report 1431-1, Defense Atomic Support Agency, Wash, DC, 29 October 1964.
11. Danek, W. L., Jr., Dargis, A. A., Particle Velocimeter for Use Close-In to Underground Explosions, Phase IV, DASA Report 1431-2, Defense Atomic Support Agency, Wash, DC, 31 December 1965.
12. Danek, W. L., Jr., Private Communication.
13. Danek, W. L., Jr., Schooley, D. L., Jerozal, F. A., Close-In Particle Velocity, Operation DISTANT PLAIN, Event 6, Project 3.09, DASA Report 2021, Defense Atomic Support Agency, 15 November 1967.

REFERENCES (cont'd)

14. Keough, D. D., Constitutive Relations from In Situ Lagrangian Measurements of Stress and Particle Velocity, DASA Report 2685, Defense Atomic Support Agency, Wash, DC, 27 January 1972.
15. Smith, C. W., Grady, D. E., Seaman, L., Petersen, C. F., Constitutive Relations from In Situ Lagrangian Measurements of Stress and Particle Velocity, DNA Report 28831, Defense Nuclear Agency, Wash, DC, January 1972.
16. Grady, D. E., Smith, C. W., Seaman, L., In Situ Constitutive Relations of Rocks, DNA Report 31722, Defense Nuclear Agency, Wash, DC, January 1973.
17. Garcia, P. R., IMHST and Particle Velocity Gage Measurements, MIDDLE GUST IV and V, Report No. AL-881, EG&G, Inc., Albuquerque, NM, 3 November 1972.
18. Renick, J. D., et al., Close-In Ground Stress Measurements, MIXED COMPANY III, Project LN 304, Report No. FOR 6633, AF Weapons Laboratory, Kirtland AFB, NM, November 1973.
19. Stern, T. E., Theory of Nonlinear Networks and Systems, An Introduction, Addison-Wesley Publishing Company, Inc., Reading, MA, 1965.
20. Seshu, S., Reed, M. B., Linear Graphs and Electrical Networks, Addison-Wesley Publishing Company, Inc., Reading, MA, 1961.
21. Terman, F. E., Radio Engineers' Handbook, McGraw-Hill Book Company, Inc., New York/London, pp 53-57, 1943.
22. Test Facilities Handbook (Tenth Edition), Arnold Engineering Development Center, Arnold AFS, TN, May 1974.
23. Bridgeman, P. W., "The Resistance of 72 Elements, Alloys, and Compounds to 100,000 kg/cm²," in Proceedings of American Academy of Arts and Sciences, 81, 1952.
24. Neutron Cross Sections, Vol I, Resonance Parameters, BNL 325, National Neutron Cross-Section Center, Brookhaven National Laboratory, Upton, New York, June 1973.